OPTIMIZING DEVELOPMENT STRATEGIES TO INCREASE RESERVES IN UNCONVENTIONAL GAS RESERVOIRS

A Thesis

by

GULCAN TURKARSLAN

Submitted to the Office of Graduate Studies of
Texas A&M University
in partial fulfillment of the requirements for the degree of

MASTER OF SCIENCE

August 2010

Major Subject: Petroleum Engineering

Optimizing Development Strategies to Increase Reserves in Unconventional Gas Reservoirs

OPTIMIZING DEVELOPMENT STRATEGIES TO INCREASE RESERVES IN UNCONVENTIONAL GAS RESERVOIRS

A Thesis

by

GULCAN TURKARSLAN

Submitted to the Office of Graduate Studies of
Texas A&M University
in partial fulfillment of the requirements for the degree of

MASTER OF SCIENCE

Approved by:

Chair of Committee,	Duane McVay
Committee Members,	Walter Ayers
	Tom Blasingame
Head of Department,	Stephen Holditch

August 2010

Major Subject: Petroleum Engineering

ABSTRACT

Optimizing Development Strategies to Increase Reserves in Unconventional Gas Reservoirs. (August 2010)

Gulcan Turkarslan, B.S., Middle East Technical University

Chair of Advisory Committee: Dr. Duane McVay

The ever increasing energy demand brings about widespread interest to rapidly, profitably and efficiently develop unconventional resources, among which tight gas sands hold a significant portion. However, optimization of development strategies in tight gas fields is challenging, not only because of the wide range of depositional environments and large variability in reservoir properties, but also because the evaluation often has to deal with a multitude of wells, limited reservoir information, and time and budget constraints. Unfortunately, classical full-scale reservoir evaluation cannot be routinely employed by small- to medium-sized operators, given its time-consuming and expensive nature. In addition, the full-scale evaluation is generally built on deterministic principles and produces a single realization of the reservoir, despite the significant uncertainty faced by operators.

This work addresses the need for rapid and cost-efficient technologies to help operators determine optimal well spacing in highly uncertain and risky unconventional gas reservoirs. To achieve the research objectives, an integrated reservoir and decision modeling tool that fully incorporates uncertainty was developed. Monte Carlo simulation was used with a fast, approximate reservoir simulation model to match and predict production performance in unconventional gas reservoirs. Simulation results were then fit with decline curves to enable direct integration of the reservoir model into a Bayesian decision model. These integrated tools were applied to the tight gas assets of Unconventional Gas Resources Inc. in the Berland River area, Alberta, Canada.

DEDICATION

in loving memory of my grandmother
Guzin Ekmekcioglu

ACKNOWLEDGEMENTS

I would like to thank my committee chair, Dr. Duane McVay, for his guidance and support throughout the course of this research. Without his help, this work would not have been possible. I also would like to thank my committee members, Dr. Walter Ayers and Dr. Tom Blasingame, for their guidance and helpful comments.

Thanks also go to my friends whose existence made my stay at Texas A&M University a pleasurable and memorable one. I thank all of them and wish best of luck in their careers and studies.

I would like to especially thank my colleague, Mr. Tugrul Tas for sharing his extensive knowledge and experience on coding. In spite of the numerous logistical limitations, never once did he hesitate to offer his sincere help, for which I am truly grateful and deeply appreciate.

I owe my sincerest gratitude to my best friend, Dr. Murat Kaya Yapici, who has always been beside me whenever I needed his help. I am greatly indebted to him for his unwavering support, endless patience and generous help.

Lastly but most importantly, I would like to express my heartfelt gratitude to my beloved parents, Efser and Muharrem, and my dear sister, Ozlem for their unconditional love and support ever since. Without their encouragement, none of this would have been possible.

TABLE OF CONTENTS

Page

ABSTRACT iii

DEDICATION iv

ACKNOWLEDGEMENTS v

TABLE OF CONTENTS vi

LIST OF FIGURES viii

LIST OF TABLES xv

CHAPTER

I INTRODUCTION 1

1.1 Statement and Significance of the Problem 1
1.2 Literature Review 2
1.2.1 Integrated Reservoir Studies 3
1.2.3 Moving Window Method 6
1.2.4 Simulation-based Regression 12
1.2.5 Limitations of Existing Methods 15
1.3 Objectives 15
1.4 Organization of Thesis 16

II GETHING RESERVOIR 17

2.1 Background 17
2.2 Gething Formation 20

III PROBABILISTIC RESERVOIR MODEL 23

3.1 Monte Carlo Probabilistic Approach 24
3.2 Reservoir Models for Different Decision Contexts 31
3.2.1 First Reservoir Model 31
3.2.2 Second Reservoir Model 38

CHAPTER Page

IV CORRELATION COEFFICIENTS 52

4.1 Variogram Analysis 52
4.2 Correlation Coefficients 60

V DECLINE CURVE MODEL 62

5.1 Background 62
5.1.1 Exponential Decline Curve 63
5.1.2 Hyperbolic Decline Curve 64
5.2 Applied Methodology 64
5.3 Results of Decline Curve Model 67

VI DECISION MODEL 81

6.1 Methodology 82
6.2 Results of the Decision Model 84

VII CONCLUSIONS AND RECOMMENDATIONS 90

7.1 Conclusions 90
7.2 Limitations 91
7.3 Recommended Future Work 91

NOMENCLATURE 93

REFERENCES 96

APPENDIX A 99

APPENDIX B 105

APPENDIX C 107

APPENDIX D 119

APPENDIX E 122

VITA 133

LIST OF FIGURES

Page

Fig.1— Location map showing the position of the study area relative to the Deep Basin of Alberta (Smith et al. 1984) 18

Fig.2— Berland River base map. Regions enclosed in blue show the sections where UGR's wells are located (provided by UGR)..... 19

Fig.3— Stratigraphic column of the Lower Cretaceous (Smith et al. 1984)..... 20

Fig.4— Type logs of the various facies of the Gething Formation (Smith et al. 1984)..... 21

Fig.5— Schematic illustration of the integrated reservoir and decision modeling tools 23

Fig.6— Block diagram representation of the applications and tools used in this study 26

Fig.7— Histograms and probability distribution functions of uncertain input variables used in the modeling of Berland River area: (a) Net pay, (b) Porosity, (c) Formation depth, (d) Reservoir size 27

Fig.8— (a) Probability distribution plot (PDF), (b) cumulative distribution plot (CDF) of permeability 28

Fig.9— Porosity-permeability cloud 29

Fig.10— Gridblocks model based on an aspect ratio of 7: (a) Grid Centroid X, (b) Grid Centroid Y 30

Fig.11— Schematic illustration showing possible existing and new well locations 32

Fig.12— Probability distribution plot of 20-year discounted cumulative gas production for Well 1 on 210 acre-spacing (Stage 1) 36

Fig.13— Crossplot of Well 1 (Stage 1) vs. Well 2 (Stage 2) 20-year discounted cumulative gas productions (Option 2) 36

Fig.14— Possible two-stage downspacing combinations. Numbers on top of arrows indicate Stage 1 wells and additional Stage 2 wells 39

Page

Fig.15— Simulated cases used in the comparison. Wells labeled in red are compared with the actual field data 41

Fig.16— Cumulative distribution plots of (a) best-month gas production and (b) stage gas production 42

Fig.17— Probability distribution plot of stage-end average gas production for Well 1 on 640 acre-spacing (Stage 1) 43

Fig.18— Crossplot of Stage 1 (640 acres) vs. Stage 2 (640 acres) gas productions 43

Fig.19— Schematic illustration showing (a) possible well locations, (b) representative well locations 46

Fig.20— Possible two-stage downspacing combinations. Numbers on top of arrows indicate Stage 1 wells and additional Stage 2 wells. Wells 1 through 4 are the representative wells 46

Fig.21— Porosity map of the Gething reservoir (provided by Schlumberger Consulting Services on Berland River area) 54

Fig.22— Variogram analysis for porosity: (a) Variogram map (distances are in meters), (b) major and (c) minor direction empirical variograms, (d) major and (e) minor direction theoretical variograms with covariance and correlation functions (provided by Schlumberger Consulting Services on Berland River area) 55

Fig.23— Net pay map of the Gething reservoir (provided by Schlumberger Consulting Services on Berland River area) 56

Fig.24— Variogram analysis for net pay: (a) Variogram map (distances are in meters), (b) major and (c) minor direction empirical variograms, (d) major and (e) minor direction theoretical variograms with covariance and correlation functions (provided by Schlumberger Consulting Services on Berland River area) 57

Fig.25— Permeability-thickness map of the Gething reservoir (provided by Schlumberger Consulting Services on Berland River area) 58

Page

Fig.26— Variogram analysis for permeability: (a) Variogram map (distances are in meters), (b) major and (c) minor direction empirical variograms, (d) major and (e) minor direction theoretical variograms with covariance and correlation functions (provided by Schlumberger Consulting Services on Berland River area) 59

Fig.27— Schematic illustration showing the representative well locations and the corresponding interwell distances in meters 60

Fig.28— Example of a simulated production profile from the reservoir model with 3-year stage length: (a) Hyperbolic decline model fitted to the first 3 years of production (b) An early hyperbolic model transitioning to exponential, fitted to the 20 years of production..... 66

Fig.29 — Cumulative distribution plot of qi for Well 1, stage-length of 1 year: (a) 1 year-qi (Stage 1), (b) 20 year-qi (Stage 1 + Stage 2) 68

Fig.30— Schematic outlining the approach used in the decision model. Production profiles from the reservoir simulation are input into the decline curve analysis to generate the decline parameters. Means, standard deviations and correlation coefficients of the decline parameters are then calculated and input into the decision model. The decision model processes these inputs and yields the optimal development strategy..... 81

Fig.31— Influence diagram for the Berland River area development plan decision..... 82

Fig.32— Partial decision tree for the Berland River area development plan..... 83

Fig.A1— Probability distribution plot of 20-year discounted cumulative gas production for Well 1 on 210 acre-spacing (Stage 2 – Option 1) 99

Fig.A2— Probability distribution plot of 20-year discounted cumulative gas production for Well 1 on 160 acre-spacing (Stage 2 – Option 2) 100

Fig.A3— Probability distribution plot of 20-year discounted cumulative gas production for Well 2 on 160 acre-spacing (Stage 2 – Option 2) 100

Fig.A4— Probability distribution plot of 20-year discounted cumulative gas production for Well 1 on 160 acre-spacing (Stage 2 – Option 3) 101

Page

Fig.A5— Probability distribution plot of 20-year discounted cumulative gas production for Well 2 on 160 acre-spacing (Stage 2 – Option 3) 101

Fig.A6— Probability distribution plot of 20-year discounted cumulative gas production for Well 3 on 210 acre-spacing (Stage 2 – Option 3) 102

Fig.A7— Probability distribution plot of 20-year discounted cumulative gas production for Well 1 on 160 acre-spacing (Stage 2 – Option 4) 102

Fig.A8— Probability distribution plot of 20-year discounted cumulative gas production for Well 2 on 160 acre-spacing (Stage 2 – Option 4) 103

Fig.A9— Probability distribution plot of 20-year discounted cumulative gas production for Well 3 on 210 acre-spacing (Stage 2 – Option 4) 103

Fig.A10— Probability distribution plot of 20-year discounted cumulative gas production for Well 4 on 210 acre-spacing (Stage 2 – Option 4) 104

Fig.B1— Crossplot of Well 1 (Stage 1) vs. Well 3 (Stage 2) 20-year discounted cumulative gas productions (Option 3) 105

Fig.B2— Crossplot of Well 1 (Stage 1) vs. Well 4 (Stage 2) 20-year discounted cumulative gas productions (Option 4) 106

Fig.C1— Probability distribution plot of stage-end average gas production for Well 1 on 640 acre-spacing (Stage 2, 640-640) 107

Fig.C2— Probability distribution plot of stage-end average gas production for Well 1 on 320 acre-spacing (Stage 2, 640-320) 108

Fig.C3— Probability distribution plot of stage-end average gas production for Well 2 on 320 acre-spacing (Stage 2, 640-320) 108

Fig.C4— Probability distribution plot of stage-end average gas production for Well 1 on 160 acre-spacing (Stage 2, 640-160) 109

Fig.C5— Probability distribution plot of stage-end average gas production for Well 2 on 160 acre-spacing (Stage 2, 640-160) 109

Fig.C6— Probability distribution plot of stage-end average gas production for Well 3 on 160 acre-spacing (Stage 2, 640-160) 110

Page

Fig.C7— Probability distribution plot of stage-end average gas production for Well 4 on 160 acre-spacing (Stage 2, 640-160) 110

Fig.C8— Probability distribution plot of stage-end average gas production for Well 1 on 320 acre-spacing (Stage 1) 111

Fig.C9— Probability distribution plot of stage-end average gas production for Well 2 on 320 acre-spacing (Stage 1) 111

Fig.C10— Probability distribution plot of stage-end average gas production for Well 1 on 320 acre-spacing (Stage 2, 320-320) 112

Fig.C11— Probability distribution plot of stage-end average gas production for Well 2 on 320 acre-spacing (Stage 2, 320-320) 112

Fig.C12— Probability distribution plot of stage-end average gas production for Well 1 on 160 acre-spacing (Stage 2, 320-160) 113

Fig.C13— Probability distribution plot of stage-end average gas production for Well 2 on 160 acre-spacing (Stage 2, 320-160) 113

Fig.C14— Probability distribution plot of stage-end average gas production for Well 3 on 160 acre-spacing (Stage 2, 320-160) 114

Fig.C15— Probability distribution plot of stage-end average gas production for Well 4 on 160 acre-spacing (Stage 2, 320-160) 114

Fig.C16— Probability distribution plot of stage-end average gas production for Well 1 on 160 acre-spacing (Stage 1) 115

Fig.C17— Probability distribution plot of stage-end average gas production for Well 2 on 160 acre-spacing (Stage 1) 115

Fig.C18— Probability distribution plot of stage-end average gas production for Well 3 on 160 acre-spacing (Stage 1) 116

Fig.C19— Probability distribution plot of stage-end average gas production for Well 4 on 160 acre-spacing (Stage 1) 116

Fig.C20— Probability distribution plot of stage-end average gas production for Well 1 on 160 acre-spacing (Stage 2, 160-160) 117

Page

Fig.C21— Probability distribution plot of stage-end average gas production for Well 2 on 160 acre-spacing (Stage 2, 160-160) 117

Fig.C22— Probability distribution plot of stage-end average gas production for Well 3 on 160 acre-spacing (Stage 2, 160-160) 118

Fig.C23— Probability distribution plot of stage-end average gas production for Well 4 on 160 acre-spacing (Stage 2, 160-160) 118

Fig.D1— Crossplot of Stage 1 (640 acres) vs. Stage 2 (320 acres) gas productions 119

Fig.D2— Crossplot of Stage 1 (640 acres) vs. Stage 2 (160 acres) gas productions 120

Fig.D3— Crossplot of Stage 1 (320 acres) vs. Stage 2 (320 acres) gas productions 120

Fig.D4— Crossplot of Stage 1 (320 acres) vs. Stage 2 (160 acres) gas productions 121

Fig.D5— Crossplot of Stage 1 (160 acres) vs. Stage 2 (160 acres) gas productions 121

Fig.E1— Cumulative distribution plot of qi for Well 2, stage-length of 1 year: (a) 1 year-qi (Stage 1), (b) 20 year-qi (Stage 1 + Stage 2) 122

Fig.E2— Cumulative distribution plot of *qi* for Well 3, stage-length of 1 year: (a) 1 year-*qi* (Stage 1), (b) 20 year-*qi* (Stage 1 + Stage 2) 123

Fig.E3— Cumulative distribution plot of *qi* for Well 4, stage-length of 1 year: (a) 1 year-*qi* (Stage 1), (b) 20 year-*qi* (Stage 1 + Stage 2) 124

Fig.E4— Cumulative distribution plot of *qi* for Well 1, stage-length of 3 years: (a) 3 year-*qi* (Stage 1), (b) 20 year-*qi* (Stage 1 + Stage 2) 125

Fig.E5— Cumulative distribution plot of *qi* for Well 2, stage-length of 3 years: (a) 3 year-*qi* (Stage 1), (b) 20 year-*qi* (Stage 1 + Stage 2) 126

Fig.E6— Cumulative distribution plot of *qi* for Well 3, stage-length of 3 years: (a) 3 year-*qi* (Stage 1), (b) 20 year-*qi* (Stage 1 + Stage 2) 127

Fig.E7— Cumulative distribution plot of *qi* for Well 4, stage-length of 3 years: (a) 3 year-*qi* (Stage 1), (b) 20 year-*qi* (Stage 1 + Stage 2) 128

Page

Fig.E8— Cumulative distribution plot of *qi* for Well 1, stage-length of 5 years: (a) 5 year-*qi* (Stage 1), (b) 20 year-*qi* (Stage 1 + Stage 2) 129

Fig.E9— Cumulative distribution plot of *qi* for Well 2, stage-length of 5 years: (a) 5 year-*qi* (Stage 1), (b) 20 year-*qi* (Stage 1 + Stage 2) 130

Fig.E10— Cumulative distribution plot of *qi* for Well 3, stage-length of 5 years: (a) 5 year-*qi* (Stage 1), (b) 20 year-*qi* (Stage 1 + Stage 2) 131

Fig.E11— Cumulative distribution plot of *qi* for Well 3, stage-length of 5 years: (a) 5 year-*qi* (Stage 1), (b) 20 year-*qi* (Stage 1 + Stage 2) 132

LIST OF TABLES

Page

Table 1— Uncertain input variables involved in the modeling of Berland River (Gething) reservoir (data from UGR)..... 26

Table 2— Input parameters employed in the Berland River reservoir model (data from UGR) 31

Table 3— Example simulation results of the first reservoir model for Option 1 (One well is drilled in Stage 1 and no additional wells are drilled in Stage 2)..... 35

Table 4— Statistics of stage-end gas productions (mean and standard deviation) and pairwise correlation coefficients between Stage 1 and Stage 2..... 37

Table 5— Possible downspacing combinations evaluated in the preliminary reservoir model..... 39

Table 6— Example simulation results of the preliminary reservoir model. In Stage 1, one well (Well 1) is producing on 640 acre-spacing. In Stage 2, an additional well is drilled (Well 2) on 320 acre-spacing 40

Table 7— Statistics of stage-end gas productions (mean and standard deviation) and pairwise correlation coefficients between Stage 1 and Stage 2..... 44

Table 8— Possible downspacing combinations evaluated in the final reservoir model..... 45

Table 9— Example simulation results of the final reservoir model for a stage-length of 1 year. In Stage 1, one well (Well 1) is producing on 640 acre-spacing. In Stage 2, three additional wells are drilled on 160 acre-spacing and represented by Well 3 in simulation..... 49

Table 10— Example simulation results of the final reservoir model for a stage-length of 3 years. In Stage 1, one well (Well 1) is producing on 640 acre-spacing. In Stage 2, three additional wells are drilled on 160 acre-spacing and represented by Well 3 in simulation..... 50

Page

Table 11— Example simulation results of the final reservoir model for a stage-length of 5 years. In Stage 1, one well (Well 1) is producing on 640 acre-spacing. In Stage 2, three additional wells are drilled on 160 acre-spacing and represented by Well 3 in simulation 51

Table 12— Correlation matrix for porosity 61

Table 13— Correlation matrix for net pay 61

Table 14— Correlation matrix for permeability 61

Table 15— Example decline curve results of the final reservoir model for a stage length of 1 year. In Stage 1, one well (Well 1) is producing on 640 acre-spacing. In Stage 2, three additional wells are drilled on 160 acre-spacing and represented by Well 3 in simulation 69

Table 16— Example decline curve results of the final reservoir model for a stage length of 3 years. In Stage 1, one well (Well 1) is producing on 640 acre-spacing. In Stage 2, three additional wells are drilled on 160 acre-spacing and represented by Well 3 in simulation 70

Table 17— Example decline curve results of the final reservoir model for a stage length of 5 years. In Stage 1, one well (Well 1) is producing on 640 acre-spacing. In Stage 2, three additional wells are drilled on 160 acre-spacing and represented by Well 3 in simulation 71

Table 18— Statistics of decline curve parameters (mean and standard deviation) and pairwise correlation coefficients between Stage 1 and Stage 2 for downspacing combinations of 640-640, 640-320, 640-160 and 640-80 (stage length of 1 year) 72

Table 19— Statistics of decline curve parameters (mean and standard deviation) and pairwise correlation coefficients between Stage 1 and Stage 2 for downspacing combinations of 320-320, 320-160 and 320-80 (stage length of 1 year) 73

Table 20— Statistics of decline curve parameters (mean and standard deviation) and pairwise correlation coefficients between Stage 1 and Stage 2 for downspacing combinations of 160-160 and 160-80 (stage length of 1 year) 74

Page

Table 21— Statistics of decline curve parameters (mean and standard deviation) and pairwise correlation coefficients between Stage 1 and Stage 2 for downspacing combinations of 80-80 (stage length of 1 year) 74

Table 22— Statistics of decline curve parameters (mean and standard deviation) and pairwise correlation coefficients between Stage 1 and Stage 2 for downspacing combinations of 640-640, 640-320, 640-160 and 640-80 (stage length of 3 years) 75

Table 23— Statistics of decline curve parameters (mean and standard deviation) and pairwise correlation coefficients between Stage 1 and Stage 2 for downspacing combinations of 320-320, 320-160 and 320-80 (stage length of 3 years) 76

Table 24— Statistics of decline curve parameters (mean and standard deviation) and pairwise correlation coefficients between Stage 1 and Stage 2 for downspacing combinations of 160-160 and 160-80 (stage length of 3 years) 77

Table 26— Statistics of decline curve parameters (mean and standard deviation) and pairwise correlation coefficients between Stage 1 and Stage 2 for downspacing combinations of 640-640, 640-320, 640-160 and 640-80 (stage length of 5 years) 78

Table 27— Statistics of decline curve parameters (mean and standard deviation) and pairwise correlation coefficients between Stage 1 and Stage 2 for downspacing combinations of 320-320, 320-160 and 320-80 (stage length of 5 years) 79

Table 28— Statistics of decline curve parameters (mean and standard deviation) and pairwise correlation coefficients between Stage 1 and Stage 2 for downspacing combinations of 160-160 and 160-80 (stage length of 5 years) 80

Table 29— Statistics of decline curve parameters (mean and standard deviation) and pairwise correlation coefficients between Stage 1 and Stage 2 for downspacing combinations of 80-80 (stage length of 5 years) 80

Table 30— Low price environment 85

Table 31— Decision model results showing the optimal development plan in low price environment. Stage length is 1 year 86

Page

Table 32— Decision model results showing the optimal development plan in low price environment. Stage length is 3 years 87

Table 33— High price environment 87

Table 34— Decision model results showing the optimal development plan in high price environment. Stage length is 1 year 88

Table 35— Decision model results showing the optimal development plan in high price environment. Stage length is 3 years 89

CHAPTER 1
INTRODUCTION

1.1 Statement and Significance of the Problem

The rapid growth in world energy demand and higher depletion rates of existing oil and gas reserves have initiated a gap between demand and supply (Zahid et al. 2007). To bridge this fast-growing energy gap and create a sustainable future energy supply, the global petroleum industry is investing heavily in exploration and development of unconventional energy sources.

During the 1980s, implementation of federal tax credits and various technical development programs in North America accelerated the development of new technologies for unconventional natural gas exploration and exploitation. With the advancement of technology, along with increasing gas prices, there has been growing interest in shales, tight sands and coalbed methane during the past decade (Xiong and Holditch 2006).

Among unconventional gas reservoirs in North America, tight sands hold the largest portion (Stark et al. 2007) and they represent an important source for future reserve growth and production. However, despite their tremendous reserve growth potential, tight gas reservoirs present significant technical and engineering challenges in characterization and exploitation, as well as uncertainties in production owing to complex heterogeneities and reservoir properties. Therefore, economic development of these assets remains risky.

Functioning within this risky domain, it is imperative that operators make sound judgements and development decisions such as determining the optimal well spacing. When making such decisions, one should conserve capital, protect the environment by avoiding over drilling and profitably maximize production by quickly achieving the optimal well spacing.

This thesis follows the style and format of the *SPE Journal*.

Examples of previous suboptimal development plans (McKinney et al. 2002) indicate potential losses of 50% in the asset value, which shows the importance of identifying the optimal well spacing early in the life of an unconventional gas field.

Traditionally, determination of the optimal well spacing has been carried out through statistical comparison of the performance of wells drilled at different spacings, from several infill programs with 10-40 year time spans. Unfortunately, for emerging tight sand plays, due to the lack of historical infill programs there is insufficient data to utilize traditional statistical comparison methods for evaluating optimal well spacing. Moreover, we do not have the luxury to develop these fields in an upcoming 40-year time span.

In summary, accelerating the development of unconventional gas reservoirs is critical to increase reserves and to meet the growing energy demand. Effective exploitation of these reservoirs can be achieved by developing fields at sufficiently dense well spacings, so that ultimate recovery is maximized while over drilling is avoided. Furthermore, the optimal well spacing must be reached early in the field's life to minimize capital expenditures and maximize profit.

1.2 Literature Review

Rapid and cost-effective assessments of optimal development strategies in marginal tight gas fields, such as well spacing and completion practices are critical to increase reserves and accelerate production, while protecting the environment. However, optimization of development strategies in tight gas fields is challenging, not only because of the complexity involved in the evaluation due to the wide range of depositional environments and large variability in reservoir properties, but also because the evaluation often has to deal with a multitude of wells, limited reservoir information, and time and budget constraints.

In recent years, the issue of determining optimal development strategies in tight gas fields has been followed with much interest in industry, and various authors have proposed techniques to address the challenges associated with geologic complexity of

these reservoirs and methods of handling large numbers of wells and limited reservoir information.

Newsham and Rushing (2001) introduced an integrated reservoir study including detailed geological, geophysical, petrophysical, reservoir engineering analyses and interpretations to evaluate infill drilling potential of a field and to determine optimal well placements. Unfortunately, such integrated studies cannot always be justified due to scarcity of data and marginal economics.

As an alternative to performing an integrated reservoir study for large, low-permeability gas reservoirs, some authors (Cipolla and Wood 1996; Guan and Du 2004; Guan and McVay 2004; Guan et al. 2002; Hudson et al. 2000; Hudson et al. 2001; Kyte and Meehan 1996; McCain et al. 1993; Voneiff and Cipolla 1996) proposed statistical moving window techniques to optimize the number and locations of wells to be drilled. While this technology can be a useful screening tool, the estimation errors for infill well performance can be quite significant as well interference effects become complicated and reservoir heterogeneity increases.

To improve upon moving window methods, some authors (Gao and McVay 2004; Cheng et al. 2006a; Cheng et al. 2006b; Cheng et al. 2008) suggested a simulation-based regression method combined with automated prediction to determine optimal well locations. The notable features of this method are (1) fast and cost-effective automatic history-matching and capability of handling hundreds of wells; (2) reliable reservoir characterization of large-scale heterogeneity for both permeability and pore volume and; (3) minimal data requirements.

In this section, we present an extensive survey of those approaches regarding the determination of optimal development strategies in marginal tight sand reservoirs.

1.2.1 Integrated Reservoir Studies

Optimizing the development of low-permeability gas reservoirs is most accurately done by conducting a full-scale reservoir evaluation involving geological, geophysical, petrophysical and reservoir engineering analyses and interpretations. This

includes developing a geological model of the field, approximating distributions of static reservoir properties such as porosity and permeability, building and calibrating an accurate reservoir simulation model of the study area and utilizing it for the estimation and optimization of reservoir development. Although, the reliability and accuracy of this approach is quite high, it is not always favorable due its time-consuming and expensive nature.

Rushing and Newsham (2001) presented an integrated work-flow process model to describe and characterize unconventional gas reservoirs. They modified and expanded the Petrophysical Integration Process Model (PPIM) of Gunter et al. (1997a, 1997b). The modified four-stage process model utilizes and integrates data from multiple and seemingly independent data sources; however, the key link among all data sources is the petrophysical model. Moreover, each stage of the process model both complements and supports other stages.

Stage 1 is a geological assessment that defines large-scale architecture and geometry of the reservoir from interpretations of structural geology, depositional environment and stratigraphy to obtain an estimate of the reservoir volume potential at deposition. Based on lithology and sedimentary structure, lithofacies are derived from core data, meanwhile well logs are used to identify vertical distributions of lithologies.

Pore-scale characterization of the rock and fluid systems are carried out in Stage 2 based on the geologic framework context that was previously defined in Stage 1. For pore-scale characterization, petrographic observations on pore structure, texture, mineralogy and diagenesis are made. As a result of this characterization, rocks are categorized into several hydraulic rock types depending primarily on their unique porosity-permeability relationships and capillary pressure characteristics.

Stage 3 is fundamentally an integration of the previously defined geological framework (Stage 1) and rock types (Stage 2) with formation evaluation techniques. This helps define reservoir flow units, seals and baffles which control fluid distribution and flow in the reservoir. For prediction of the vertical distribution of hydraulic rock types

along with their properties at each depth increment, petrophysical models formed on the basis of geophysical well log data are used.

In Stage 4, the geological and petrophysical models obtained in Stages 1-3 are calibrated with various reservoir models. The objective of this stage is to develop three-dimensional wellbore and reservoir flow models which can be employed in predicting future well performance and optimizing field development.

Reservoir models are defined as multi-well flow models incorporating both large-scale geological elements and small scale rock properties. Such models are useful for a variety of reasons. First, they provide a venue for optimizing well spacing through the analysis of production performance. Second, reservoir models could be used to evaluate targeted versus blanket infill drilling development practices. Third, they could serve as a means to quantify reserve growth in current production scenarios. Typically, reservoir models are classified into two as, stochastic and deterministic models.

Reservoir models that are built on principles of statistics and probability are termed as stochastic models. Such models use distributions to provide information on geological structures and rock properties, along with estimates on corresponding uncertainties on these distributions. Stochastic models have a variety of applications including the capturing of large-scale geological elements and small-scale petrophysical properties, as well as incorporating all reservoir heterogeneities. Other applications could be listed as, quantification of probable sand continuity between wells and determining rock property anisotropies and their distributions between wells. Usually, a large number of grids with small dimensions are used in constructing reservoir models, so that the range and sensitivity of the model is suitable for capturing variations at all scales. It is important to note that, stochastic models incorporate only static properties.

Deterministic models divide the reservoir into discrete grids; assign rock and fluid properties to each grid, and model vertical and horizontal fluid flow through the system. Since deterministic models employ larger grid blocks due to computational restrictions, properties from the finer-grid stochastic model are upscaled before being used in the coarse-grid deterministic models. Wellbore models; well stimulation

efficiencies in terms of fracture height, length, orientation, and conductivity; and hydrocarbon pore volume in pressure communication with the wellbore are also incorporated to the model. Major elements of a deterministic study include history matching field production, predicting future performance based on existing operating strategies and evaluating alternative operating and development strategies.

History matching is an inverse process that adjusts wellbore and reservoir parameters based on the historical production data. Once the model performance is matched to the actual production profile, future performance can be predicted for both existing and alternative development strategies.

Optimizing the development of low-permeability gas reservoirs is most accurately done by conducting a full-scale reservoir evaluation. This includes geological, geophysical, petrophysical and reservoir engineering studies, analyses and interpretations. Some key points in reservoir evaluation include, the development of a geological model of the field, approximating distributions of static reservoir properties such as porosity and permeability, developing and adjusting an accurate reservoir simulation model of the study area and utilizing it for the estimation and optimization of reservoir development. Although, the reliability and accuracy of this approach is quite high, it is not always favorable due its time-consuming and expensive nature.

1.2.3 Moving Window Method

As an alternative to conducting full-scale reservoir evaluations for large, low-permeability gas reservoirs having large data sets, some researchers (Guan and McVay 2004; Guan et al. 2002; Hudson et al. 2000; Hudson et al. 2001; Kyte and Meehan 1996; McCain et al. 1993; Voneiff and Cipolla 1996) conducted statistical moving window techniques to model variable well performance.

Essentially, the moving window techniques perform a statistical analysis of production data using defined performance indicators which serve as proxies for reservoir properties, production response and reservoir pressure. Based on the comparison of performance indicators between new and old wells within areal windows

throughout the study area, judgments are made concerning interference between existing wells, areas of depletion and undrained acreage. These judgments are then used to optimize the location of infill wells for maximum recovery and drainage of the reservoir with the fewest number of wells.

The moving domain technology incorporates a multitude of local analyses in areal windows each of equal size. The size of the window depends on the average spacing between data locations and on the dimensions of the study area. However, a margin of at least a few wells should be set within each window for a reliable calculation of summary statistics. When the number of wells in a window is less than a threshold value, then a regional or global regression is employed rather than a local regression, lowering prediction accuracy.

The major advantages of the moving domain technology over the integrated reservoir studies are its speed and its reliance on simply well locations and production profiles, which makes it a preferable screening tool for large infill development projects.

McCain et al. (1993) first introduced a statistical technique to determine the appropriate well density in complex, low-permeability gas reservoirs. This method is noteworthy, as it describes an objective way of comparing well performance, indicating regions that should be subjected to advanced analysis, and describing the areal locations where specific conclusions can be made.

Importance is given on making a clear and thorough geological and petrophysical description, and judging the coherence of reservoir descriptions established via independent geological and reservoir engineering methods.

This statistical technique is performed by building and analyzing graphs of well performance vs. date of first production. Well performance was characterized by the following productivity indicators: the maximum monthly production rate, the average monthly production rate for the best 12 consecutive months and the monthly production rate at the time a specific cumulative production was reached.

McCain et al. (1993) divided the entire field into equal sized study units. Each study unit included 10 to 20 wells. The three performance indicators of each study unit

were then plotted against the date of first production and a least-squares straight line was fitted to each of the data sets. Slope of the line fitted to the well performance data could serve as an indicator for interference between wells. More explicitly, a negative slope is interpreted as a sign of depletion at infill well locations due to overlapping well drainage areas, whereas a slope of zero indicates identically performing wells. Evaluating slopes of the least-squares lines on the performance indicator plots, areas of depleted infill locations were determined.

Voneiff and Cipolla (1996) improved the statistical method used by McCain et al. (1993) in their study on the Ozona field and named it "moving domain" technology. Basically, this technology appraises location and performance of existing wells to find evidence of depletion and to determine the optimal well spacing.

The moving domain technology described by Voneiff and Cipolla can be applied in two phases. The first phase is a scoping study provides the preliminary infill estimates, areas of depletion, and areas required for detailed conventional engineering. The second phase involves a more detailed engineering evaluation to calculate drainage areas, undrained acreage, recovery per acre, and infill reserves.

Guan et al. (2002) used a model-based analysis in each window. The model is based on a combination of the material-balance equation and the pseudosteady state flow equation, defined as,

$$\ln q = \ln(kh) + C_1 + \ln\left(p_i - p_{wf} - C_2 \frac{G_p}{A} \right) - \ln\left(\ln(\sqrt{A}) + C_3\right)$$

where

$$C_1 = -\ln(141.2\mu B)$$

$$C_2 = 0.00742 \frac{\pi B}{c_t h \phi}$$

$$C_3 = 0.40428 + s + 0.5\ln\left(C_A {r_w}^2\right)$$

In generalized form,

$$y = a_0 + a_1 x_1 + a_2 x_2 + a_3 x_3$$

where

a_0, a_1, a_2 and a_3 are the regression coefficients that are assumed to be constant for a moving window.

$$y = \ln q$$

$$x_1 = \ln(kh)$$

$$x_2 = \ln\left(\frac{G_p}{A}\right)$$

$$x_3 = \ln\left(\ln(\sqrt{A})\right)$$

In this model, production rate (q), permeability-thickness product or reservoir quality (kh) and drainage area (A) are substituted by best year (BY), virgin best year (VBY) and well spacing, respectively. The moving window technology is based on this 4D regression model that correlates BY vs. VBY, cumulative withdrawal per acre and well spacing.

BY is simply the arithmetic average of the best 12 consecutive months of production, which often correlates well with long-term production. VBY is the BY of a well at virgin conditions and is determined by performing a 2D regression of BY vs. time. Well spacing is the area of voronoi polygon around each well based on x/y well locations.

The first step of the moving window technology is performing the 2D regression of BY vs. time to determine the VBY used in the subsequent 4D regression. The next step is regressing BY on VBY, cumulative withdrawal per acre and well spacing of wells within each window to determine the corresponding regression coefficients. Once the 4D regression equation is established for each window, performance of a candidate infill well in that window can be estimated.

Guan et al. (2002) provided a systematic assessment of the validity and accuracy of moving window technology in determining the optimum infill drilling strategy of low-permeability gas reservoirs. Performing a reservoir simulation study on an area of 100 producing wells from a field in Canada, they generated synthetic production data sets to be analyzed in the moving window technique. To examine the impact of

heterogeneity on prediction accuracy of this model-based statistical approach, they built 4 reservoir models with different degrees of heterogeneity but the same average permeability, 0.2 md. All the remaining parameters were kept the same for all cases.

To quantify the accuracy of moving window technology in assessment of VBY, which serves as a proxy for kh in the 4D regression model, Guan et al. made a separate simulation run for each existing well in which they produced only that well for one year. Comparison of the VBY from the 2D regression to the VBY determined from simulation indicated that increased heterogeneity reduces the estimation accuracy. Accordingly, the best correlation was observed in the homogeneous reservoir model.

The next step was to determine the accuracy of moving window technology in predicting the infill well performance. This was achieved by placing in each grid block a new well that is produced for one year following the end of the performance history and generating the distribution of incremental production attributed to a new well at any possible location in the area. To convert the simulation-based infill well performance estimates from cell to well basis, a surrounding region on the simulation grid was attributed to each well. A well's region comprises all simulation cells closer to that well than to any other well. The arithmetic average of new well 1-year cumulative production, i.e. the infill BY, was then computed for each region and compared to the BY derived from the 4D regression model.

Comparison of infill BY from the moving window technology and reservoir simulation for different degrees of reservoir heterogeneity indicated that although estimates of infill well performance are mostly erroneous in individual well basis, the moving window technology predicts the average infill well performance well. Another conclusion that was reached from this analysis was that the moving window technology looses its effectiveness as the reservoir heterogeneity increases. The technique employed by Guan et al. (2002) is based on three assumptions:

The first assumption is that reservoir properties do not vary considerably within any moving window throughout the study area. As mentioned before, the reservoir model employed in this technique is established on a combination of the material

balance and pseudo-steady state flow equations, simplified by assuming that the reservoir is homogeneous within an individual moving window. The result is a 4D linear regression equation applied within each window. The second assumption is that completion and production techniques applied to each well are identical, regardless of when the well was drilled and completed.

Another assumption of the moving window technique is that at least a few wells in each part of the study area have reached the boundary-dominated flow, which may take several years of production for a tight gas well. This is required to compute drainage area and recovery per acre.

The analysis of moving domain technique in its entirety reveals three limitations of this method based on the three assumptions above.

While the first assumption is reasonable for most reservoirs, there also exist reservoirs that have rapid and dramatic change in their properties within a small area. For instance, some labyrinth-type reservoirs are comprised of narrow channel-fill bodies and substantial changes in rock properties may occur between sand units in jigsaw-puzzle reservoirs. In such cases, the estimations obtained by the use of moving domain technology may have errors and may not be reliable.

Another limitation of moving domain technology is that, in case the performance of the new wells are worse than prior ones, there is no clear indication of whether depletion or variation in rock properties have led to poor well performance. Moreover, various changes in completion and production technology over time could also suppress the effect of depletion.

The last limitation of this technique is the requirement that a certain number of wells exist in each part of the field, and that they display adequate production history to experience boundary-dominated flow. This condition is necessary for accurate calculation of the drainage area and recovery per acre. However, typically some low-permeability reservoirs require between 9 to 14 years to reach boundary-dominated flow. Therefore, moving window technology may not be applicable for some gas fields that have only short production profiles less than 10 years.

Despite these assumptions and limitations, this moving domain technique has been applied to the Ozona (Canyon) gas sands (Voneiff and Cipolla 1996), Milk River formation in Canada (Hudson et al. 2000), Cotton Valley in East Texas (Hudson et al. 2001; McCain et al. 1993), Mesaverde formation in the San Juan Basin (Hudson et al. 2001), and the Morrow formation in the Permian Basin (Hudson et al. 2001) to quantify infill potential.

1.2.4 Simulation-based Regression

To improve upon moving window methods, some authors (Cheng et al. 2006a; Cheng et al. 2006b; Cheng et al. 2008; Gao and McVay 2004) suggested combining conventional reservoir simulation with automated methods for assessment of infill potential in tight gas basins. Reservoir simulation inversion techniques aims to combine the greater accuracy of simulation-based methods with the short analysis times and low costs associated with statistical methods.

The simulation-based inversion technology developed by Gao and McVay (2004) differs from typical simulation inversion applications in that, rather than focusing on small-scale, high-resolution problems; it focuses on large-scale, coarse-resolution studies consisting of thousands of wells. This technique consists of two major components: forward modeling and inverse modeling.

The forward model used to calculate reservoir and well performance is a conventional 2D, single-phase, finite-difference gas reservoir simulator. This forward model is based on GasSim, a single-phase simulator for modeling real-gas flow in gas reservoirs. The main equations used in this simulator are,

(1) Real gas pseudo-pressure

$$p_p = 2\int_0^p \frac{p}{z\mu} dp$$

(2) 2D flow equation

$$-a_N p_{pi,j-1}^{n+1} - a_W p_{pi-1,j}^{n+1} + a_C p_{pi,j}^{n+1} - a_E p_{pi+1,j}^{n+1} - a_S p_{pi,j+1}^{n+1} = d$$

where

$$a_C = a_N + a_W + a_E + a_S + \alpha$$

$$d = \alpha . p_{pi,j}^{n} - q$$

$$\alpha = \frac{1}{\Delta t}\left(\frac{T_{sc}}{p_{sc}T}\right)\frac{\left(\frac{V_p p}{z}\right)_i^{n+1} - \left(\frac{V_p p}{z}\right)_i^{n}}{p_{pi}^{n+1} - p_{pi}^{n}}$$

(3) PI equation

$$q = J'\left(p_{pi,j}^{n+1} - p_{pwf}\right)$$

where

$$J' = \frac{0.01988khT_{sc}}{p_{sc}T\left(\ln\frac{r_o}{r_w} + s\right)}$$

The reservoir simulator calculates individual well and field-wide production responses based on input static geologic model and other available reservoir data. However, since the initial geologic model is derived from static data only, it should be adjusted to the dynamic response of the reservoir through history matching.

Inverse modeling consists of an automatic history matching process that continuously adjusts reservoir properties until the best fit of calculated response to historical production data is achieved. The inversion of performance history is accomplished by sensitivity coefficient based algorithms, which requires the calculation of partial derivatives of production response variables with respect to reservoir parameters.

Gao and McVay (2004) employed the modified generalized pulse-spectrum technique (MGPST) for sensitivity calculation. Since the sensitivity coefficients obtained by partially differentiating the 2D flow equation with respect to gridblock permeability, they can be calculated internally by the simulator during a forward model run. Usually, sensitivity coefficients are calculated based on only those gridblocks with wells on production. This is mainly because of the availability of production data for

history matching being limited to gridblocks with wells and at time steps after wells start producing.

The procedure of simulation-based inversion is briefly described as follows: (1) run the forward model and calculate the sensitivity coefficients of production response; (2) perform inverse modeling to estimate the change in permeability required to honor production data and, update the permeability field correspondingly; and (3) assess infill drilling potential using forward modeling with the inverted permeability field.

Cheng et al. (2006a, 2006b, 2008) advanced the simulation-based regression approach by implementing a sequential inversion of both reservoir permeability and pore volume distributions. Adding pore volume to the regression enhances the quality of the history match, improves the resolution of reservoir characterization and lays a foundation for reliable prediction of future performance and assessment of infill drilling potential.

The sequential inversion of and infill assessment procedure is summarized briefly as follows: (1) run the forward model and compute the sensitivity coefficients of production response with respect to permeability; (2) perform inverse modeling to estimate the change in permeability required to honor production data and, update the permeability field accordingly; (3) run the forward model with the calibrated permeability field and determine the sensitivity coefficients of production response with respect to pore volume; (4) perform inverse modeling to estimate the change in pore volume required to honor production data and, update the pore volume field accordingly; (5) attempt to reach convergence between inversion on permeability and pore volume; (6) run several iterations until convergence between inversion on permeability and pore volume is reached and; (7) assess infill drilling potential using forward modeling with the inverted permeability and pore volume fields.

Later on, Cheng et al. (2006a, 2006b) improved this inversion algorithm by calculating porosity from the permeability-porosity correlation after the permeability field is calibrated and, then using the updated porosity field in the inversion of pore volume.

1.2.5 Limitations of Existing Methods

Among the existing methods, full-scale reservoir evaluation is the most accurate way to optimize development of unconventional gas reservoirs, but it is not routinely employed by small- to medium-sized operators given its time-consuming and expensive nature. On the other hand, while statistical moving-window and simulation-based regression techniques can provide rapid and cost-effective solutions, they employ deterministic principles and produce only a single representation of the reservoir. Hence, they do not account for uncertainties inherent in highly heterogeneous, complex reservoirs and quantify the risk involved in development decisions. Also, deterministic methods cannot model interdependencies present in tight gas reservoirs. Therefore, to model the production uncertainty and capture the impact of dependencies between parameters, a suitable approach would be to integrate stochastic and deterministic methods.

Given the considerable amount of uncertainty associated with unconventional resources, practical and flexible decision models are also needed to evaluate multiple development scenarios and hence, to assess the full spectrum of potential economic outcomes. Such models provide operators strategic insights for making profitable investment decisions in the face of significant risk.

Therefore, it is necessary to establish new methods which would allow assessment of optimal well spacing in a timely manner and also effectively manage uncertainties to achieve feasible development of unconventional reservoirs.

1.3 Objectives

The long-term objective of the overall project of which I am a part is to develop practical reservoir and decision modeling tools to help operators determine the optimal well spacing in highly uncertain and risky unconventional gas reservoirs as early in the reservoir life as possible. The technology and tools developed will be applied in UGR's tight gas assets in the Berland River area, Alberta.

The specific objective of this research work is to develop a fast, approximate, probabilistic reservoir model that assesses uncertainty in key reservoir parameters and allows prediction of production profiles as function of well spacing. Use of a probabilistic model will also provide a venue for modeling dependencies between parameters such as porosity, permeability and net pay. The reservoir model needs to be fast since it will be combined with a decision model and run thousands of times.

1.4 Organization of Thesis

This research focuses on the development and calibration of a probabilistic reservoir model for UGR's tight gas assets in Berland River area. Integration of this reservoir model with a Bayesian decision model will provide the basis for determining optimal well spacing for the area. The thesis is organized as follows:

Chapter I presents an overview of the problem, provides a review of literature on the subject and states the project goals. Chapter II gives a brief review of the general geology, depositional environments and stratigraphy of the Berland River area and the Gething Formation. Chapter III reports the tools and applications used in the construction of the probabilistic reservoir model, describes the reservoir simulation and Monte Carlo techniques that were employed, and explains different reservoir models established on different decision contexts. Chapter IV discusses the variogram analysis conducted to determine correlation coefficients between pairs of well porosities, net pay thicknesses and permeabilities, which were then incorporated into the reservoir model. Chapter V discusses the decline curve analysis performed on the simulated production profiles to facilitate the integration of the reservoir and decision models. Chapter VI briefly describes the decision model and presents the preliminary results. Chapter VII presents the conclusions, discusses the limitations of the study, and provides recommendations for future work.

CHAPTER II
GETHING RESERVOIR

The technology and tools developed in this project will be used to determine optimal well spacing strategies for Deep Basin tight gas sands in the Berland River area, Alberta. Unconventional Gas Resources Canada Operating, Inc. (UGR) is an active operator in the area, and is our industry collaborator.

In this chapter, a brief review of the general geology, depositional environments and stratigraphy of the study area are presented.

2.1 Background

The Berland River area is located on the edge of the Deep Basin of Western Alberta, Canada. Discovered in 1976, the Deep Basin of Alberta is considered as one of North America's giant gas fields with recoverable gas reserves ranging between 50 to 150 Tcf (Masters, 1979).

Fig. 1 shows the approximate location of the Berland River area. As with most tight gas fields, success depends upon identifying areas of good porosity and permeability, so-called sweetspots which are usually associated with coarse-grained sandstones and conglomerates (Smith et al. 1984).

The study area encompasses approximately 236 km^2 (58,240 acres and 91 sections) and includes about 120 wells. **Fig. 2** displays the Berland River base map in which regions outlined in blue show the sections where most of UGR's wells are located.

Fig. 3 depicts the stratigraphic view of the Berland River area. The various depositional environments are: 1) Cadomin - alluvial fan and plain, 2) Gething - fluvial deposits and flood plain, 3) Bluesky - shoreface sand and shales (Smith et al. 1984). The formation of interest in this study is the Gething.

Fig. 1—Location map showing the position of the study area relative to the Deep Basin of Alberta (Smith et al. 1984).

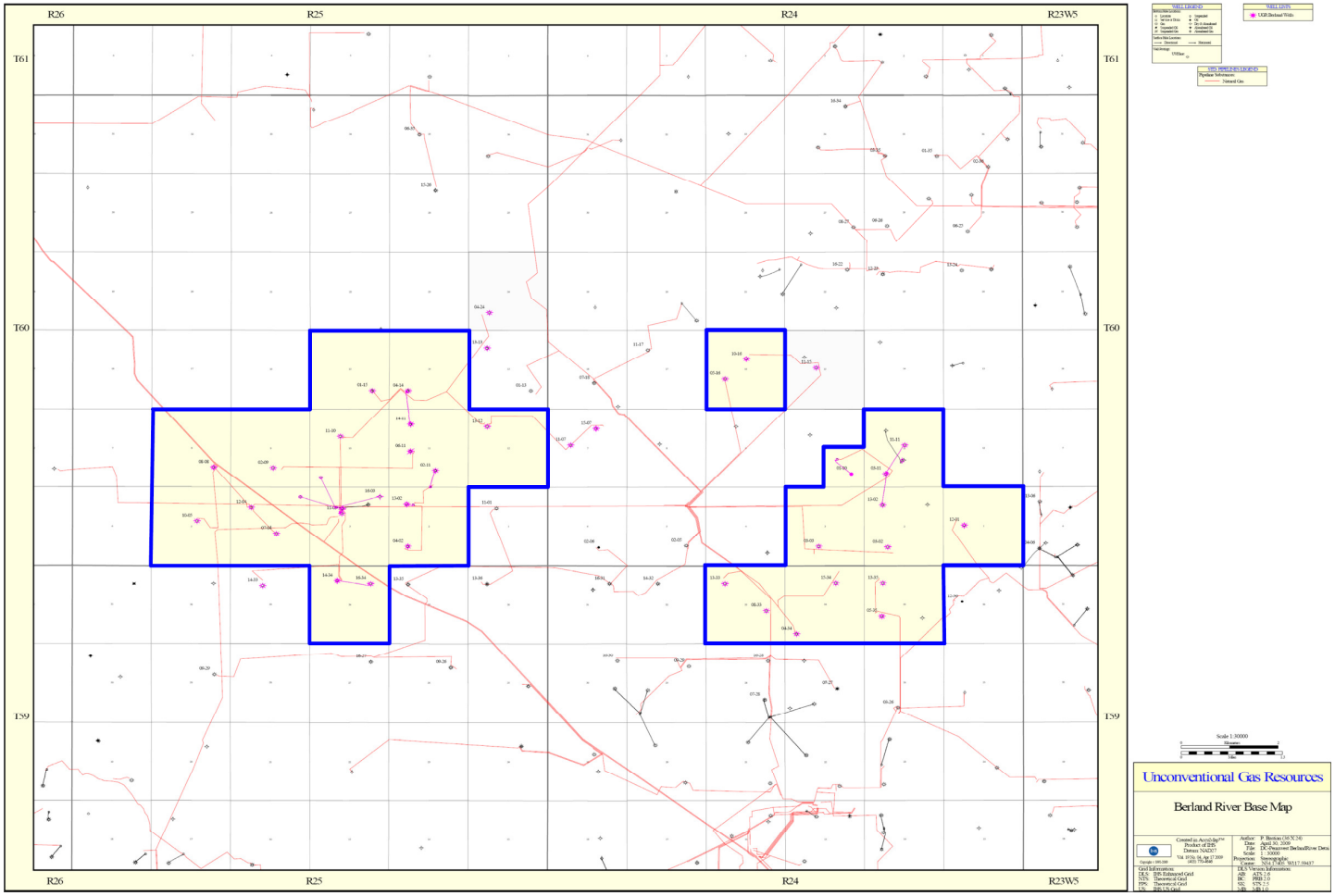

Fig. 2— Berland River base map. Regions enclosed in blue show the sections where UGR's wells are located (provided by UGR).

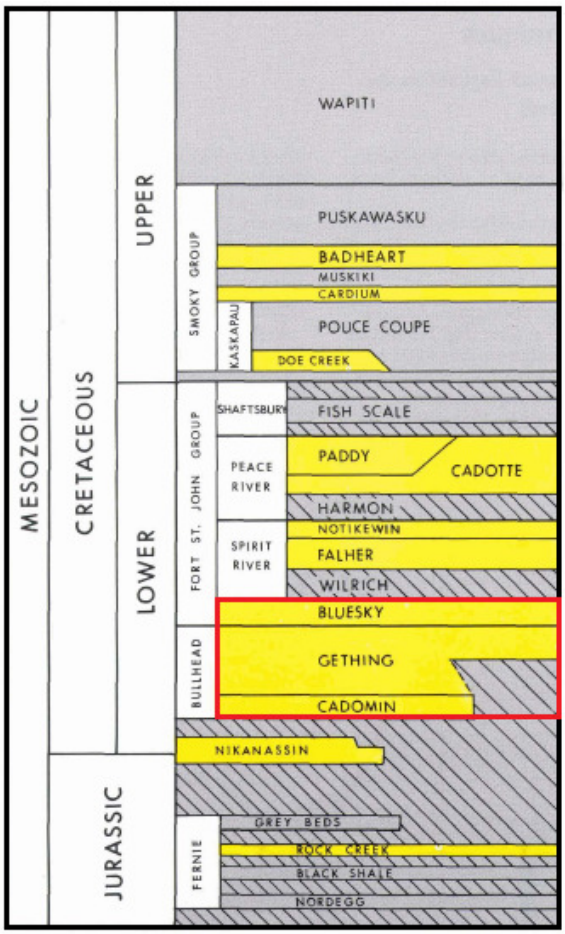

Fig. 3—Stratigraphic column of the Lower Cretaceous (Smith et al. 1984).

2.2 Gething Formation

The Gething formation consists primarily of interbedded fine- to medium-grained sandstones, siltstones, mudstones and coal sediments **(Fig. 4).** The sequence is terrestrial and is described as a low relief interior drainage plain on the eastern flank of the Cordillera.

Sandstones are fining upward or thin-bedded. Trough and planar cross-bedded, ripple-bedded and parallel-laminated sandstones are common. Plant material including fossil leaves, stems, logs, stumps, and other carbonaceous debris are also present.

Coalbeds exist throughout the Gething, and dinosaur foot prints have been discovered in Peace River.

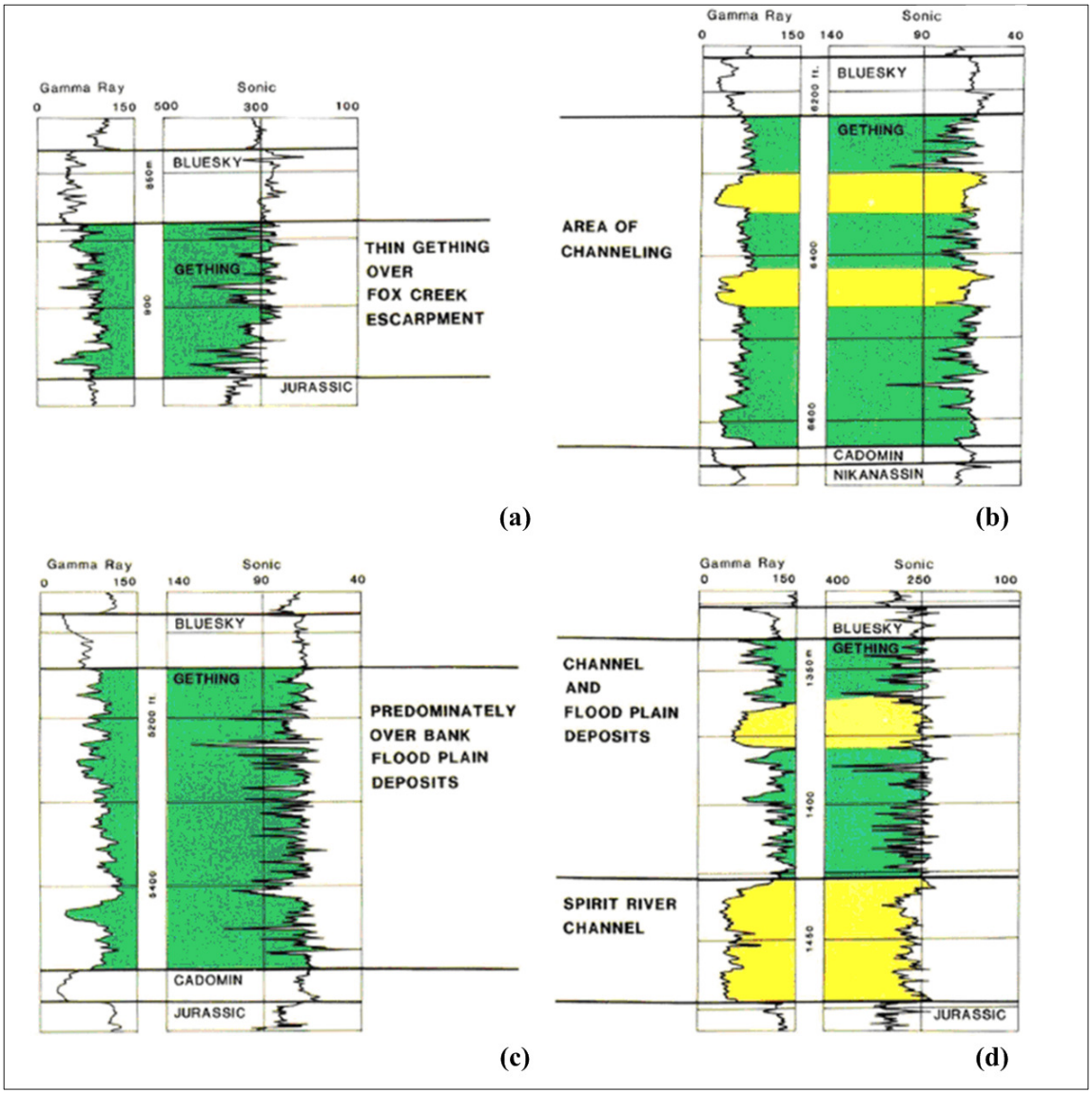

Fig. 4—Type logs of the various facies of the Gething Formation (Smith et al. 1984).

The representative drainage pattern of the Gething sandstones is an active channel system that trended northeast at the time of deposition. With the burial of the

Fox Creek Escarpment by Gething sediments, there remained no local constraint on drainage which resulted in eastward expansion of the drainage plain. The physiography of this larger drainage system was a low-lying swampy plain with numerous shallow lakes and the area was heavily forested with conifers, cycads, and ferns. No evidence of marine sedimentation was observed in the study area although the coastline was not far away (Smith et al. 1984).

CHAPTER III
PROBABILISTIC RESERVOIR MODEL

The core of the technology developed in this work is a reservoir model that involves explicit modeling of subsurface uncertainty and an advanced decision model that fully incorporates uncertainty to optimally manage risk **(Fig. 5).**

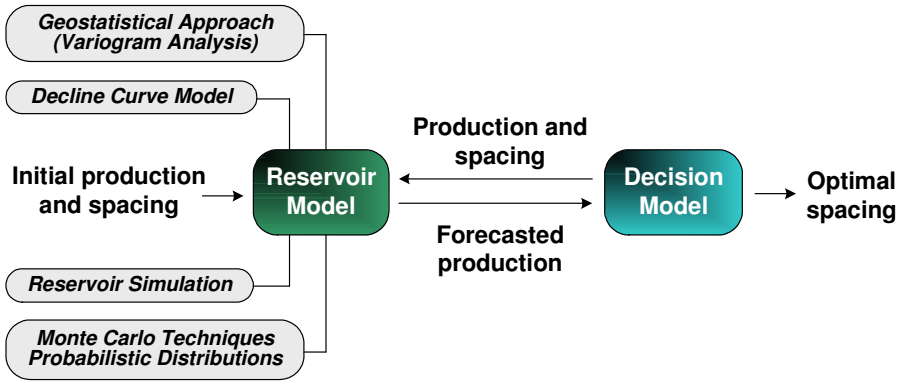

Fig. 5 — Schematic illustration of the integrated reservoir and decision modeling tools

The reservoir model uses (1) reservoir simulation techniques and (2) conventional Monte Carlo methods to predict production profiles with a wide variety of reservoir properties and under different development scenarios; (3) geostatistical techniques to model dependencies in production response among wells and; (4) decline curve analysis to specify the decline parameters that best capture production profiles. To integrate all the different techniques used in constructing the reservoir model and automate the performing of thousands of simulations, a VBA code was developed. In this way, the reservoir model can provide a full spectrum of production profiles under different downspacing scenarios.

Once the reservoir model is established, it serves as a basis to construct a practical decision model. The decline parameters obtained from the decline curve model

will be inputs for the decision model which will yield estimates of the expected net profit under different scenarios. Hence, the model will allow operators to select the optimal development strategy with the objective of maximizing profitability.

In this project, two probabilistic reservoir models that allow for two development stages (a primary development stage followed by one stage of downspacing) were built for the modeling studies of UGR's tight gas assets in the Berland (Gething) reservoir. The first reservoir model is based on UGR's specific development strategy in the Berland River area. The second model follows a more general approach based on simulating a variety of downspacing combinations to evaluate different development scenarios.

In this chapter first the tools and applications used in the construction of the probabilistic reservoir model are reported. Then, the reservoir simulation and Monte Carlo techniques employed in the model are described and the input variables are presented. Finally, the two different models established on different decision contexts are discussed in detail.

3.1 Monte Carlo Probabilistic Approach

Most tight gas reservoirs are characterized by complex geological, geophysical and petrophysical properties and a high level of heterogeneity and hence, involve considerable uncertainty. Because of the large number of unknowns, a merely deterministic approach remains inadequate to quantify the range of variability in outcomes such as cumulative gas production or net present value and, therefore, to assess the risk associated with future performance predictions. Consequently, to model production uncertainties and quantify the risk involved in the development decisions, a suitable approach would be to integrate stochastic and deterministic methods.

To address these issues, a stochastic modeling tool, @Risk from Palisade Group is coupled to CMG's full featured simulator, IMEX from Computer Modeling Group so that thousands of simulations can be run to evaluate combinations of unknown parameters within their ranges of uncertainty.

A single-well, one-layer, single-phase reservoir model was built for the modeling studies of Berland River (Gething) reservoir. The reservoir simulator was formulated for the analysis of hydraulically fractured gas wells.

The Gething reservoir is a commingled, stratified multilayer system. In other words, there is no formation crossflow and vertical permeabilities of all layers are assumed to be zero. The flow capacity of such a system would be equal to the arithmetic sum of the flow capacities of all layers. Therefore, summing all the reservoir layers and representing them by a single simulation model layer will be a reasonable assumption.

A VBA code was generated in Excel to perform thousands of simulations automatically. An example input file to be run in IMEX was created and uncertain parameters were defined by @Risk distribution functions. **Fig. 6** is a block diagram representation of the applications and tools used in the construction of the Gething reservoir model.

The uncertain parameters and their associated distributions involved in modeling of Berland River (Gething) reservoir are presented in **Table 1.** The histograms and the corresponding probability distribution functions of these uncertain input variables obtained from a simulation of one thousand iterations are illustrated in **Fig. 7.**

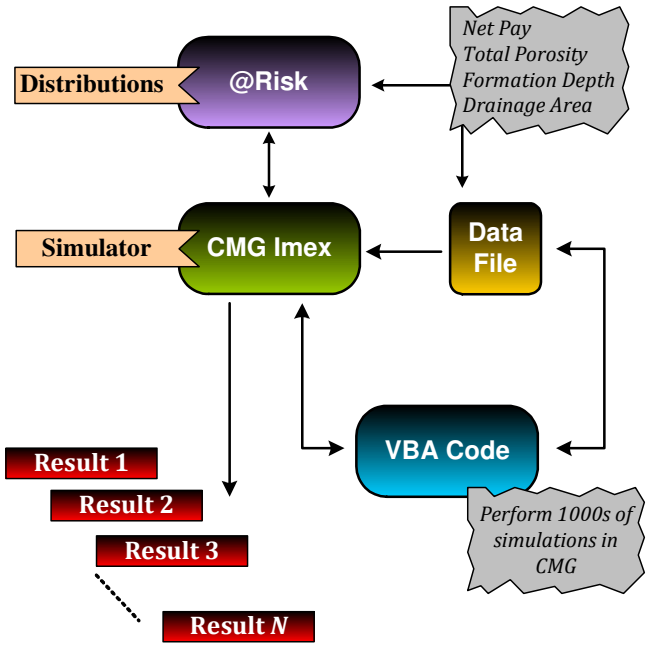

Fig. 6— Block diagram representation of the applications and tools used in this study.

Table 1— Uncertain input variables involved in the modeling of Berland River (Gething) reservoir (data from UGR).

	Units	Distribution Type	Minimum	Maximum	Mean	Most Likely	Std dev.	Shift
Net Pay	m	Log-normal	0.4	15	6.5	-	4.45	0.6
Total Porosity	%	Normal	6	14	10.2	-	1.4	-
Formation Depth	m	Normal	2600	3100	2780	-	91	-
Drainage Area	acre	Triangular	40	640	-	160	-	-

In addition to the parameters defined in Table 1, the average reservoir pressure is also uncertain since it is computed in the model by multiplying a constant pressure gradient with the formation depth which itself is an uncertain variable defined with a normal distribution.

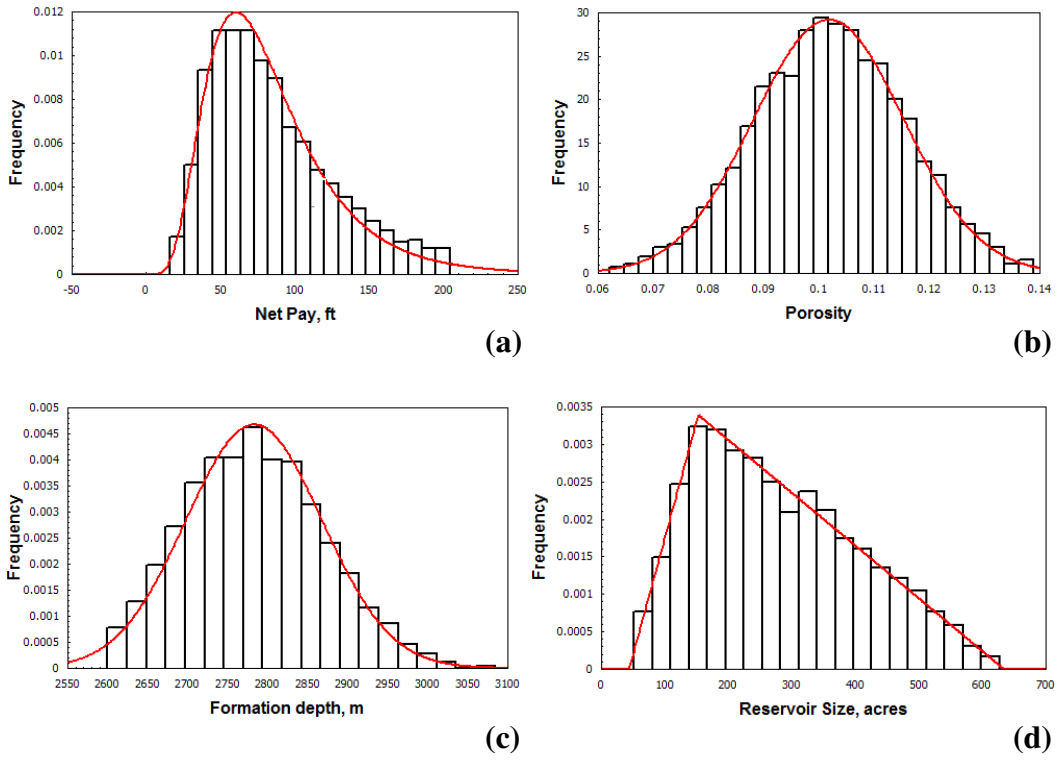

Fig. 7— Histograms and probability distribution functions of uncertain input variables used in the modeling of Berland River area: (a) Net pay, (b) Porosity, (c) Formation depth, (d) Reservoir size.

The permeability model is based on a porosity-permeability relationship assumed to honor the heterogeneity and core data from the field. The correlation is given by,

$$k_{gas}(md) = 0.0071 * \exp(47.517 * \text{Gas Porosity})$$

A scalar factor of 1.92 was added to this correlation to calibrate the simulation model to the well performance data. Applying the scalar factor and rearranging,

$$k_{gas}(md) = 1.92 * \exp(47.517 * \text{Gas Porosity} + \ln 0.0071)$$

Uncertainty is incorporated into the permeability model as well, by assigning a normal distribution to the porosity-permeability correlation defined above. The expression inside the exponential function is assigned as the mean of this normal

distribution and a standard deviation of 0.55 is used (data from UGR). As expected, the generated synthetic permeability data set shows a log-normal distribution **(Fig. 8).**

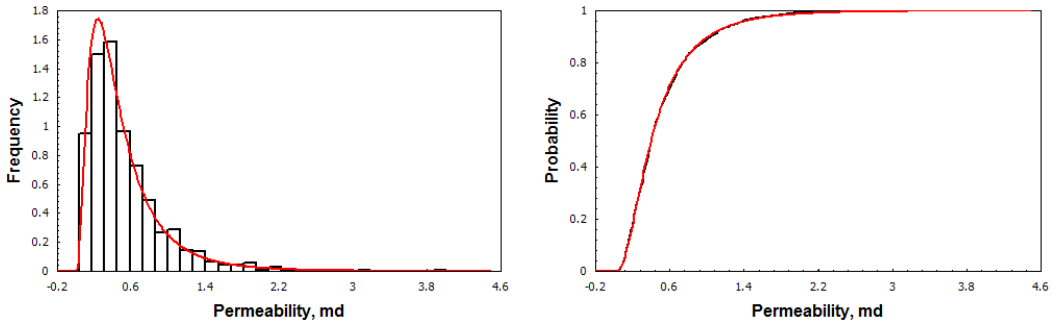

(a) **(b)**

Fig. 8— (a) Probability distribution plot (PDF), (b) cumulative distribution plot (CDF) of permeability.

Fig. 9 shows the permeability cloud which was obtained from a simulation of one thousand iterations based on the described porosity-permeability correlation. The red line is the regression line computed deterministically at 6% and 12% gas porosity. The permeability-porosity cloud is represented by the black dots, and the trendline shows the least-squares regression through the cloud data. The overlapping regression lines indicate an excellent match between deterministic and probabilistic models.

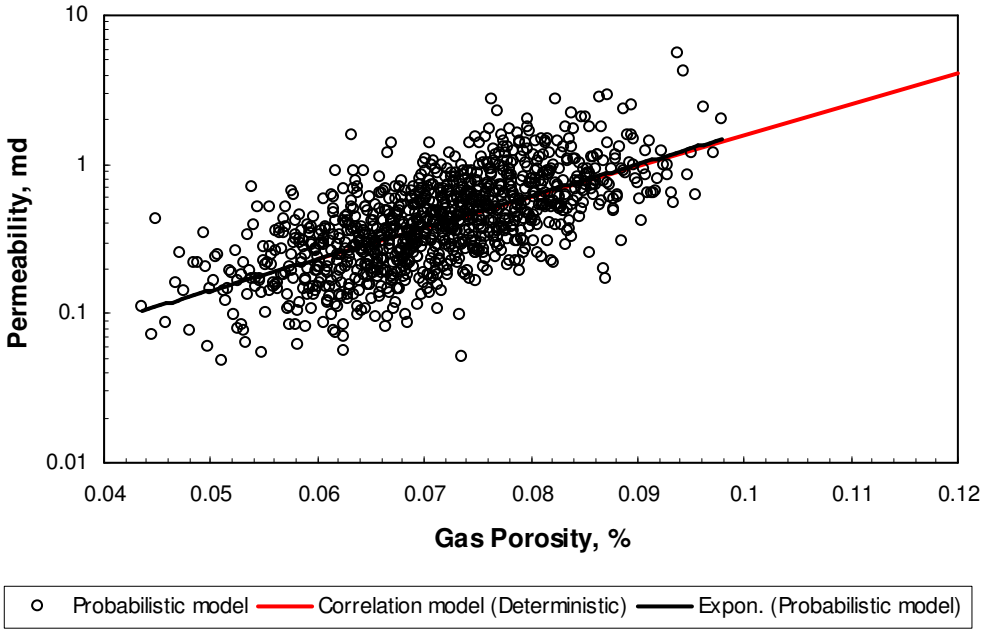

Fig. 9—Porosity-permeability cloud.

Reservoirs that originate in non-marine, channel (fluvial) environments such as the Berland River (Gething) reservoir are often characterized by laterally discontinuous sand bodies. The fluvial channel geometry is generally defined by its width/thickness (aspect) ratio. An aspect ratio of 7 was used in the modeling of the Berland River (Gething) reservoir.

The reservoir model depicts a quarter of the section; however, during simulation the thickness is multiplied by four and extended to cover the entire section. Representative gridblocks in one quarter of the model are drawn (**Fig. 10**) to show the positions of the gridblocks' centroids (centroid X and centroid Y) with respect to the well location, as well as the aspect ratio of the gridblocks. The model includes a hydraulic fracture near the wellbore, along the x-axis. To accurately model gas flow in the hydraulically fractured well, the hydraulic fracture is explicitly modeled by refined grids along the fracture and around the wellbore (Fig. 10).

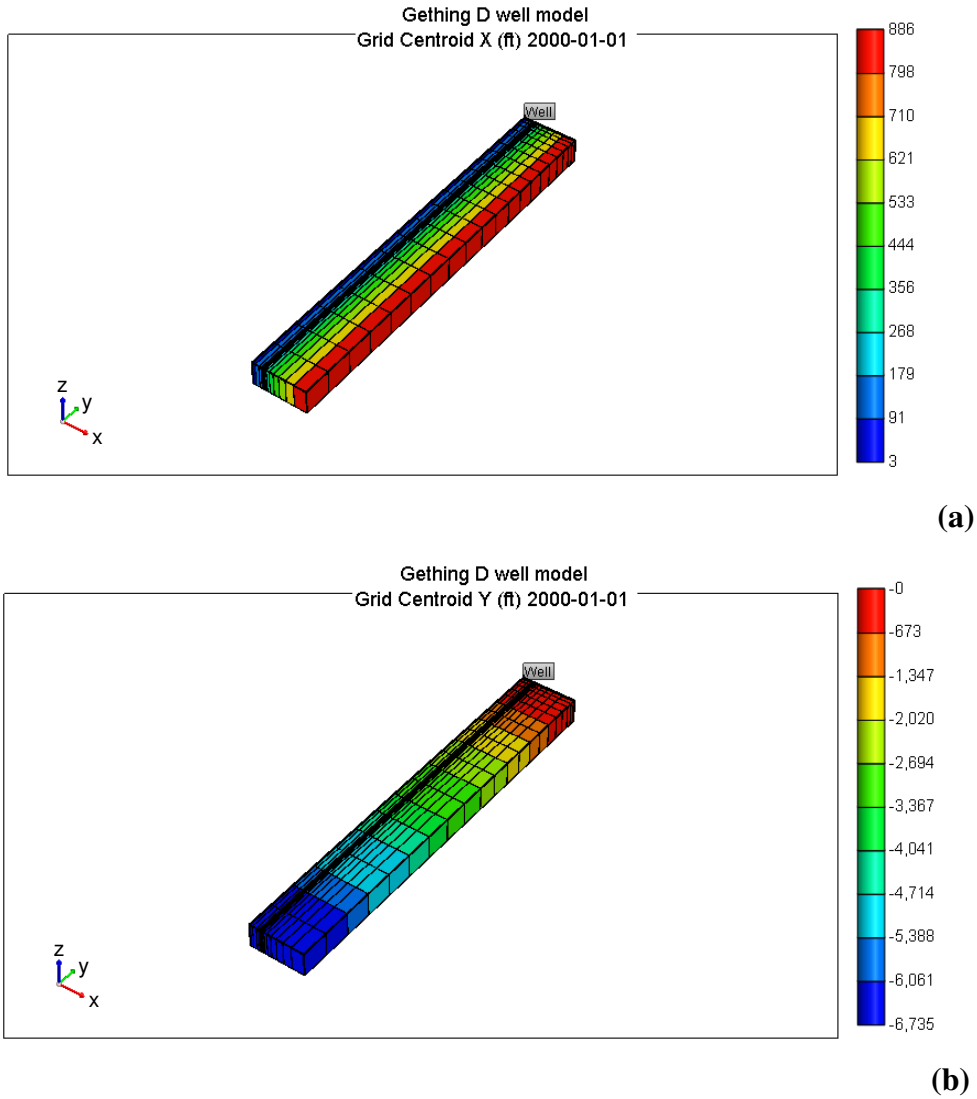

Fig. 10—Gridblocks model based on an aspect ratio of 7: (a) Grid Centroid X, (b) Grid Centroid Y.

Other input parameters in the Berland River reservoir model are as follows; initial pore pressure gradient (0.28 psi/ft), water saturation (30%), reservoir temperature (90°C) and gas gravity (0.71). The hydraulic fracture has a length of 200 ft and an approximate width of 0.04 ft. The dimensionless fracture conductivity (F_{cD}) used in the model is 1.3 (**Table 2**).

The fracture permeability is computed as,

$$k_f\,(md) = \frac{F_{cD} * L_f * k}{w}$$

However, observing that an F_{cD} of 1.3 resulted in extremely high fracture conductivities for the higher permeability wells, wk_f was limited to a maximum value of 150 md-ft, which means that the fracture permeability, k_f cannot exceed 3750 md.

Table 2— Input parameters employed in the Berland River reservoir model (data from UGR).

	Units	Value
Pressure Gradient	psi/ft	0.28
Reservoir Temperature	°C	90
Aspect Ratio	-	7
Gas Gravity		0.71
Water Saturation	%	30
Fracture Length	ft	200
Fracture Width	ft	0.04
Dimensionless Fracture Conductivity	-	1.3

3.2 Reservoir Models for Different Decision Contexts

3.2.1 First Reservoir Model

The first reservoir model was established on UGR's specific development decision for the Berland River (Gething) reservoir. In our discussions, UGR stated their interest in developing some specific sections in the left region that is enclosed in blue in the base map (Fig. 2). The intention was to drill one well in those sections and then decide on whether to downspace or not, based on the first stage production results. UGR considered the drilling of up to 3 additional wells in the second stage.

The information provided by UGR and the base map of the Berland River area (Fig. 2) suggests that the study area is mainly developed on 320-acre spacing. Considering that there are already two wells in almost each section of the field, the reservoir model is built under the assumption that up to four more wells will be drilled in

a section. Among these, two will be in the same section as the existing wells, whereas the other two will be placed in neighboring sections **(Fig. 11).**

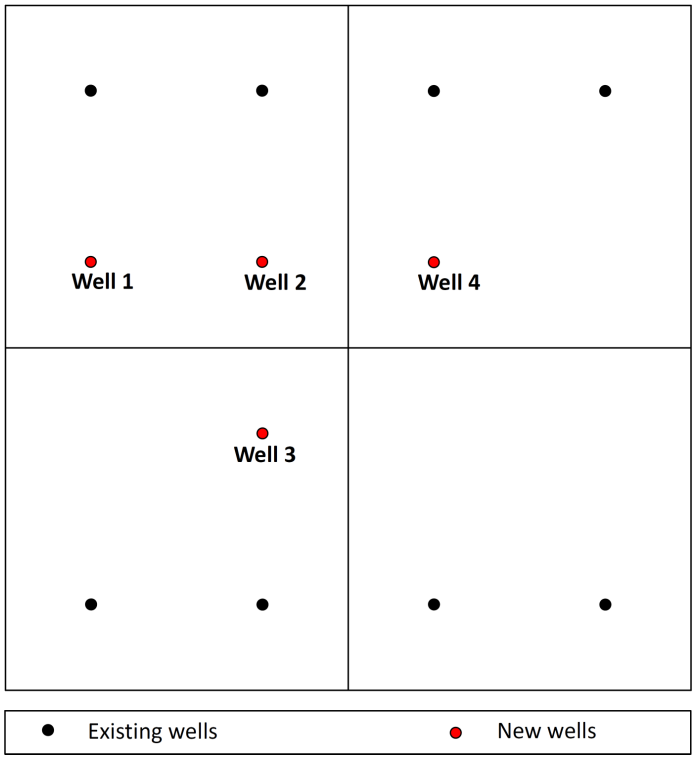

Fig. 11— Schematic illustration showing possible existing and new well locations.

The development decision modeled for the Gething reservoir is established on a two-stage downspacing with stage length of 1 year. In the first stage, a single well will be drilled in a section, which will increase the number of wells to three and reduce the well spacing to 213 acres in this section. As for the second stage, either no wells or up to three additional wells may be drilled. The first option is to continue production from existing wells, without including additional wells. The second option is to drill one new well, which marks the fourth well in that particular section, hence decreasing the well

spacing down to 160 acres. The third option is to drill two wells, one of them being in the section under consideration (fourth well in this particular section) and the other one in a neighboring section (third well in the neigboring section). The fourth option is similar to the third option except that one more well is drilled in another neighboring section (one well on 160 acre-spacing in the particular section, and two wells on 213 acre-spacing in two different neighboring sections).

The average reservoir pressure is computed in the model using a pressure gradient of 0.2 psi/ft which was reported in a reservoir characterization study of the Berland River area conducted by Schlumberger Data and Consulting Services, College Station, TX. This average reservoir pressure is designated as the initial pressure of the first stage. Since drainage interference is assumed to exist only within the same section, i.e., the section boundaries are assumed to be no-flow boundaries, the final pressure of the first well (Stage 1) is assigned as the initial pressure of the second well (Stage 2) while the reservoir pressure is assumed to be the initial pressure of the third and fourth wells (Stage 2).

Simulation results quantify best-month gas production, stage-end average pressure, stage-end gas production and the discounted cumulative production for each well. Table 3 display example simulation results of the first reservoir model for Option 1 where one well is drilled in Stage 1 and no additional wells are drilled in Stage 2.

Use of a reservoir simulation model with Monte Carlo techniques provided production estimations in forms of probabilistic distributions. **Fig. 12** depicts the probability distribution plot of the discounted cumulative gas production of Well 1 on 210 acre-spacing (Stage 1) which showed a log-normal distribution with a median of 497.5 MMscf. Probability distribution plots of other production data sets are presented in Appendix A.

Crossplots of Stage 1 vs. Stage 2 gas productions were generated to provide insights on dependencies between primary and secondary development plans. **Fig. 13** shows the crossplot of Stage 1 and Stage 2 gas productions for Option 2 where one well is producing in Stage 1 (Well 1) and one additional well (Well 2) is drilled in Stage 2. Remaining crossplots are included in Appendix B.

The statistics (mean and standard deviation) of each production data set and the pairwise correlation coefficients between Stage 1 and Stage 2 productions are displayed in **Table 4**.

The model described in this section was based on UGR's specific development decision, and is important in showing the capability of our technology in adjusting to different decision contexts.

Table 3— Example simulation results of the first reservoir model for Option 1 (One well is drilled in Stage 1 and no additional wells are drilled in Stage 2).

Run #	Stage 1, Well 1 (210 acres)					Stage 2, Well 1 (210 acres)				
	Initial Pressure (psi)	1st Month Gas Prod (MMscf)	Stage-end Avr Pressure (psia)	Stage-end Gas Prod (MMscf)	20-year Disc Cum Prod (MMscf)	Initial Pressure (psi)	1st Month Gas Prod (MMscf)	Stage-end Avr Pressure (psia)	Stage-end Gas Prod (MMscf)	20-year Disc Cum Prod (MMscf)
1	1847.958327	43.434	1691.3	264.33	921.708464	1691.3	31.185	1493.6	332.62	691.2364195
2	1732.016918	14.98	1430.9	91.949	258.2518839	1430.9	12.669	1058.7	111.39	182.3007145
3	1848.171206	42.463	1233.1	189.87	365.384659	1233.1	19.188	769.2	137.44	186.1087757
4	1854.271424	55.225	1510.8	391.58	1102.841876	1510.8	54.056	1046.6	519.74	799.0925788
5	1762.319627	34.8	1502.4	194.11	568.4087961	1502.4	22.306	1213.3	213.54	390.9165021
6	1953.218346	20.318	1534.1	115.96	294.4178043	1534.1	13.268	1096.9	119.36	189.3056056
7	1777.528678	43.338	1430.6	255.08	676.0007934	1430.6	30.423	1046	277.11	448.920792
8	1820.34424	32.189	1480.5	185.97	502.0603305	1480.5	22.291	1104	202.66	336.2386593
9	1823.714374	59.047	1512.7	332.45	927.7813708	1512.7	39.074	1170.1	361.57	627.2836196
10	1758.475183	23.399	1461.6	133.14	373.140126	1461.6	15.921	1129	146.86	253.8501334
11	1800.298521	44.324	1328.8	278.71	634.4007043	1328.8	31.326	840.58	278.82	387.194479
12	1843.805778	9.5199	1566.7	49.232	140.511287	1566.7	5.4749	1276.1	51.242	94.42083212
13	1944.738084	19.952	1587	123.05	340.5687106	1587	16.711	1153.2	147.56	238.3655174
14	1900.971808	29.623	1566.1	160.7	440.6725832	1566.1	18.113	1213.5	167.72	292.0395166
15	1711.831633	12.096	1510.3	80.884	269.3625844	1510.3	12.142	1217.3	116.08	211.9921571
16	1845.8447	81.283	1406.9	516.47	1249.846602	1406.9	60.822	925.69	551	798.2445576
17	1713.194817	29.745	1536.3	172.48	562.9343328	1536.3	20.131	1324.6	204.98	408.8773068
18	1886.18743	17.497	1601.2	98.013	286.2659097	1601.2	11.386	1283.5	108.51	197.3065111
19	1837.373309	12.353	1534.9	75.38	217.5263584	1534.9	10.015	1164.3	91.142	154.4750435
20	1811.182736	32.47	1274.3	162.86	338.3193203	1274.3	18.23	807.7	136.34	188.0045317
990	1798.545401	25.597	1514.5	143.96	413.0917853	1514.5	16.854	1197.9	158.55	282.7705435
991	1806.152916	53.4	1636.8	315.25	1060.123346	1636.8	37.35	1428.4	386.03	783.8892062
992	1832.506835	100.82	1382.6	556.48	1302.074124	1382.6	61.054	945.53	526.77	790.1881688
993	1782.93341	70.839	1415.9	401.93	1032.66114	1415.9	47.708	1023.3	420.86	671.1751593
994	1743.788509	45.429	1327.5	274.17	655.0327693	1327.5	31.777	888.26	280.61	410.893478
995	1816.220977	15.766	1529	97.85	287.7663684	1529	13.285	1167.7	121.42	207.4329777
996	1718.844828	43.979	1435.4	262.92	750.595951	1435.4	32.737	1101.7	304.28	521.9771825
997	1843.255799	21.338	1616.9	139.32	455.6259997	1616.9	20.038	1302.3	192.01	351.4536417
998	1785.609949	46.579	1412.6	269.2	688.6262163	1412.6	32.915	1005.8	286.94	449.9259437
999	1971.735801	20.593	1793.3	117	391.0552899	1793.3	13.181	1583.8	137.56	284.2576545
1000	1859.542736	43.394	1371	250.37	566.8781144	1371	25.95	906.16	231.63	336.1247045

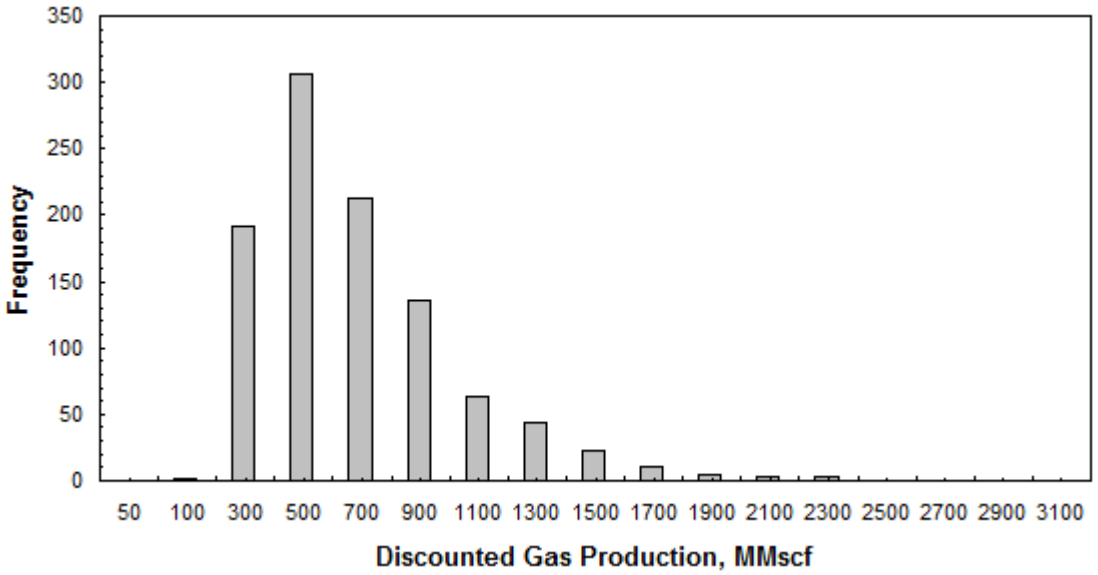

Fig. 12— Probability distribution plot of 20-year discounted cumulative gas production for Well 1 on 210 acre-spacing (Stage 1).

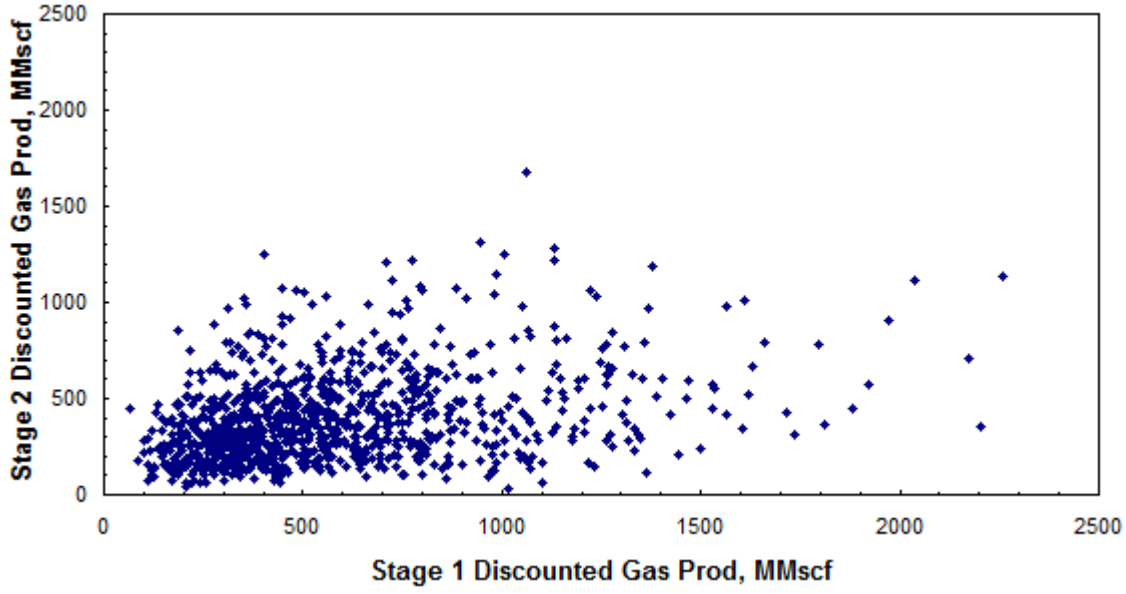

Fig. 13— Crossplot of Well 1 (Stage 1) vs. Well 2 (Stage 2) 20-year discounted cumulative gas productions (Option 2).

Table 4— Statistics of stage-end gas productions (mean and standard deviation) and pairwise correlation coefficients between Stage 1 and Stage 2.

	Stage 1, Well 1 (210 acres)
	Discounted Gas Production (MMscf)
mean	578.1171876
std dev	342.592303
corr coeff	

	Stage 1, Well 1 (210 acres)	Stage 2, Well 2 (160 acres)
	Discounted Gas Production (MMscf)	Discounted Gas Production (MMscf)
mean	578.1171876	394.5165458
std dev	342.592303	231.8910878
corr coeff		0.345554511

	Stage 1, Well 1 (210 acres)	Stage 2, Well 2 (160 acres)	Stage 2, Well 3 (210 acres)
	Discounted Gas Production (MMscf)	Discounted Gas Production (MMscf)	Discounted Gas Production (MMscf)
mean	578.1171876	394.5165458	530.94404
std dev	342.592303	231.8910878	305.8012089
corr coeff		0.345554511	0.429385547

	Stage 1, Well 1 (210 acres)	Stage 2, Well 2 (160 acres)	Stage 2, Well 3 (210 acres)	Stage 2, Well 4 (210 acres)
	Discounted Gas Production (MMscf)	Discounted Gas Production (MMscf)	Discounted Gas Production (MMscf)	Discounted Gas Production (MMscf)
mean	578.1171876	394.5165458	530.94404	529.4859974
std dev	342.592303	231.8910878	305.8012089	310.137433
corr coeff		0.345554511	0.429385547	0.441159866

3.2.2 Second Reservoir Model

The second reservoir model follows a more general approach and analyzes all possible two-stage downspacing combinations to study the effect of downspacing in the Berland River area, and to determine the optimal development strategy for the asset. More specifically, the decision context to be modeled consists of two development decisions: the primary and secondary well spacings. The intention is to start development on a specific well spacing and then decide on whether to downspace or not, based on the primary production results. For this purpose, first a preliminary model was developed and the feasibility of the approach was tested. Later, the preliminary model was revised to provide a complete, final reservoir model. The following sections discuss these models in detail.

3.2.2.1 Preliminary Model

The decision context behind the preliminary version of the reservoir model was to start development on 640, 320 or 160 acre-spacings and then, to decide on the secondary well spacing based on the primary production results. Therefore, the model is built to evaluate all possible two-stage downspacing combinations between 640, 320 and 160 acres **(Table 5).** Four wells were modeled in a section and, depending on the downspacing alternative; the corresponding well(s) was/were simulated **(Fig. 14).** For instance, when downspacing from 640 acres (Stage 1) to 160 acres (Stage 2), 1 well is producing in Stage 1 and 3 more will be drilled in Stage 2. In this model, a fixed stage-length of 2 years is used. Hence, Well 1 will produce for 2 years after which Wells 2 through 4 will be drilled, and all will produce for another 2 years.

To account for variability in reservoir properties at different well locations, all wells are modeled individually, but sampled from the same probabilistic distributions. In other words, the reservoir heterogeneity is modeled to a certain extent although a single-well model is used. Spatial dependencies in reservoir properties are also modeled and incorporated into the reservoir model.

Table 5—Possible downspacing combinations evaluated in the preliminary reservoir model.

Stage 1 \ Stage 2	640	320	160
640	X		
320	X	X	
160	X	X	X

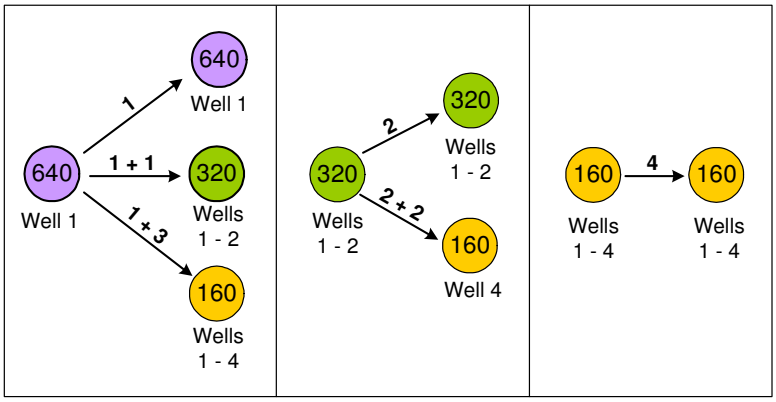

Fig. 14— Possible two-stage downspacing combinations. Numbers on top of arrows indicate Stage 1 wells and additional Stage 2 wells.

The average reservoir pressure is computed using the initial pore pressure gradient specified as 0.2 psi/ft by UGR and is assigned as the initial pressure of the first-stage wells. On the other hand, based on an initial assumption that drainage interference is likely to exist throughout the section, the average pressure at the end of first stage is assigned as the initial pressure of second-stage wells.

Once the reservoir model was established, a reservoir simulation of one thousand iterations was conducted to quantify best-month gas production, stage-end average pressure and stage-end gas production for each well **(Table 6).**

Table 6— Example simulation results of the preliminary reservoir model. In Stage 1, one well (Well 1) is producing on 640 acre-spacing. In Stage 2, an additional well is drilled (Well 2) on 320 acre-spacing.

Run #	Stage 1, Well 1 (640 acres)				Stage 2, Well 1 (320 acres)				Stage 2, Well 2 (320 acres)			
	Initial Pressure (psi)	Stage-end Gas Prod (MMscf)	Stage-end Avr Pres (psia)	1st Month Produced (MMscf)	Initial Pressure (psi)	Stage-end Gas Prod (MMscf)	Stage-end Avr Pres (psia)	1st Month Produced (MMscf)	Initial Pressure (psi)	Stage-end Gas Prod (MMscf)	Stage-end Avr Pres (psia)	1st Month Produced (MMscf)
1	2514.996772	475.13	2173	54.564	2173	369.77	1822.5	44.526	2173	629.98	1783.2	75.218
2	2738.058299	490.4	2460.8	55.33	2460.8	385.07	2174.9	42.706	2460.8	670.43	2132.1	72.314
3	2657.178056	417.34	2094.7	48.138	2094.7	301.46	1705.5	37.467	2094.7	447.44	971.66	71.513
4	2483.17818	282.94	1971.7	34.034	1971.7	198.88	1622.4	25.223	1971.7	416.49	1570.2	51.734
5	2608.439499	753.35	2043.4	95.264	2043.4	550.43	1693.3	67.456	2043.4	167.81	1869.6	20.369
6	2702.318567	598.52	1687.5	85.706	1687.5	288.58	1213.7	41.328	1687.5	153.23	1553.7	19.072
7	2483.942907	412.26	2199.7	44.323	2199.7	340.67	1913.9	39.884	2199.7	252.87	1927	32.209
8	2489.906505	259.72	1960.7	33.276	1960.7	202.33	1760.7	23.447	1960.7	254.32	1663.6	29.543
9	2470.9865	501.61	2089.3	62.193	2089.3	356.57	1824.8	42.242	2089.3	353.07	1773.6	41.717
10	2521.552856	392.4	1709.8	50.177	1709.8	214.45	1275.9	28.622	1709.8	251.31	1488.9	34.272
11	2699.938117	422.97	2180.6	53.178	2180.6	287.19	1843.5	35.014	2180.6	93.864	1666.8	13.329
12	2529.879886	368.86	1936.3	49.51	1936.3	230.26	1577	30.172	1936.3	343.05	1683.1	40.742
13	2662.13392	1094.4	1846.2	129.31	1846.2	683.35	1356.1	91.704	1846.2	115.69	1670.2	14.574
14	2554.97214	759.99	2030.3	88.049	2030.3	547.17	1665.6	67.822	2030.3	98.566	1417.3	16.515
15	2608.157515	1146.4	1948.2	136.14	1948.2	819.19	1522.5	101.56	1948.2	385.05	1120.9	60.733
16	2468.785165	131.07	2239.1	16.374	2239.1	93.568	2078	10.212	2239.1	288.16	1737.2	31.726
17	2765.702156	416	1941.4	46.289	1941.4	281.22	1412.3	37.177	1941.4	704.36	1645.8	89.233
18	2602.964113	397.2	1643.3	57.948	1643.3	190.51	1192.7	27.327	1643.3	111.45	1200.6	14.618
19	2501.805014	406.87	2089.6	47.729	2089.6	298.13	1692.1	36.603	2089.6	392.71	1395.1	59.64
20	2577.301556	1822.9	1674.5	207.53	1674.5	877.73	1088.5	116.67	1674.5	456.05	1169.4	59.223
990	2528.069526	456.45	2137.6	59.28	2137.6	318.7	1872.4	38.165	2137.6	201.68	1119.1	30.904
991	2422.702983	160.5	2178.7	17.753	2178.7	118.62	1902.4	13.835	2178.7	112.89	1634.2	13.38
992	2549.60562	1217.7	690.64	244.69	690.64	163.69	418.13	32.083	690.64	18.528	496.42	3.5412
993	2629.664961	310.14	2235.7	34.513	2235.7	211.96	1798	25.691	2235.7	1066.7	1847.1	129.54
994	2497.506333	257.36	1928.9	35.068	1928.9	160.06	1585.1	20.896	1928.9	108.37	1574	13.194
995	2480.764997	807.28	1792.3	97.354	1792.3	490.14	1384.6	62.539	1792.3	416.18	1588.9	51.91
996	2596.181978	390.24	2183.7	52.818	2183.7	262.41	1914.8	31.457	2183.7	454.18	1689.6	54.572
997	2555.231925	428.28	2217.7	43.715	2217.7	364.28	1801.5	44.14	2217.7	130.89	2049.5	15.899
998	2451.309545	101.68	2080.6	14.218	2080.6	69.494	1832.7	8.6848	2080.6	275.15	1978.6	29.993
999	2527.789509	478.83	2209.6	49.616	2209.6	456.57	1915.7	53.463	2209.6	698.84	1751.2	82.539
1000	2553.220063	448.01	2226.2	46.759	2226.2	340.33	1790.2	41.268	2226.2	545.55	1058.9	94.38

To test and validate this simple, preliminary model, simulated best-month and 24-month productions were compared with actual field data. Comparison was made for simulated cases which include 2 wells, since the study area is mainly developed on 320-acre spacing **(Fig. 15).**

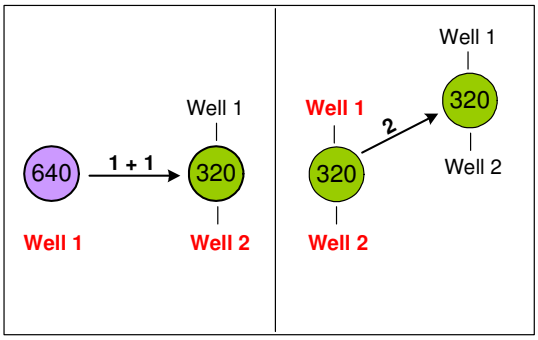

Fig. 15— Simulated cases used in the comparison. Wells labeled in red are compared with the actual field data.

Fig. 16 shows the cumulative distribution plots of the best-month and 24-month gas productions. The production distributions estimated by the reservoir model closely match the actual production distributions, which confirm the feasibility of the approach. Following the development and verification of the preliminary model, a more advanced, final model was developed which will be discussed in the next section.

Fig. 17 depicts the probability distribution plot of the stage-end gas production of Well 1 on 640 acre-spacing (Stage 1) which showed a log-normal distribution with a median of 515 MMscf. Probability distribution plots of other production data sets are presented in Appendix C.

We also generated crossplots of Stage 1 vs. Stage 2 gas productions to illustrate the dependency of Stage 2 on Stage 1 (Appendix D). **Fig. 18** shows an example where

first and second stage productions of Well 1 on 640 acres are plotted against each other. Stage 2 exhibits strong dependence on Stage 1 with a correlation coefficient of 0.894.

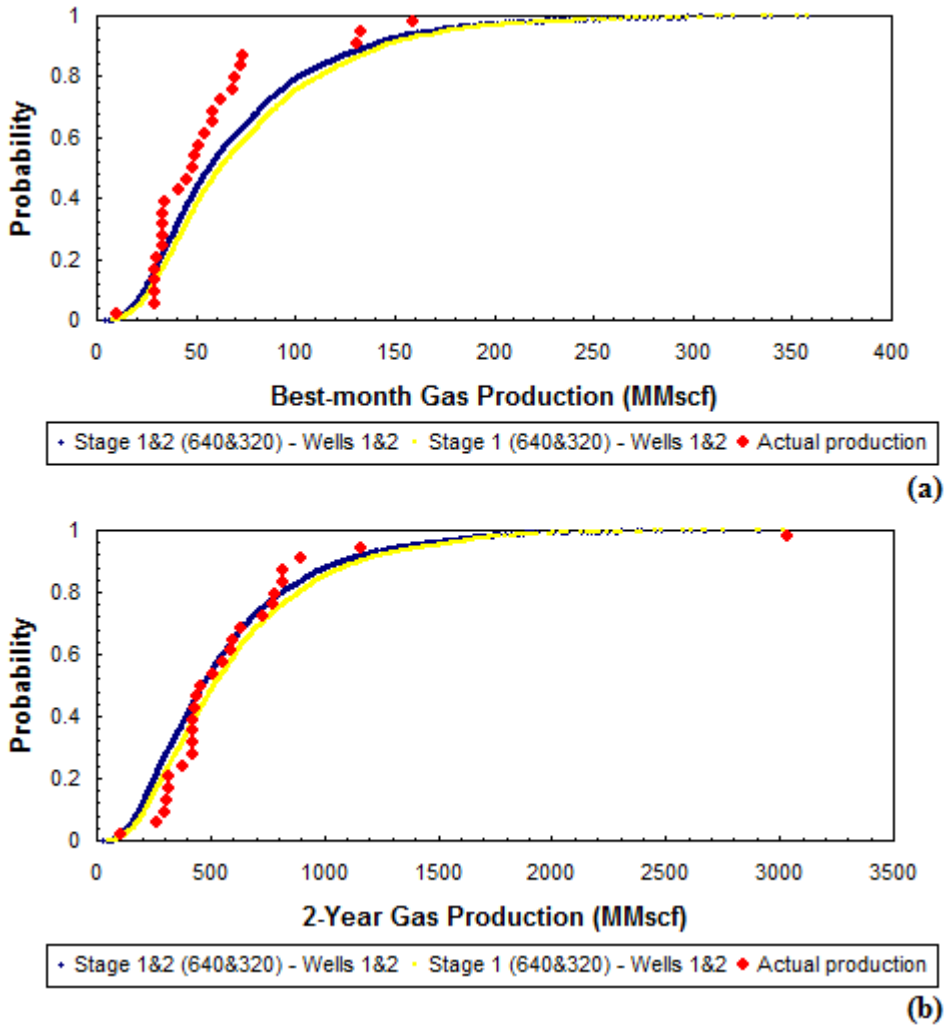

Fig. 16— Cumulative distribution plots of (a) best-month gas production and (b) stage gas production.

Table 7 displays the statistics (mean and standard deviation) of each production data set and the pairwise correlation coefficients between Stage 1 and Stage 2 productions.

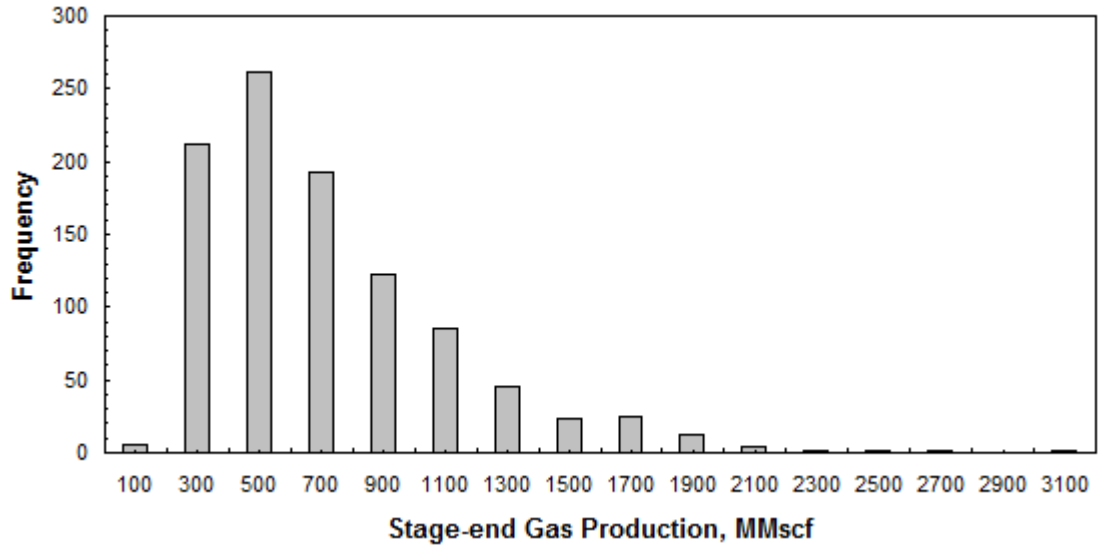

Fig. 17— Probability distribution plot of stage-end average gas production for Well 1 on 640 acre-spacing (Stage 1).

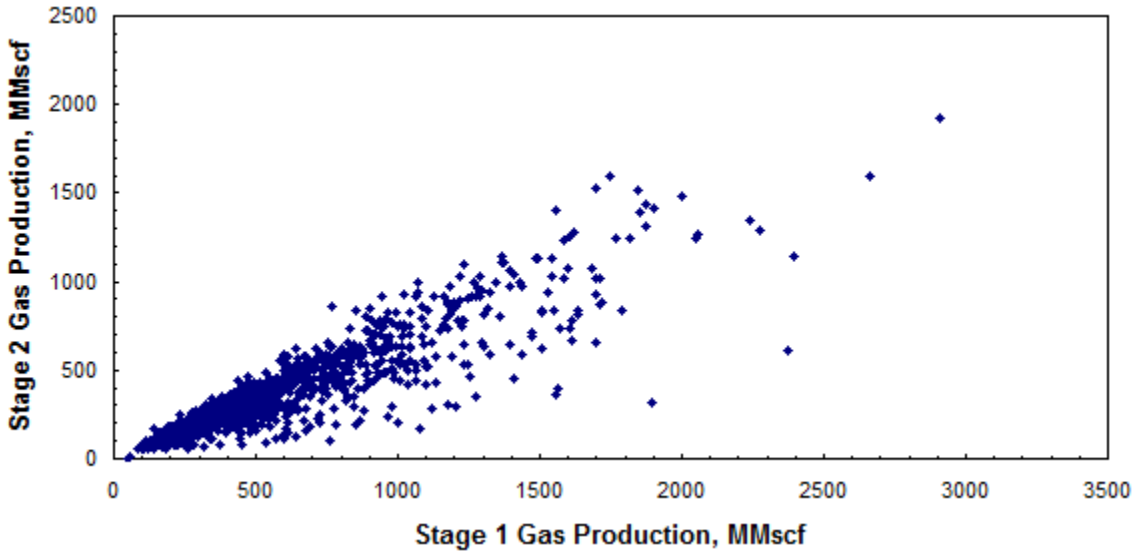

Fig. 18— Crossplot of Stage 1 (640 acres) vs. Stage 2 (640 acres) gas productions.

Table 7— Statistics of stage-end gas productions (mean and standard deviation) and pairwise correlation coefficients between Stage 1 and Stage 2.

	Stage 1 (640 acres)	Stage 2 (640 acres)	Stage 2 (320 acres)	Stage 2 (160 acres)
	Stage-end Gas Production (MMscf)	Stage-end Gas Production (MMscf)	Stage-end Gas Production (MMscf)	Stage-end Gas Production (MMscf)
mean	622.354554	397.600547	778.1964011	1369.503003
std dev	407.0426255	271.720798	392.8931037	545.3583681
corr coeff		0.894294773	0.638702947	0.399614956

	Stage 1 (320 acres)	Stage 2 (320 acres)	Stage 2 (160 acres)
	Stage-end Gas Production (MMscf)	Stage-end Gas Production (MMscf)	Stage-end Gas Production (MMscf)
mean	1239.384558	751.652797	1328.134775
std dev	629.3279747	339.4555214	451.969589
corr coeff		0.8761713	0.614559565

	Stage 1 (160 acres)	Stage 2 (160 acres)
	Stage-end Gas Production (MMscf)	Stage-end Gas Production (MMscf)
mean	2156.403983	1086.852833
std dev	841.7607305	310.3790517
corr coeff		0.776464689

3.2.2.2 Final Model

This model follows the same approach used to develop the preliminary model, but with two major improvements. First, the downspacing alternatives also include 80-acre spacing, allowing more development scenarios to be evaluated **(Table 8).** Second, production is forecasted over a total period of 20 years and each well's production profile is estimated.

Table 8—Possible downspacing combinations evaluated in the final reservoir model.

Stage 1 \ Stage 2	640	320	160	80
640	X			
320	X	X		
160	X	X	X	
80	X	X	X	X

This final version of the reservoir model is established assuming the drilling of up to 8 wells in a section **(Fig. 19a).** The wells are numbered according to the drilling sequence to be followed during development of Berland River area. For simplicity and shorter computation times, only four of the eight wells (**Fig. 19b)** are modeled.

Wells 1 through 4 are assigned to well spacings of 640, 320, 160 and 80 acres, respectively. For each downspacing combination, only one well is used to represent all the wells that will be drilled at each stage **(Fig. 20).** For instance, when downspacing from 320 acres (Stage 1) to 80 acres (Stage 2), 2 wells are producing in Stage 1 and 6 more will be drilled in Stage 2. In this case, Well 2 and Well 4 will be simulated to represent all Stage 1 and Stage 2 wells, respectively.

Although a single-well model is used in the reservoir characterization of the Gething Formation, the heterogeneity is modeled by attributing different reservoir properties to each well. That is, each well were modeled individually but sampled from the same statistical distributions.

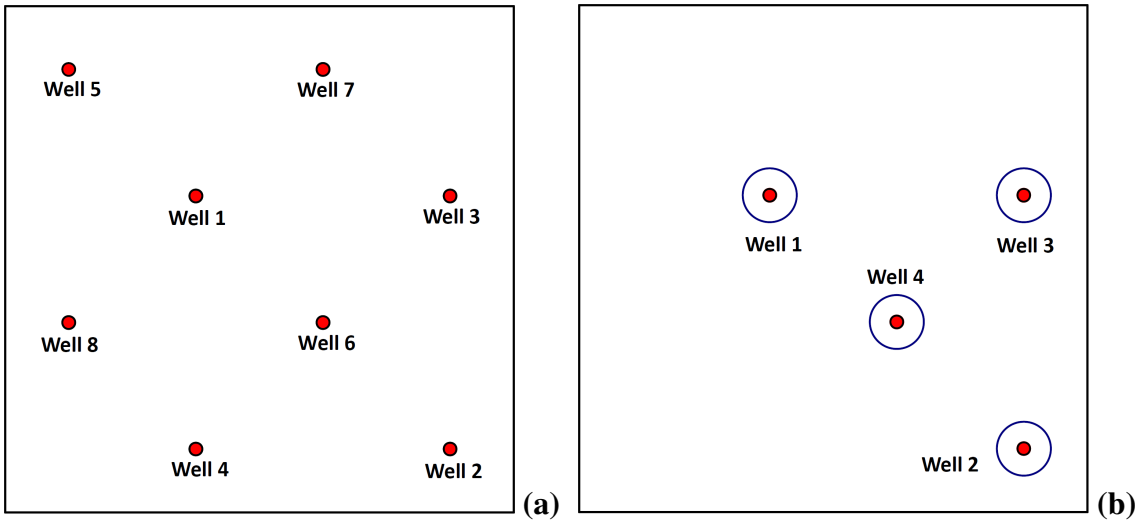

Fig. 19— Schematic illustration showing (a) possible well locations, (b) representative well locations.

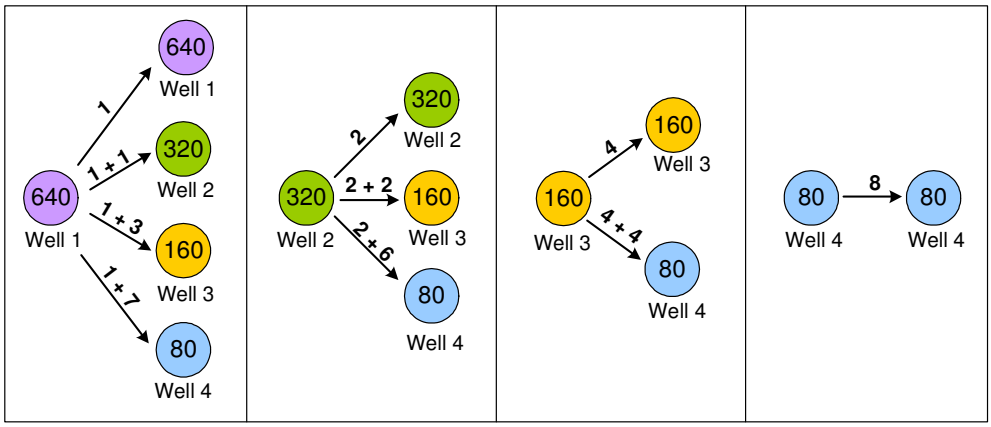

Fig. 20— Possible two-stage downspacing combinations. Numbers on top of arrows indicate Stage 1 wells and additional Stage 2 wells. Wells 1 through 4 are the representative wells.

At first, the average reservoir pressure was assigned as the initial pressure of first-stage wells, whereas the initial pressure of second-stage wells were modeled probabilistically on the rough assumption that there may be 75% chance of communication (i.e., pressure interference) between the second- and first-stage wells, and 25% chance of no communication. This assumption was made based on a quick analysis of Berland River permeability maps, which reveal drainage interference roughly in three forth of the study area.

To establish the probabilistic pressure model, a uniform distribution that generates random numbers between 0 and 1 was assigned for each well to represent its likelihood of having pressure interference with the adjacent wells. If the random number generated for a well by its @Risk uniform distribution function is lower than 0.25, the average reservoir pressure is designated as the initial pressure of this particular well; otherwise, the final pressure of the first stage- well(s) is/are assigned as the initial pressure of the same well.

However, in reality pressure interference between first- and second-stage wells depends on the well spacing, i.e., number of wells drilled in a section and areas that are being drained by these wells. Therefore, one would expect a greater chance of communication between wells when the field is developed on a smaller spacing. In other words, as more wells are drilled, the probability of pressure interference increases. Also, the greater the reservoir size of each well, the higher the chance of communication between adjacent wells.

Thus, to illustrate the effect of well spacing and drainage area on production interference, different probabilities representing pressure interference were assigned for each production scenario based upon well spacing and reservoir size of the first-and second-stage well/wells.

Completion efficiency of Berland River (Gething) wells was also modeled probabilistically. Based on information provided by UGR, a failure rate of 10% was assumed and incorporated into the reservoir model. To do so, a uniform distribution that generates random numbers between 0 and 1 is assigned for each well to represent its likelihood of having stimulation failure. If the random number generated for a well by its @Risk uniform distribution function is lower than 0.1, meaning that the fracture treatment failed, the fracture conductivity, k_f is equal to the permeability; otherwise, it is defined by the following equation; $k_f(md) = \frac{F_{cD} * L_f * k}{w}$ where F_{cD} is fixed at 1.3 and k_f cannot exceed 3750 md.

Once established, the reservoir model was run with 1-, 3- and 5-year stages to understand the trade-off between Stage 1 spacing and duration and illustrate how the value of learning about the primary development plan varies with stage length. **Tables 9 through 11** show example simulation results of the model for stage-lengths of 1, 3 and 5 years, respectively.

The remaining chapters (Chapter IV - correlation coefficients, Chapter V - decline curve model, Chapter VI - decision model) will all be based on the final reservoir model that was presented in this section.

Table 9— Example simulation results of the final reservoir model for a stage-length of 1 year. In Stage 1, one well (Well 1) is producing on 640 acre-spacing. In Stage 2, three additional wells are drilled on 160 acre-spacing and represented by Well 3 in simulation.

Run #	Stage 1 - Well 1 (640 acres)					Stage 2 - Well 1 (160 acres)					Stage 2 - Well 3 (160 acres)				
	Pressure & Production Data					Pressure & Production Data					Pressure & Production Data				
	Initial Pressure (psi)	1st Month Gas Prod (MMscf)	Stage-end Avr Pres (psia)	Stage-end Gas Prod (MMscf)	20-year Disc Cum Prod (MMscf)	Initial Pressure (psi)	1st Month Gas Prod (MMscf)	Stage-end Avr Pres (psia)	Stage-end Gas Prod (MMscf)	20-year Disc Cum Prod (MMscf)	Initial Pressure (psi)	1st Month Gas Prod (MMscf)	Stage-end Avr Pres (psia)	Stage-end Gas Prod (MMscf)	20-year Disc Cum Prod (MMscf)
1	1783.22837	10.053	1518.9	61.706	185.3372894	1518.9	7.6421	1330.6	87.205	182.6647478	1518.90	10.853	1330.4	107.84	217.9880179
2	1883.20217	18.655	1725.2	134.7	514.0624949	1725.2	14.729	1353.6	157.7	285.2009219	1725.20	13.149	1460.3	111.39	210.9721154
3	1870.67853	54.846	1528.4	360.78	1011.608833	1528.4	42.43	984.39	374.94	535.2293215	1528.40	30.676	730.68	194.69	223.7801212
4	1753.79564	49.077	1595.7	321.21	1147.905756	1595.7	26.259	1296.6	301.88	574.9093259	1595.70	20.047	1132.6	150.06	234.0154083
5	1798.84626	25.898	1607.7	168.34	574.626961	1607.7	26.924	1273.6	232.7	412.8879469	1798.85	16.664	1370.8	153.54	264.3698432
6	1743.4777	21.021	1634.7	128.02	464.7397565	1634.7	19.813	1363.3	169.06	315.7013967	1743.48	31.766	1221.1	306.98	482.3075496
7	1890.63737	13.324	1726.8	87.993	319.9229551	1726.8	9.4729	1369.4	95.547	173.7871329	1726.80	11.994	1322.1	109.47	188.9058349
8	1831.71446	29.434	1596.2	194.57	627.7634089	1596.2	26.858	1089.6	234.55	355.0397452	1596.20	23.062	1153.9	194.66	312.0364377
9	1838.55696	16.265	1692.7	94.995	330.9800268	1692.7	9.2365	1495.7	102.48	215.7108985	1692.70	6.9916	1519	67.701	139.4191788
10	1845.64992	37.63	1385.5	199.22	460.8881308	1385.5	27.988	1090.7	249.97	439.3705058	1385.50	14.445	1179.3	131.13	251.6849695
11	1862.83384	68.009	1322.7	331.62	699.2177266	1322.7	32.884	1048.2	329.67	590.9800882	1862.83	51.922	1481.4	441.57	789.755486
12	1841.73088	38.964	1504.7	270.28	763.8743477	1504.7	28.977	969.43	280.25	400.6940906	1504.70	42.328	996.09	364.56	532.9166628
13	1996.16358	19.085	1383.7	98	201.74329	1383.7	11.321	1049.3	104.77	176.98656	1383.70	9.5386	1014.2	85.186	137.9922751
14	1733.42915	19.988	1525.2	123.22	398.0890276	1525.2	15.76	1145.5	136.34	227.63303	1525.20	14.653	1231.9	131.1	238.1240198
15	1784.44816	63.482	1652.5	443.14	1711.586542	1652.5	47.269	1225.8	453.99	757.4889663	1652.50	43.632	1193.2	383.93	617.7706654
16	1795.44141	18.172	1542.6	107.94	327.895396	1542.6	15.605	1218.3	136.74	241.7600947	1542.60	20.506	1215.5	192.12	341.6844573
17	1804.5523	15.565	1657	90.717	314.3142892	1657	13.421	1380.2	112.54	209.3368159	1657.00	22.054	1342.8	231.96	434.9399048
18	1747.14491	41.727	1644.1	321.36	1370.827116	1644.1	47.331	1176.8	410.94	654.2767218	1644.10	54.792	1202.3	477.65	778.2935649
19	1955.42176	40.234	1481.9	212.04	500.7518316	1481.9	31.588	1170.8	274.69	484.6061009	1955.42	28.406	1488.7	255.02	439.6303693
20	1817.44404	36.887	1566.9	245.12	776.2420706	1566.9	27.296	992.88	232.11	326.7424252	1566.90	31.122	1106.6	275.58	431.8326242
990	1881.86959	27.895	1783.1	165.33	608.3019224	1783.1	22.372	1559.8	212.07	424.3591578	1783.10	23.331	1488.3	255.58	502.204015
991	1788.9879	30.996	1228.1	159.78	320.8152616	1228.1	13.513	791.93	119.34	167.4068502	1788.99	44.753	1373.5	386.68	666.5695603
992	1778.46942	25.14	1622.5	172.39	633.6605125	1622.5	22.513	1177.2	194.41	313.6367063	1622.50	70.67	1112.2	630.17	959.8713265
993	1824.79852	35.85	1731.4	212.27	813.9350645	1731.4	25.433	1512.3	248.03	498.5996196	1731.40	15.989	1570.4	157.91	330.4923438
994	1743.7617	25.063	1655	202.39	915.2539892	1655	25.925	1301.8	277.86	503.1748877	1743.76	30.971	1155.8	267.94	396.3616046
995	1723.1206	50.734	1645.8	380.46	1683.864365	1645.8	54.644	1276.2	496.3	866.0219773	1645.80	93.595	1160.5	899.46	1418.023382
996	1858.6468	22.515	1447.5	113.54	277.8302094	1447.5	16.766	1178.5	146.27	266.5129634	1447.50	16.493	1128.9	164.43	290.1775565
997	1909.09059	77.435	1390.2	379.7	833.5851853	1390.2	37.955	1120.8	387.49	713.6717794	1390.20	33.093	1131.9	306.62	563.0283573
998	1788.32771	18.184	1681.5	129.84	530.1243145	1681.5	18.976	1288.6	164.4	282.0383249	1681.50	25.898	1190.6	206.87	324.2468778
999	1868.04354	12.088	1464.3	55.821	136.318546	1464.3	8.1852	1211.2	69.079	127.3128072	1868.04	25.807	737.43	180.95	193.8385712
1000	1858.23701	10.714	1531.5	55.703	151.2656699	1531.5	7.6623	1167.4	61.283	103.1094724	1858.24	17.377	1415.3	146.91	250.7524903

Table 10— Example simulation results of the final reservoir model for a stage-length of 3 years. In Stage 1, one well (Well 1) is producing on 640 acre-spacing. In Stage 2, three additional wells are drilled on 160 acre-spacing and represented by Well 3 in simulation.

	Stage 1 - Well 1 (640 acres)					Stage 2 - Well 1 (160 acres)					Stage 2 - Well 3 (160 acres)				
	Pressure&Production Data					Pressure&Production Data					Pressure&Production Data				
Run #	Initial Pressure (psi)	1st Month Gas Prod (MMscf)	Stage-end Avr Pres (psi)	Stage-end Gas Prod (MMscf)	20-year Disc Cum Prod (MMscf)	Initial Pressure (psi)	1st Month Gas Prod (MMscf)	Stage-end Avr Pres (psi)	Stage-end Gas Prod (MMscf)	20-year Disc Cum Prod (MMscf)	Initial Pressure (psi)	1st Month Gas Prod (MMscf)	Stage-end Avr Pres (psi)	Stage-end Gas Prod (MMscf)	20-year Disc Cum Prod (MMscf)
1	1832.80251	29.659	1326.2	397.56	615.2829383	1326.2	16.274	843.79	183.05	86.70444101	1326.20	14.113	882.12	161.11	83.77039345
2	1817.23246	48.267	1004.4	414.39	528.1347145	1004.4	16.85	722.42	169.67	97.21037637	1004.40	17.415	728.83	230.83	140.7187201
3	1856.27647	14.474	1633.1	209.76	384.0377408	1633.1	11.819	1216.4	129.23	85.27576849	1633.10	15.758	1129.4	195.8	114.5748258
4	1934.56636	52.352	1448.5	671.85	1066.938244	1448.5	32.499	943.92	363.74	183.6419559	1448.50	40.863	893.21	448.57	202.2109936
5	1818.40424	47.431	1158.3	480.84	668.9689794	1158.3	17.467	853.83	213.15	135.5902938	1158.30	10.816	996.57	123.74	101.1931367
6	1758.99499	27.477	1578.5	459.08	878.0121709	1578.5	28.413	1190.4	324.48	220.1192722	1578.50	24.485	1026.2	299.62	153.889752
7	1819.40689	53.07	1179.9	539.44	759.6306864	1179.9	24.424	855.93	262.57	158.8255746	1179.90	42.804	638.06	499.4	162.5973567
8	1808.89313	70.622	1493.2	1001.5	1737.340628	1493.2	35.716	1098.1	493.72	328.9323901	1493.20	25.777	967.03	289.71	145.2185808
9	1794.77766	29.411	1118	378.71	521.321008	1118	16.681	760.17	190.77	100.7142739	1794.78	18.569	1169.4	199.56	103.5597587
10	1735.52523	23.805	1011.1	207.82	272.009778	1011.1	7.9478	825.57	101.16	78.48050972	1735.53	25.503	1289.9	304.49	204.7076338
11	1848.952	15.966	1482.7	215.44	362.8711706	1482.7	10.61	1161	135.62	100.4044353	1482.70	15.968	1085.9	194.26	125.519673
12	1936.03219	57.045	1703.6	887.6	1647.789706	1703.6	54.874	1268.6	599.5	396.8942011	1703.60	68.772	1078.6	813.33	399.5892494
13	1754.32952	83.222	1047.1	955.61	1275.358566	1047.1	33.855	728.32	408.75	225.4239744	1754.33	69.222	1074.1	765.09	351.868886
14	1860.73232	137.21	568.52	1027.1	1067.171677	568.52	15.195	429.12	201.09	107.9818561	568.52	11.435	461.79	145.7	98.72605694
15	1815.9464	69.519	1172.3	935.37	1323.301833	1172.3	26.1	647.64	304.33	103.5829104	1172.30	16.009	739.41	183.57	83.27381865
16	1782.03023	64.232	1284.9	791.48	1212.38443	1284.9	34.868	829.25	398.04	193.3091279	1782.03	25.468	1241.9	279.44	164.9600392
17	1787.31985	11.469	1600.8	146.76	265.9457214	1600.8	9.2797	1334.7	103.65	81.74842219	1600.80	27.559	1169.3	392.18	260.9587253
18	1814.5272	49.061	1407.5	686.76	1129.945019	1407.5	37.212	998.56	414.33	246.7661228	1407.50	37.006	951.04	444.15	242.2381232
19	1789.86545	19.517	975.01	200.42	253.6634217	975.01	6.9915	649.41	75.263	36.44731911	975.01	12.588	707.05	147.82	87.8230436
20	1869.00932	43.854	1058.6	382.18	494.4999036	1058.6	16.258	847.12	190.25	139.56963	1058.60	14.865	793.46	198.96	131.7863712
990	1752.13888	91.278	390.68	522.05	512.4179161	390.68	3.6702	316	50.869	21.47159517	390.68	2.0356	354.36	27.511	22.0855266
991	1842.53397	49.177	1507.9	616.45	1039.616042	1507.9	34.387	1108.7	386.52	248.6277185	1507.90	17.945	1117.6	215.63	142.5283157
992	1809.46293	37.351	1403.3	448.71	725.3079459	1403.3	23.509	979.92	259.58	149.5996051	1403.30	38.086	746.51	426.7	141.8027657
993	1707.4735	40.898	747.77	334.13	382.189121	747.77	8.7893	578.96	109.21	71.47816827	747.77	5.2704	555.36	60.473	35.19363433
994	1818.16561	14.329	1574.4	194.21	347.2576656	1574.4	9.5717	1198.5	112.08	77.68734858	1574.40	15.212	1131.9	198.16	125.6054596
995	1846.61387	6.9523	1505.7	93.873	160.1456625	1505.7	4.9215	1214.8	63.305	49.45469653	1505.70	9.7787	1153.3	130.36	93.60806889
996	1873.49492	20.639	1086.3	220.35	289.7095469	1086.3	10.648	852.35	125.14	88.8686229	1086.30	18.008	815.48	227.36	150.0828562
997	1718.59996	36.837	1311.5	455.22	729.1279594	1311.5	23.984	995.48	275.46	186.2845456	1311.50	18.046	964.41	222.75	143.5635031
998	1864.14949	35.502	950.53	297.91	365.2276816	950.53	11.405	741.38	128.7	88.16830974	950.53	14.069	736.3	162.32	110.0023971
999	1773.4257	20.935	1004.5	192.8	248.8452238	1004.5	7.833	803.94	95.343	70.42497007	1004.50	6.7803	797.01	85.404	62.57419937
1000	1836.62994	26.388	1577	394.43	712.2180186	1577	20.843	1115.8	230.24	138.0287825	1836.63	34.95	1157.7	404.5	199.1401057

Table 11— Example simulation results of the final reservoir model for a stage-length of 5 years. In Stage 1, one well (Well 1) is producing on 640 acre-spacing. In Stage 2, three additional wells are drilled on 160 acre-spacing and represented by Well 3 in simulation.

	Stage 1 - Well 1 (640 acres)					Stage 2 - Well 1 (160 acres)					Stage 2 - Well 3 (160 acres)				
	Pressure&Production Data					Pressure&Production Data					Pressure&Production Data				
Run #	Initial Pressure (psi)	1st Month Gas Prod (MMscf)	Stage Avr Pres (psi)	Stage Gas Prod (MMscf)	20 year Disc Cum Prod (MMscf)	Initial Pressure (psi)	1st Month Gas Prod (MMscf)	Stage Avr Pres (psi)	Stage Gas Prod (MMscf)	20 year Disc Cum Prod (MMscf)	Initial Pressure (psi)	1st Month Gas Prod (MMscf)	Stage Avr Pres (psi)	Stage Gas Prod (MMscf)	20 year Disc Cum Prod (MMscf)
1	1774.15363	41.14	1319.5	663.31	813.5132642	1319.5	24.521	877.02	355.84	249.2524139	1319.50	32.393	829.24	556.63	382.707681
2	1801.26352	14.734	817.56	156.5	161.3177711	817.56	2.9061	640.31	52.422	38.73457009	817.56	5.8	671.59	106.37	79.92694354
3	1821.46744	41.209	1557.6	1025.5	1376.201402	1557.6	33.635	1031.9	573.54	403.9838017	1557.60	27.949	1009.1	472.26	329.8922324
4	1914.40177	43.548	1122.1	914.57	1021.542491	1122.1	18.827	514.29	262.6	162.7815566	1914.40	61.551	732.89	780.99	478.9010646
5	1838.90436	73.702	957.93	1027.5	1099.893532	957.93	16.213	668.54	317.63	225.430083	957.93	3.9126	860.91	57.328	43.38314547
6	1839.26509	28.54	1418.6	615.28	779.9026759	1418.6	20.45	843.07	296.84	200.470212	1839.27	41.884	752.61	562.95	348.6175932
7	1750.19548	55.368	546.56	516.03	497.0659736	546.56	5.0829	423.87	95.755	68.57913085	546.56	4.8092	434.52	83.325	60.39828977
8	1868.84101	47.473	1376.7	794.19	973.2370944	1376.7	27.447	888.91	408.4	283.5776859	1376.70	36.188	755.11	580.49	381.6149655
9	1888.19756	24.715	1496.9	488.68	623.6600607	1496.9	17.227	947.62	244.03	168.6025558	1496.90	34.116	395.26	305.81	178.1848117
10	1830.12487	14.611	1528.8	286.69	372.758511	1528.8	8.8895	1101.2	151.77	110.1232268	1528.80	12.201	853.25	205.7	136.4441987
11	1860.38342	8.359	1637.9	169.86	225.8747151	1637.9	7.6486	1247	111.8	82.0665193	1860.38	8.8505	1451.2	169.37	127.0666452
12	1730.97635	22.165	1425.6	528.65	691.8773369	1425.6	16.109	942.11	301.71	212.1130841	1730.98	16.435	1237.2	246.32	177.9585321
13	1868.37818	24.589	843.69	340.22	350.0624111	843.69	7.7343	630.75	131.59	95.34558976	843.69	13.001	534.67	230.49	155.4175322
14	1952.03536	85.569	1339.2	1843.9	2212.381786	1339.2	39.177	621.65	568.08	356.6349569	1952.04	37.318	993.84	518.18	337.6697018
15	1816.36929	37.93	1527	781.52	1022.562388	1527	21.255	1123.8	406.48	298.4029685	1816.37	19.569	1276.2	330.28	238.3521081
16	1934.9201	5.4194	1262.2	69.879	81.16276743	1262.2	2.1973	1059.7	40.984	31.14866134	1262.20	1.4793	1067.3	28.947	22.12011285
17	1883.26842	53.872	1497.9	1367.7	1775.40953	1497.9	47.619	878.74	791.3	533.1361486	1497.90	40.74	811.8	624.07	410.0915614
18	1753.911	21.717	1038.7	335.43	374.8069927	1038.7	8.2202	677.39	128.15	88.47609887	1038.70	11.049	695.14	181.39	126.5826648
19	1824.8248	26.382	1201.9	298.5	346.6101715	1201.9	12.794	952.08	173.15	127.1956741	1201.90	11.273	978.94	248.08	189.4442595
20	2017.35981	35.379	1432.9	902.73	1108.392011	1432.9	29.535	723.73	422.36	271.682063	1432.90	17.042	771.87	240.43	157.5028456
990	1765.07165	11.137	894.51	120.64	127.9826009	894.51	2.5732	714.87	46.924	35.0123551	894.51	3.8255	723.48	70.5	52.83583463
991	1927.7197	22.888	908.62	314.62	327.7385367	908.62	6.4724	576.43	95.55	64.73865819	1927.72	60.796	743.05	796.9	489.1801103
992	1736.09679	36.401	1183.5	619.15	733.5950931	1183.5	17.85	724.44	279.32	189.367652	1183.50	30.181	660.53	448.28	294.5000419
993	1854.91173	26.003	1567.6	430.65	549.9179323	1567.6	16.958	1219.9	275.31	204.1139548	1567.60	18.9	1166.7	350.5	258.0962405
994	1819.02319	33.523	1313.3	790.06	972.7317799	1313.3	19.571	688.55	311.15	201.4119584	1313.30	20.724	730.68	301.74	198.9239023
995	1828.07626	23.613	1474.6	437.08	558.1201764	1474.6	10.854	1166.8	231.13	174.8605853	1828.08	23.222	1113.5	310.66	212.9322954
996	1863.54483	16.304	1451.1	343.66	436.9334755	1451.1	11.705	929.28	178.57	123.84747	1863.54	15.975	1128.4	238.89	163.6872921
997	1833.47154	51.05	825.13	646.53	664.7475841	825.13	12.124	526.83	176.78	119.2725851	825.13	20.828	489.57	293.31	192.1517455
998	1805.60225	19.008	931.53	211.28	225.5045541	931.53	5.1149	739.09	87.814	65.2118773	931.53	2.4804	782.55	42.849	32.30897494
999	1810.86784	27.222	708.27	356.67	355.3496828	708.27	6.0279	429.43	82.425	53.52998042	1810.87	27.777	947.56	382.68	250.6123045
1000	1960.97791	24.301	1145.9	331.27	369.6232478	1145.9	8.7295	797.94	135.26	96.05904102	1960.98	74.306	826.56	1100.6	686.3150359

CHAPTER IV
CORRELATION COEFFICIENTS

The motivation of this study was to build a reservoir model using fast simulation techniques paired with stochastic methods to provide production profiles within a wide range of reservoir properties and under multiple development scenarios. Stochastic methods include Monte Carlo simulation to quantify uncertainty in reservoir properties in forms of probabilistic distributions and geostatistical analysis to honor spatial variations of these reservoir properties within the reservoir.

Previous chapters discuss the reservoir characterization study of the Gething formation where statistical distributions are attributed to uncertain parameters for a subsequent Monte Carlo simulation, and also present the stepwise development of the probabilistic reservoir model.

In this chapter, the geostatistical analysis performed to provide spatial distribution of the reservoir properties is presented and the correlation coefficients incorporated to the reservoir model are reported.

Since spatial variations of reservoir properties in the Gething tight gas formation are considered to determine dependencies in production response between wells for decision modeling, dependencies in reservoir properties were identified based on a geostatistical study performed by Schlumberger Data and Consulting Services, College Station, TX. A variogram analysis was conducted and, based on interwell distances, the correlation coefficients for porosity, permeability and net pay were computed, which were then incorporated into the probabilistic reservoir model.

4.1 Variogram Analysis

Variograms are the most widely used tools in geostatistics to investigate spatial variability of lithofacies and petrophysical properties. Building variograms in a particular direction provides insight in determining spatial distribution of some reservoir parameters such as porosity and permeability in that direction. A display that quickly

reveals directional anisotropies is a contour map of the sample variogram surface. Contour maps may serve as useful means of establishing the minimum and maximum continuity directions (Isaaks and Srivastava, 1989).

A variogram analysis was performed for Berland River area to generate possible representations of porosity, permeability and net pay at interwell locations and determine the correlation coefficients between wells separated by specific distances. Then, examining the variogram maps created for the Gething D formation, the major and minor directions of continuity were determined and the corresponding variograms are plotted.

Fitting a variogram model to each of these reservoir properties, the theoretical variograms were reproduced in an Excel spreadsheet for both major and minor directions of continuity. These theoretical variograms were plotted with their associated covariance and correlation functions.

Porosity map and porosity variogram map of the Gething reservoir are shown in **Fig. 21** and **Fig. 22a**, respectively. Based on the variogram map, the major and minor continuity directions for porosity are determined as 68° and 338°. The corresponding major and minor direction empirical variograms and the theoretical models fitted to these experimental variograms are shown in **Figs. 22b and 22c.** These empirical variograms are of exponential type with a sill of 1.055 and nugget of 0.034. The major range is established as 3913 m and the minor range as 2015 m.

Fitting an exponential model to the empirical porosity variograms, the theoretical variograms are generated for both major and minor directions of continuity, along with their associated covariance and correlation functions **(Figs. 22d and 22e).** For the exponential variogram which is a commonly used transition model, the following standardized equation is used:

$$\gamma(h) = C_0 + C_1\left[1 - \exp\left(-\frac{3h}{a}\right)\right]$$

where $\gamma(h)$ is the semi-variogram, C_0 is the nugget which provides discontinuity at the origin, C_1 is the difference between sill (or covariance at 0 separation distance, $C(0)$)

and nugget, a is the range providing a distance beyond which the variogram remains essentially constant and h is the separation or lag distance between pairs.

To compute the covariance function of porosity represented in red in Figs. 22d and 22e, the relationship between variogram and covariance expressed as $C(h) = C(0) - \gamma(h)$ is utilized. On the other hand, the correlation functions shown in yellow in Figs. 22d and 22e are derived from the covariance function using the formula $\rho(h) = \frac{C(h)}{C(0)}$.

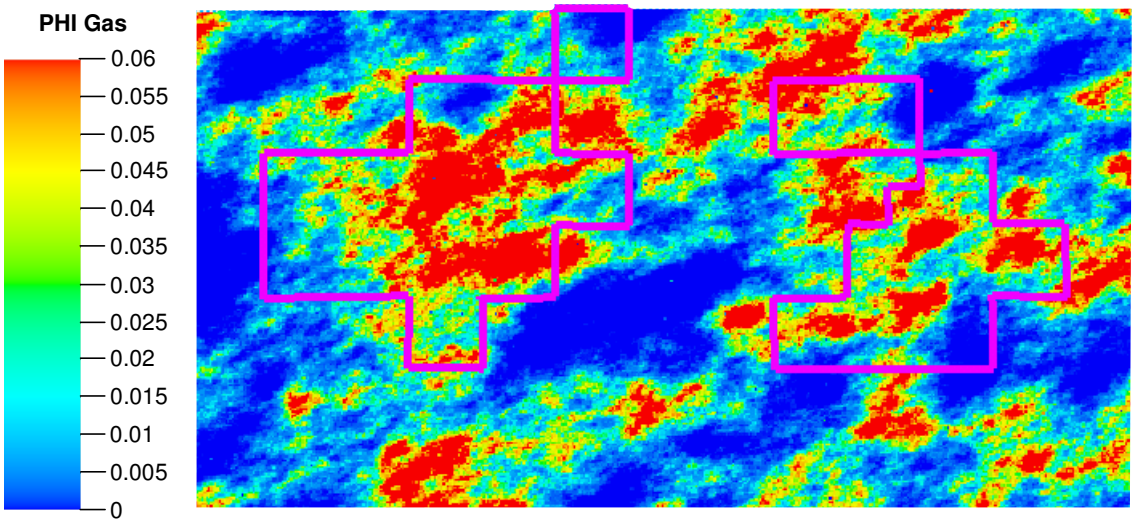

Fig. 21—Porosity map of the Gething reservoir (provided by Schlumberger Consulting Services on Berland River area).

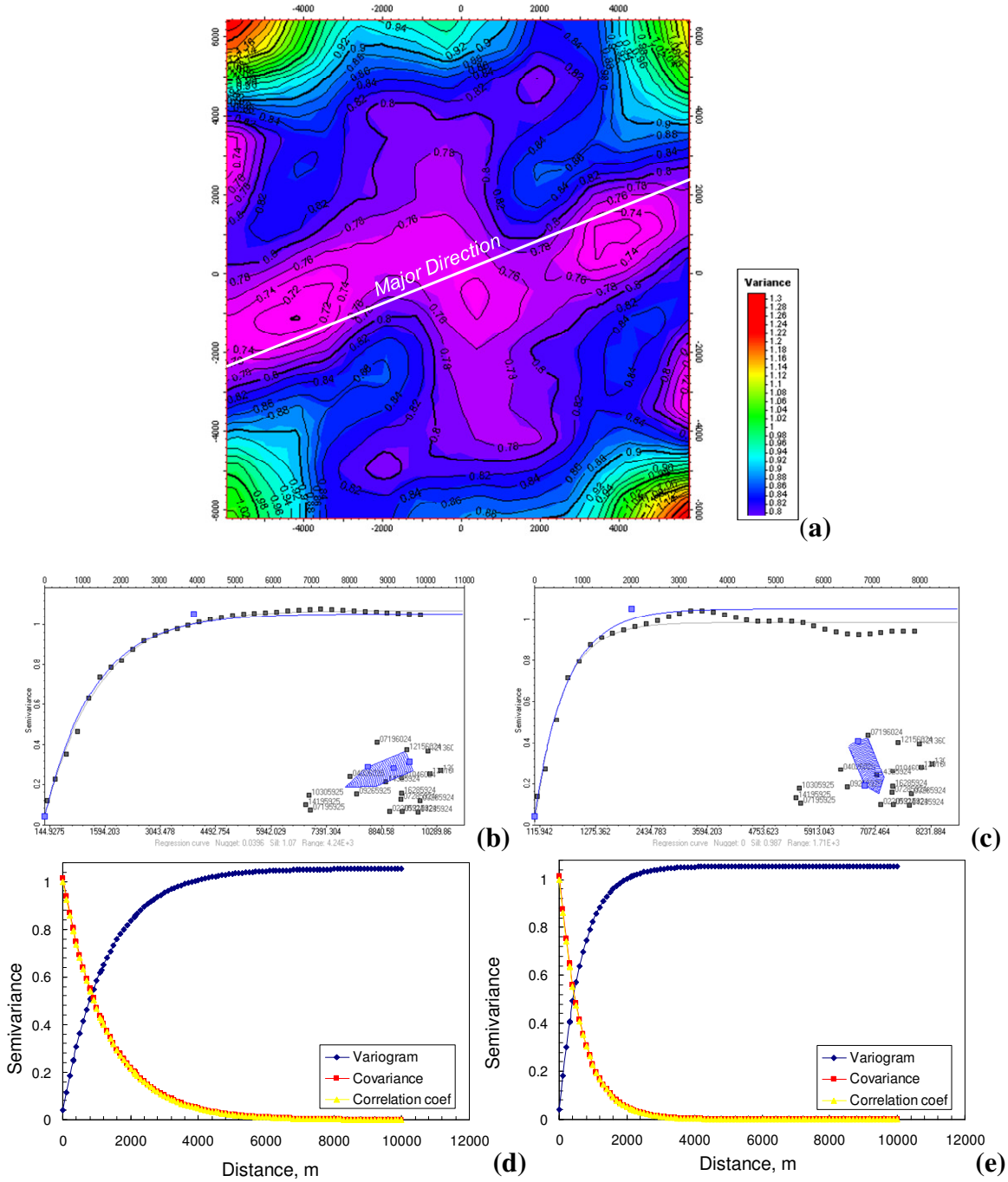

Fig. 22—Variogram analysis for porosity: (a) Variogram map (distances are in meters), (b) major and (c) minor direction empirical variograms, (d) major and (e) minor direction theoretical variograms with covariance and correlation functions (provided by Schlumberger Consulting Services on Berland River area).

Net pay map and net pay variogram map of the Gething reservoir are shown in **Fig. 23** and **Fig. 24a**, respectively. According to the variogram map, the major and minor continuity directions for net pay are noted as 297° and 207°. The corresponding major and minor direction empirical variograms and the theoretical models fitted to these experimental variograms are shown in **Figs. 24b and 24c.** These experimental variograms are Gaussian with a sill of 0.952 and nugget of 0.116. The major range is established as 2570 m and the minor range as 2470 m. The relationship between variogram and covariance is used to compute the covariance function which is then employed to derive the correlation function.

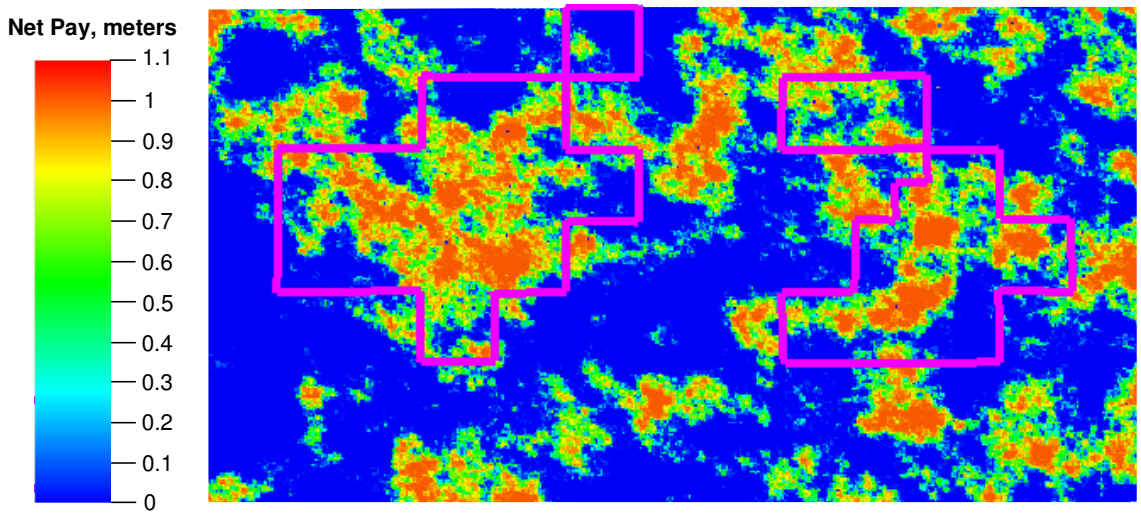

Fig. 23—Net pay map of the Gething reservoir (provided by Schlumberger Consulting Services on Berland River area).

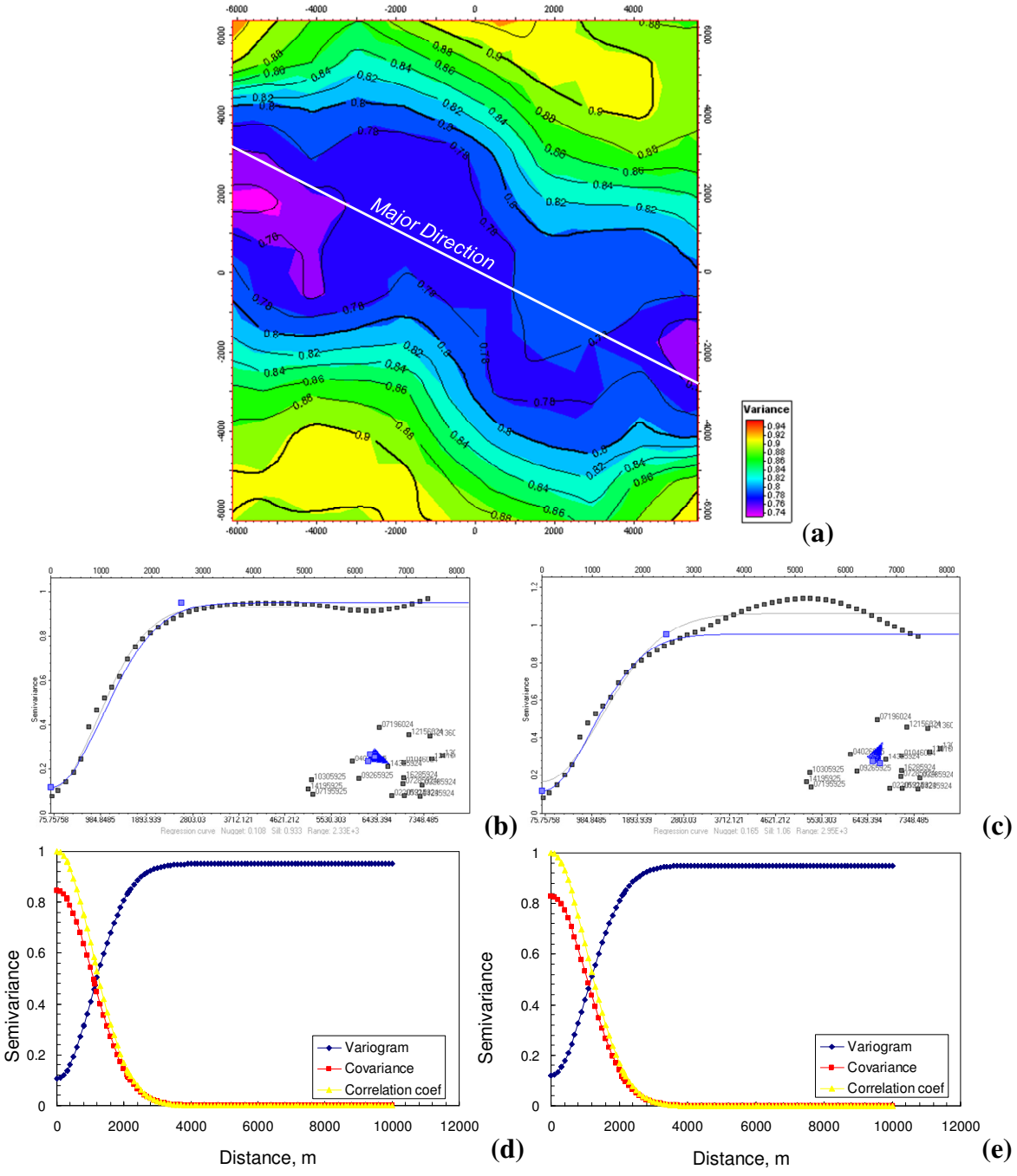

Fig. 24—Variogram analysis for net pay: (a) Variogram map (distances are in meters), (b) major and (c) minor direction empirical variograms, (d) major and (e) minor direction theoretical variograms with covariance and correlation functions (provided by Schlumberger Consulting Services on Berland River area).

Permeability-thickness map and permeability variogram map of the Gething reservoir are shown in **Fig. 25** and **Fig. 26a**, respectively. Based on this variogram map, the major and minor continuity directions for permeability are established as 264° and 174°. The associated major and minor direction empirical variograms and the theoretical models fitted to these experimental variograms are shown in **Figs. 26b and 26c.** These empirical variograms are of spherical type with a sill of 0.997 and a zero nugget. The major range is determined as 2520 m and the minor range as 2430 m.

A spherical model is fitted to the empirical major and minor direction variogram estimates of permeability and theoretical variograms are generated along with their associated covariance and correlation functions **(Figs. 26d and 26e).** The spherical variogram functions are computed based on the following standardized equation:

$$\gamma(h) = C_0 + C\left[1.5\frac{h}{a} - 0.5\left(\frac{h}{a}\right)^3\right]$$

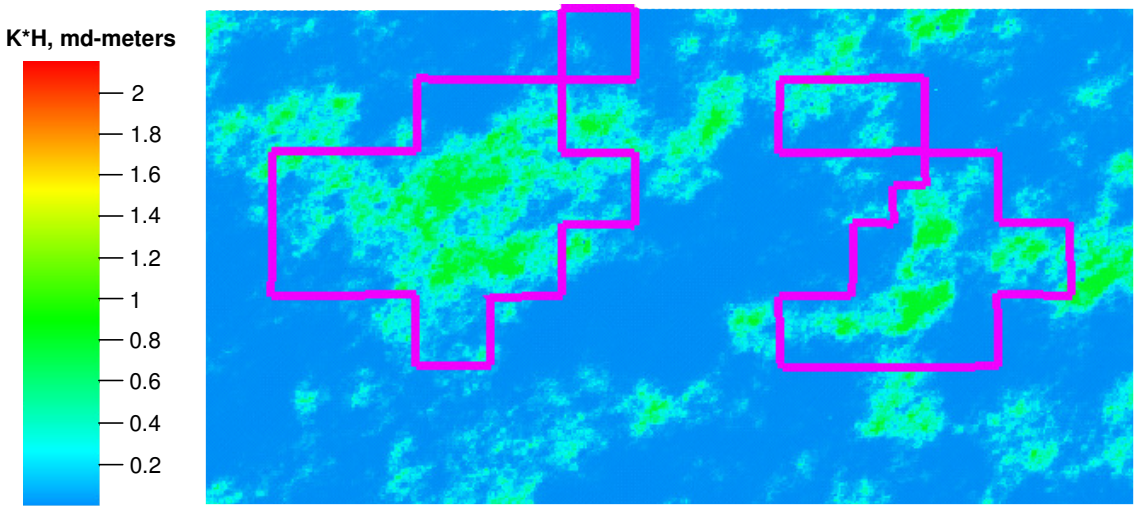

Fig. 25—Permeability-thickness map of the Gething reservoir (provided by Schlumberger Consulting Services on Berland River area).

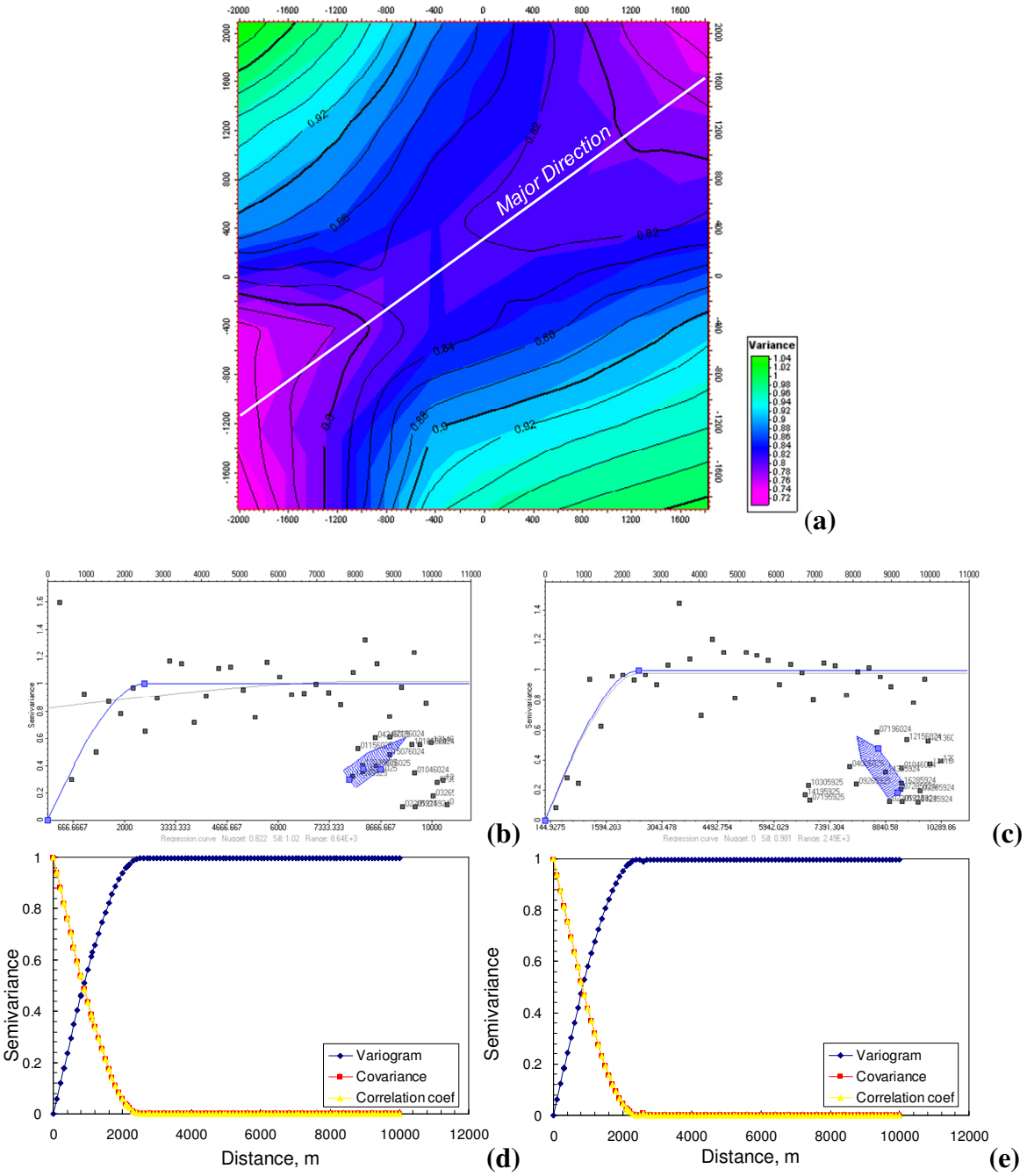

Fig. 26—Variogram analysis for permeability: (a) Variogram map (distances are in meters), (b) major and (c) minor direction empirical variograms, (d) major and (e) minor direction theoretical variograms with covariance and correlation functions (provided by Schlumberger Consulting Services on Berland River area).

Once the theoretical variograms are built, the corresponding covariance and correlation functions are computed based on aforementioned variogram-covariance and correlation-covariance relationships.

4.2 Correlation Coefficients

A variogram analysis is conducted to assess the spatial variations of reservoir properties within the Gething formation. Theoretical variogram, covariance and correlation functions are established for major and minor directions of continuity. Correlation functions are utilized to compute the correlation coefficients for porosity, permeability and net pay based on the planned well locations in a section.

As discussed in Chapter III, while the Gething reservoir model is built based on the assumption that at most 8 wells will be drilled in a section, only 4 of those are modeled. **Fig. 27** is a schematic illustration of the described well configuration with the 4 representative wells and the separation distances between them.

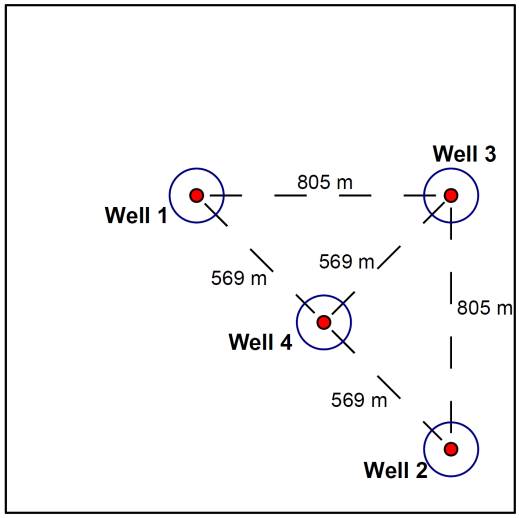

Fig. 27— Schematic illustration showing the representative well locations and the corresponding interwell distances in meters.

Tables 12 through 14 present the correlation matrices which display the correlation coefficients between all pairs of well porosities, net pay thicknesses and permeabilities. These correlation coefficients are later incorporated to the reservoir model to account for dependencies in reservoir properties between wells.

Table 12—Correlation matrix for porosity.

Well no.	1	2	3	4
1	1			
2	0.18	1		
3	0.30	0.30	1	
4	0.43	0.43	0.43	1

Table 13—Correlation matrix for net pay.

Well no.	1	2	3	4
1	1			
2	0.56	1		
3	0.75	0.75	1	
4	0.87	0.87	0.87	1

Table 14—Correlation matrix for permeability.

Well no.	1	2	3	4
1	1			
2	0.37	1		
3	0.54	0.54	1	
4	0.67	0.67	0.67	1

CHAPTER V
DECLINE CURVE MODEL

Reservoir simulation combined with Monte Carlo techniques provided a practical and quick method to predict a multitude of production profiles with various reservoir properties, under different development scenarios. These production profiles will be incorporated to a flexible decision model and allow calculation of the expected net present value for each scenario which will be used as a means to decide on the optimal development strategy. To facilitate the integration of the reservoir and decision models, simulated production profiles are fit with decline curves. The regressed decline parameters are then used in the decision model along with their means, standard deviations and pairwise correlation coefficients to specify a joint probability distribution for each development scenario.

This chapter provides background information on conventional decline curve analysis and describes the methodology followed in constructing the decline curve model in this work.

5.1 Background

Decline curve analysis is one of the most widely used techniques to predict future production performance and estimate reserves from available production data in conventional reservoirs. This technique is based on the assumption that the past production trend can be mathematically described by so-called Arps' rate-time equations and utilized to forecast future performance. Decline curve analysis may serve as an effective and powerful tool for reserve estimation and economic evaluation of an asset if applied under the appropriate conditions (Cheng et al. 2008).

Conventional decline curve analysis applies to cases in which there is a single-layer reservoir where the transient flow has died out and the well production is maintained at steady-state flow conditions with constant bottomhole pressure. It is important that the decline curve analysis is performed only after boundary-dominated

flow conditions are reached, that is when the change of reservoir pressure with time (dP/dt) is constant at all points for constant rate production. If the analysis were to be performed during transient flow conditions, predictions on future well performance would be inaccurate and misleading; since the effective drainage area of the well increases during this flow regime. Also there should not be any changes in completions. Under these conditions the Arps' equations can be effectively used for decline curve analysis (Cheng et al., 2008).

The three types of rate-time decline curves are (1) exponential decline, (2) hyperbolic decline and (3) harmonic decline. Detailed explanation on the first two methods will be provided next, whereas the last method will be omitted as it is beyond the scope of this work.

5.1.1 Exponential Decline Curve

Exponential decline which is also referred as constant percentage decline is the most commonly used Arps' model defined by an exponential equation of the form $y = ae^{bx}$. The equations used to interpret exponential decline curves are,

(1) Production rate at time t,

$$q = q_i e^{-Dt}$$

(2) Cumulative production,

$$N_p = \frac{q_i - q}{D}$$

where the decline rate, D is expressed as,

$$D = \frac{\ln\left(\frac{q_i}{q}\right)}{t}$$

The rate-time equation governing exponential decline includes two constants which are the initial production rate, q_i and the decline rate, D. The decline rate is the rate of change in production with respect to time and, for exponential decline, is constant for all time (Fattah 2006).

5.1.2 Hyperbolic Decline Curve

Hyperbolic decline occurs when the decline rate varies with producing time. The equations that define hyperbolic decline curves are,

(1) Production rate at time t,

$$q = q_i \left(1 + bD_i t\right)^{-1/b}$$

(2) Cumulative production,

$$N_p = \frac{q_i^b}{D_i \left(1-b\right)} \left(q_i^{1-b} - q^{1-b}\right)$$

The rate-time equation defining hyperbolic decline incorporates three constants, the initial production rate, q_i the initial decline rate, D_i, which is defined at the same time as the initial production rate, and the hyperbolic exponent, b. The decline rate is no longer constant, but varies with time. The hyperbolic exponent is the rate of change of the decline rate with respect to time, or the second derivative of production rate with respect to time.

The hyperbolic decline model often results in unrealistically high reserve estimates and a long lifetime since the curve continually flattens with time. In contrast, the exponential decline model yields more conservative reserve estimates and predicts a relatively rapid depletion compared to the hyperbolic decline model (Fattah, 2006).

5.2 Applied Methodology

Conventional practices of decline curve analysis in tight gas reservoirs pose significant technical challenges and may often result in unrealistic production forecasts and inaccurate reserve estimates (Cheng et al., 2008). It is typical for tight gas reservoirs to have production performances with rapid initial decline rates and lengthy transition flow periods. In our model, to account for long-duration transient effects inherent in tight gas reservoirs, the early production data are matched with a hyperbolic decline which later assumes an exponential form. Equations for the combined hyperbolic and exponential production decline used in our model are derived as,

(1) Hyperbolic Decline Segment

The production rate at time t can be expressed as,

$$q = q_i \left(1 + bD_i t\right)^{-1/b}$$

The cumulative production,

$$N_p = \frac{q_i^b}{D_i \left(1-b\right)} \left(q_i^{1-b} - q^{1-b}\right)$$

(2) Exponential Decline Segment

The initial exponential production rate may be obtained by substituting t_o in the rate-time equation describing the hyperbolic decline,

$$q = q_i \left(1 + bD_i t_o\right)^{-1/b}$$

The exponential decline rate, D, which will be constant during the exponential decline segment can be determined by,

$$D = \frac{D_i}{1 + bD_i t_o}$$

A production rate in the exponential decline segment can be expressed as:

$$q = q_i \left(1 + bD_i t_o\right)^{-1/b} \exp\left[\frac{-D_i (t - t_o)}{1 + bD_i t_o}\right]$$

The cumulative production,

$$N_p = \frac{q_i \left(1 + bD_i t_o\right)^{-1/b} - q}{\frac{D_i}{1 + bD_i t_o}}$$

Based on these equations and with the help of the Solver add-in of Excel, production profiles are matched with a decline curve. A VBA code automates the decline curve analysis of thousands of production profiles generated by random simulation runs of the reservoir model. The early production data during Stage 1 is acquired on a monthly basis and matched with a hyperbolic model; whereas, the rest of the performance history is collected on a yearly basis and matched using a hyperbolic decline that becomes exponential once boundary effects are felt **(Fig. 28).**

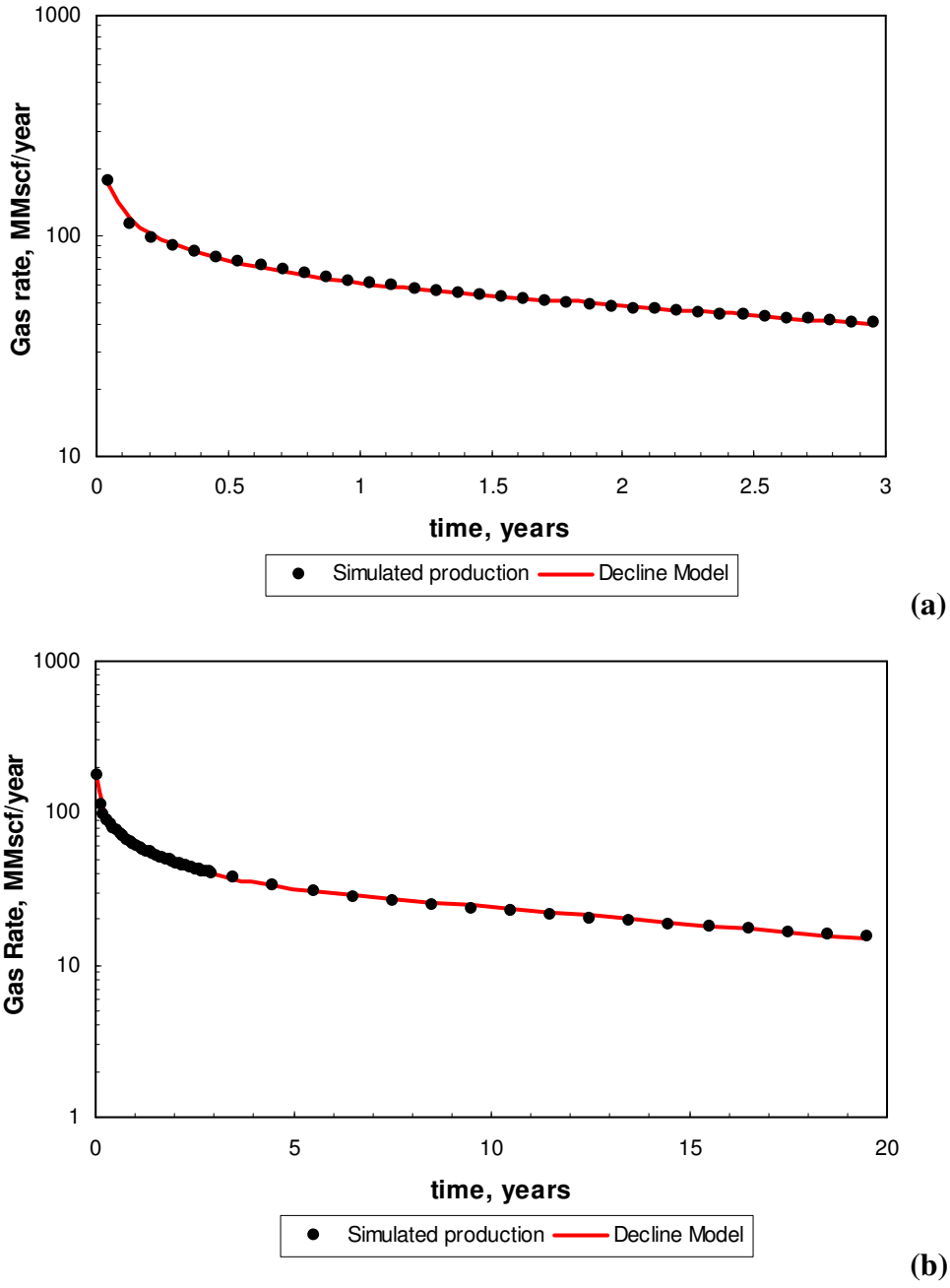

Fig. 28— Example of a simulated production profile from the reservoir model with 3-year stage length: (a) Hyperbolic decline model fitted to the first 3 years of production (b) An early hyperbolic model transitioning to exponential, fitted to the 20 years of production.

Decline parameters of Stage 1 (initial production rate q_i, initial decline rate D_i, and hyperbolic exponent b) and Stage 2 (q_i, D_i, b and transition time t_o) are determined along with their pairwise correlation coefficients to serve as inputs to the decision model.

5.3 Results of Decline Curve Model

As previously mentioned, the reservoir model was run with 1-, 3- and 5-year stages to illustrate how the value of learning about the primary development plan varies with stage length. **Tables 15 through 17** show example decline curve results for stage-lengths of 1, 3 and 5 years, respectively while **Tables 18 through 29** present the important statistics of decline parameters (mean and standard deviation) and pairwise correlation coefficients between Stage 1 and Stage 2.

These statistics (means, standard deviations and correlation coefficients) are input into the decision model. The decision model processes these inputs and yields the optimal development strategy.

The preliminary decision model that will be outlined in the following chapter only uses the initial production rate, q_i in the analysis. **Fig. 29** shows the cumulative distribution plots of the first well's 1 year- and 20 year-q_is (stage length is 1 year). The remaining CDF plots are provided in Appendix E.

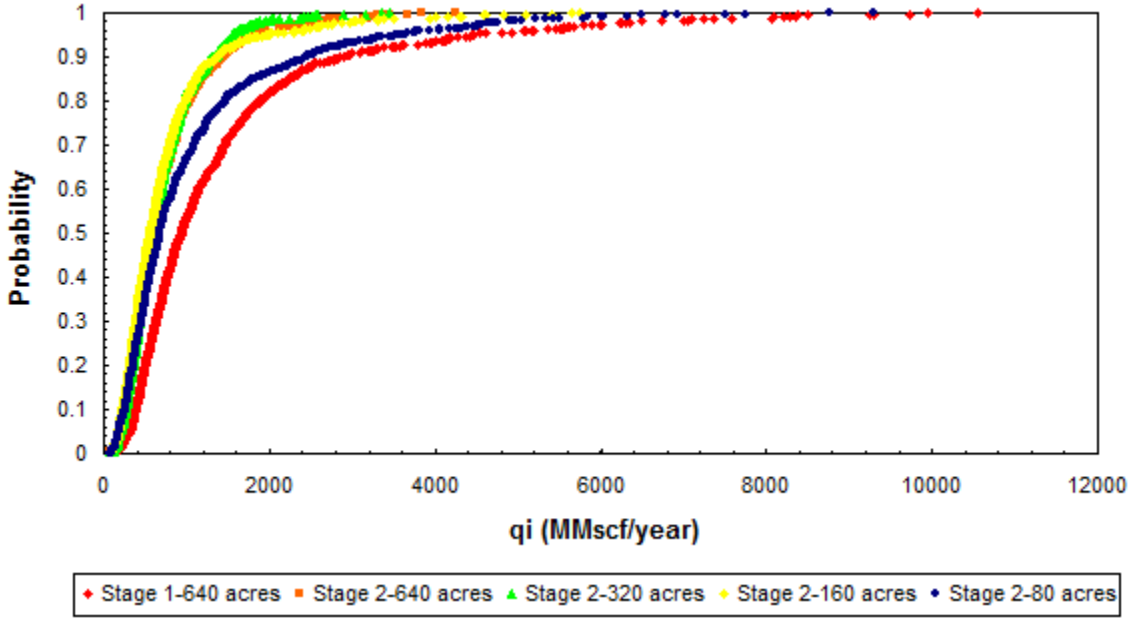

(a)

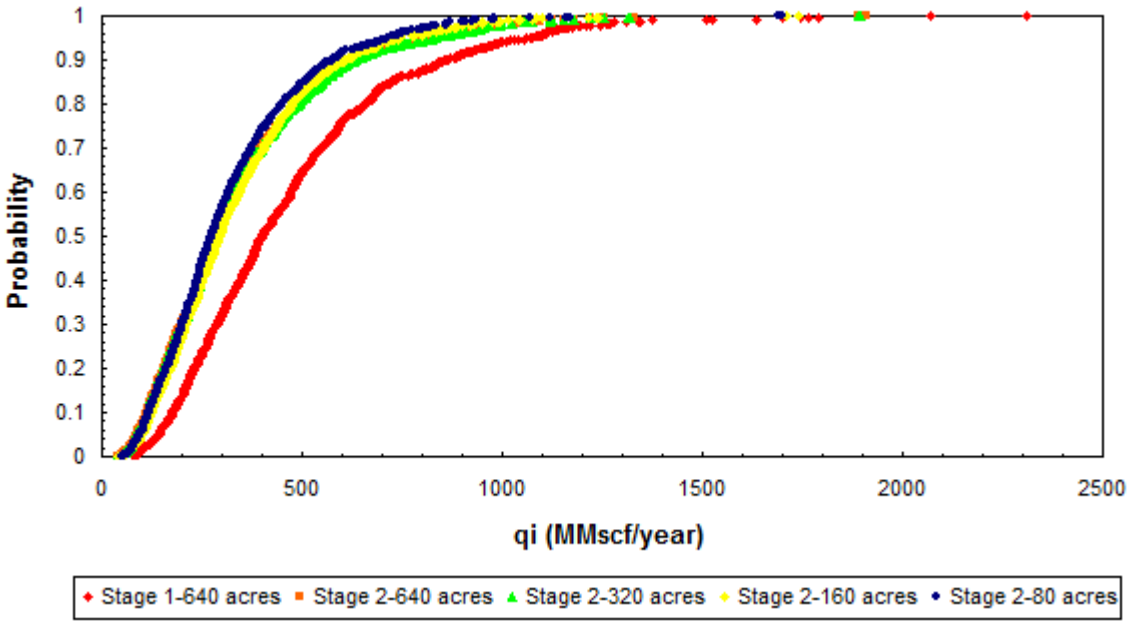

(b)

Fig. 29 — Cumulative distribution plot of qi for Well 1, stage-length of 1 year: (a) 1 year-qi (Stage 1), (b) 20 year-qi (Stage 1 + Stage 2).

Table 15— Example decline curve results of the final reservoir model for a stage length of 1 year. In Stage 1, one well (Well 1) is producing on 640 acre-spacing. In Stage 2, three additional wells are drilled on 160 acre-spacing and represented by Well 3 in simulation.

	Stage 1, Well 1 (640 acres)								Stage 2, Well 3 (160 acres)				
	1st Year Decline Parameters			20-Year Decline Parameters					20-Year Decline Parameters				
Run #	Qi (MMscf/year)	Di (1/year)	b	Qi (MMscf/year)	Di (1/year)	b	to (year)	Dmin (1/year)	Qi (MMscf/year)	Di (1/year)	b	to (year)	Dmin (1/year)
1	2610.745864	12437.60545	4.080451901	443.1460416	4.388831324	2.817587418	8.016332324	0.043831643	387.3400666	3.931397481	1.877686335	4.787463367	0.108181589
2	357.617596	53.66774016	2.21795993	160.745991	3.531827839	1.056512041	5.013307951	0.179219187	278.5837007	3.487353461	1.493808711	4.754628208	0.135331632
3	737.8511804	11.5784229	2.964754744	551.7557544	2.554713899	1.827984776	4.8319219	0.108411509	428.724	3.273691602	1.341723139	4.776484084	0.148938409
4	329.3896343	402.6950761	2.767950425	108.2946198	10.92718119	2.201203662	6.961977398	0.064866639	199.596	2.275061841	1.68319454	4.683181875	0.120159745
5	1076.231152	12.1180792	4.052144909	833.8520052	2.160054308	2.469426254	5.563239862	0.070417765	1663.68	2.433505577	0.907316496	5.665204775	0.180145658
6	811.9982463	17.72808576	2.682857305	545.8470653	3.125486156	1.679991615	4.823894398	0.118707714	346.68	2.83385004	1.206747969	4.885981083	0.160024975
7	4179.785257	8441.633221	4.23893643	795.7367779	3.469568406	2.756887063	7.635248332	0.046865325	1075.272	2.268437992	0.934528853	5.600536627	0.176220923
8	458.7424297	31.71975729	3.899274099	300.6227846	2.955521868	2.470193961	6.098354163	0.064924663	300.084	3.136985617	1.365622661	4.779577167	0.146073339
9	1961.309255	42.60103165	2.020761493	929.316	3.099032954	0.760016044	5.703609826	0.21470671	225.54	3.916066857	1.763683563	19.88824247	0.028303015
10	5790.377856	27896.18748	2.973470292	519.1575563	12.67691497	2.403948782	9.890472276	0.041919806	395.0936507	3.003319193	2.06586021	4.950989935	0.094687841
995	476.1405381	9.836829294	3.723846461	380.0792242	2.231779889	2.320367153	5.207150715	0.079804802	281.892	3.369327149	1.308382253	4.81169796	0.151691312
996	1181.51032	522.7202272	3.423803863	370.0136436	4.80575733	2.327847884	6.339149235	0.066824109	552.42	2.784811947	1.31595938	4.843669236	0.148518617
997	710.975528	20048.59339	3.692724509	98.41934403	7.295663954	2.795006483	8.202784603	0.043357794	124.8041402	5.315827639	2.216109698	6.010564713	0.074029173
998	631.8829809	15105.57089	4.313097259	116.0100582	5.214035135	3.147042529	8.008871888	0.039376201	267.7112891	3.387121812	2.125291637	5.14062563	0.089122075
999	246.8527113	14.06230946	3.23755053	187.9489399	3.175220146	2.166106296	5.188604409	0.086550057	184.961529	6.0664862	2.087335188	5.4535352	0.086593612
1000	1538.594363	10.6887689	2.940211804	1166.449033	2.477243004	1.794743291	4.790932499	0.111084346	786.5366048	8.071281776	1.92946513	5.00155695	0.102309894

	Stage 1, Well 1 (640 acres)								Stage 2, Well 3 (160 acres)				
	1st Year Decline Parameters			20-Year Decline Parameters					20-Year Decline Parameters				
	Qi (MMscf/year)	Di (1/year)	b	Qi (MMscf/year)	Di (1/year)	b	to (year)	Dmin (1/year)	Qi (MMscf/year)	Di (1/year)	b	to (year)	Dmin (1/year)
mean	1417.325454	2745.535707	2.852973224	468.837637	18.02441819	1.801787237	5.820370482	0.11585522	376.034896	5.079640652	1.716431261	5.358470257	0.117998285
std dev	1476.410001	6503.888623	0.708232695	292.4082637	280.4714013	0.648743725	1.469282791	0.058358883	243.6482803	2.70100729	0.426903732	1.392107789	0.039688428
corr coeff				0.272223737	0.277342734	0.880668382			0.086641667	-0.10465795	-0.02899776		
max	10548.5	45496.4	5.4	2312.3	7408.8	3.7	19.8	0.5	1831.8	20.2	2.9	19.9	0.3
min	106.0	5.2	0.9	77.6	1.5	0.4	4.5	0.0	46.0	1.8	0.5	3.9	0.0
mean/std dev	0.959980935	0.422137565	4.028299235	1.603366578	0.064264728	2.777348229	3.961368442	1.985219956	1.543351324	1.880646776	4.020651806	3.849177699	2.973115579
mean-1.28(std dev)	-472.4793477	-5579.44173	1.946435374	94.55505953	-340.978976	0.971395268	3.939688509	0.041155849	64.16509712	1.622351321	1.169994484	3.576572287	0.067197096

Table 16— Example decline curve results of the final reservoir model for a stage length of 3 years. In Stage 1, one well (Well 1) is producing on 640 acre-spacing. In Stage 2, three additional wells are drilled on 160 acre-spacing and represented by Well 3 in simulation.

	Stage 1, Well 1 (640 acres)								Stage 2, Well 3 (160 acres)				
	3-Year Decline Parameters			20-Year Decline Parameters					20-Year Decline Parameters				
Run #	Qi (MMscf/year)	Di (1/year)	b	Qi (MMscf/year)	Di (1/year)	b	to (year)	Dmin (1/year)	Qi (MMscf/year)	Di (1/year)	b	to (year)	Dmin (1/year)
1	415.4361556	5.770857033	2.324747002	355.908	2.823772516	1.887517675	4.480736699	0.113486692	169.356	3.411570166	1.627792424	4.138712803	0.142245781
2	1306.399157	51.95417231	2.026219619	517.3858154	3.576532721	1.260398276	4.393076377	0.171920964	208.98	2.749473342	1.806745272	4.166868144	0.126707778
3	223.5574928	11.45889175	3.074422038	176.4353968	3.674928643	2.548895848	7.701522395	0.050244963	189.096	3.070735441	1.743807884	4.308456076	0.127570961
4	799.9569383	8.727856641	2.408506286	628.224	3.200328774	1.917140629	5.156797952	0.098050994	490.356	3.189784202	1.448366097	4.097682811	0.1600398
5	941.1039175	22.85410564	2.168284329	571.2467531	4.318250982	1.593053639	4.253284718	0.142708605	158.4482944	9.367347005	2.265916539	7.963798628	0.055090176
6	381.8817053	6.420692298	3.459785928	329.724	2.548661231	2.799091636	7.452000483	0.047056177	293.82	2.764300009	1.561012145	4.158199686	0.145926702
7	920.0960058	14.75728215	2.052601671	640.0405751	4.438402137	1.628044171	4.321547931	0.137722509	513.648	1.710402592	0.863079651	5.143261227	0.199056402
8	995.9560181	6.485791095	2.647293107	876.6495655	3.503869824	2.302821793	6.060784358	0.070213354	309.324	3.397867815	1.581415284	4.136121136	0.146300912
9	382.3220906	3.858191184	1.925356055	352.932	2.155792791	1.385491074	4.357795061	0.153809414	222.8655868	3.923731626	1.635446133	4.251839854	0.138724838
10	457.9236134	20.42002442	1.873396975	285.8488569	5.078425242	1.446695995	4.084946392	0.163757594	337.5742644	5.191956213	2.001738663	4.777086114	0.102510654
995	100.9154381	7.47639826	2.542718533	88.59811712	4.138983509	2.243273589	6.025263135	0.072685412	122.3873014	3.577693163	2.056823101	4.833577735	0.097834683
996	291.0298055	6.537158243	1.819176007	247.668	3.048757194	1.334233286	4.269212906	0.165999116	217.102085	3.353666179	1.90491255	4.636867179	0.109516939
997	562.6237996	9.185060643	2.345974333	483.6670275	4.92030023	2.064650637	5.017450865	0.094674352	217.2486379	3.424355965	1.862726487	4.662057065	0.111406178
998	916.1879006	44.99668672	1.981220008	426.024	4.153392529	1.189904821	4.226009373	0.189777954	192.6653908	6.217327969	2.021802162	4.921726836	0.098896329
999	341.3951267	12.06120487	1.810941647	251.22	4.199860074	1.364466859	4.116204783	0.170807957	88.70702143	4.826625218	2.112424925	5.136971063	0.090426952
1000	371.0320272	6.64382471	2.903064412	316.883989	2.987543052	2.444602253	6.957692332	0.057658444	419.4	3.051776635	1.530218888	4.170693716	0.149036799

	Stage 1, Well 1 (640 acres)								Stage 2, Well 3 (160 acres)				
	3-Year Decline Parameters			20-Year Decline Parameters					20-Year Decline Parameters				
	Qi (MMscf/year)	Di (1/year)	b	Qi (MMscf/year)	Di (1/year)	b	to (year)	Dmin (1/year)	Qi (MMscf/year)	Di (1/year)	b	to (year)	Dmin (1/year)
mean	581.2792986	145.4158645	2.220772232	460.7254315	27.29207781	1.790508753	5.660691688	0.121484994	294.2405605	4.471879346	1.82251178	5.101428083	0.117410292
std dev	388.666244	1466.206018	0.675621468	298.9237657	538.5537777	0.651710927	1.633840471	0.061145064	244.0130949	2.213039365	0.39440547	1.447916973	0.042906923
corr coeff				0.806235075	0.87068791	0.974179772			0.345044689	-0.08242712	-0.03046719		
max	4927.0	34903.0	4.4	1866.6	15225.3	3.7	19.9	0.4	2254.9	21.6	2.8	19.9	0.4
min	73.7	1.9	0.4	62.3	1.3	0.3	4.0	0.0	9.5	1.5	0.4	2.7	0.0
mean/std dev	1.495574436	0.09917833	3.28700661	1.541280702	0.050676606	2.747397166	3.464653856	1.986832384	1.205839222	2.020695798	4.62090898	3.523287715	2.736395077
mean-1.28(std dev)	83.78650635	-1731.32784	1.355976753	78.10301143	-662.056758	0.956318767	3.569375885	0.043219311	-18.09620096	1.639188958	1.317672778	3.248094358	0.062489431

Table 17— Example decline curve results of the final reservoir model for a stage length of 5 years. In Stage 1, one well (Well 1) is producing on 640 acre-spacing. In Stage 2, three additional wells are drilled on 160 acre-spacing and represented by Well 3 in simulation.

	Stage 1, Well 1 (640 acres)								Stage 2, Well 3 (160 acres)				
	5-Year Decline Parameters			20-Year Decline Parameters					20-Year Decline Parameters				
Run #	Qi (MMscf/year)	Di (1/year)	b	Qi (MMscf/year)	Di (1/year)	b	to (year)	Dmin (1/year)	Qi (MMscf/year)	Di (1/year)	b	to (year)	Dmin (1/year)
1	604.989061	8.239680019	2.222006365	575.400529	6.812340383	2.154633911	6.502311742	0.070636964	388.716	3.075914915	1.849982425	4.396848721	0.118214497
2	176.873288	5.257100854	1.429970822	176.808	5.029523305	1.386734986	4.166302558	0.167325272	74.96091038	4.82452998	2.337925923	7.26150347	0.058193224
3	498.8269082	2.671253219	3.040292671	494.508	2.365009091	2.889157984	7.194356035	0.04715099	335.5396418	3.41043714	1.921726308	4.696500755	0.107312181
4	522.576	1.788858164	1.77660828	522.576	1.72457547	1.712487191	4.170759606	0.129496352	738.612	2.250928149	0.956286226	5.014397824	0.190859336
5	884.9701548	3.829849108	1.612068317	884.424	3.669682907	1.562750576	4.207246239	0.146041268	103.4064194	74.70355702	2.570539119	8.622766645	0.04508862
6	357.2380548	3.266112103	2.521460479	342.48	2.652700567	2.397171524	6.005179033	0.067693723	502.608	2.247462776	1.037899872	4.8119871	0.18384695
7	664.416	3.166708899	0.866101259	664.416	2.870036105	0.792669369	5.168221222	0.22496589	63.55942264	5.061688961	2.170512015	5.282749948	0.085735097
8	679.8575371	7.181421764	2.239421706	649.0911287	5.980892026	2.168256066	6.227736696	0.073150069	434.256	2.75713338	1.563829291	4.146875992	0.146034399
9	322.4160235	4.767183466	2.534138084	306.5211476	3.769522707	2.417476063	6.823902711	0.059659083	409.392	2.200565049	0.534936763	5.776934926	0.282109442
10	197.649994	6.388314637	2.720379791	182.0800077	4.402726551	2.56145255	7.762548695	0.049725188	146.412	2.600426353	1.613785695	4.175488023	0.140392351
995	322.9284296	6.434465192	2.515068303	302.7934654	4.877522653	2.400430372	7.458685186	0.055220927	342.6292816	8.828479977	1.900295614	4.551020065	0.114135014
996	205.6113981	3.563587057	2.521365432	195.8386408	2.822372298	2.391207137	6.314131021	0.06471358	193.0239493	4.162118771	1.821348481	4.576437053	0.116610611
997	612.6	3.483318784	1.354252223	612.6	3.297149706	1.295953284	4.30230224	0.170100573	250.1079504	3.799396662	1.615341361	3.923216519	0.151502903
998	229.6756715	6.08660963	1.611239536	230.3139173	5.900114825	1.573402043	4.295364188	0.144345489	33.33801579	6.46303959	2.370996003	8.260965609	0.05065486
999	326.664	2.349496075	1.044161025	326.664	2.127380866	0.949305744	5.051837008	0.189904687	333.324	3.807160872	1.57512852	4.195075052	0.145550974
1000	351.7418176	8.100082763	1.902478604	335.9209428	6.901675772	1.841444852	4.376378665	0.12189544	891.672	1.920300062	1.038661022	4.919896459	0.177592872

	Stage 1, Well 1 (640 acres)								Stage 2, Well 3 (160 acres)				
	5-Year Decline Parameters			20-Year Decline Parameters					20-Year Decline Parameters				
	Qi (MMscf/year)	Di (1/year)	b	Qi (MMscf/year)	Di (1/year)	b	to (year)	Dmin (1/year)	Qi (MMscf/year)	Di (1/year)	b	to (year)	Dmin (1/year)
mean	485.8140538	29.71721177	1.914712496	459.298298	17.66057389	1.802754927	5.519220169	0.122939993	247.7718523	4.5434288	1.886092488	5.200177699	0.112115366
std dev	313.1800035	515.7909688	0.684292847	308.3363746	333.6497451	0.64608329	1.469682016	0.062336116	227.0431232	3.348501025	0.393836166	1.549469164	0.042460053
corr coeff				0.974675357	0.955002372	0.993768427			0.365604858	-0.02653814	-0.01185563		
max	2461.3	16182.1	3.9	2461.3	10024.6	3.4	20.0	0.4	2388.2	74.7	2.9	19.9	0.3
min	69.3	1.4	0.4	64.1	1.3	0.4	4.1	0.0	2.6	1.6	0.4	3.0	0.0
mean/std dev	1.551229479	0.057614835	2.798089303	1.489601409	0.052931477	2.790282544	3.755383891	1.972211323	1.091298643	1.356854535	4.789028152	3.356102734	2.640490472
mean-1.28(std dev)	84.94364931	-630.495228	1.038817652	64.62773854	-409.4111	0.975768315	3.638027188	0.043149765	-42.84334541	0.257347488	1.381982195	3.216857168	0.057766498

Table 18— Statistics of decline curve parameters (mean and standard deviation) and pairwise correlation coefficients between Stage 1 and Stage 2 for downspacing combinations of 640-640, 640-320, 640-160 and 640-80 (stage length of 1 year).

	Stage 1, Well 1 (640 acres)			Stage 2, Well 1 (640 acres)				
	1st Year Decline Parameters			20-Year Decline Parameters				
	Qi (MMscf/year)	Di (1/year)	b	Qi (MMscf/year)	Di (1/year)	b	to (year)	Dmin (1/year)
mean	1417.325454	2745.535707	2.852973224	343.1555727	4.484499107	1.90304242	5.755026809	0.11110386
std dev	1476.410001	6503.888623	0.708232695	235.1702862	2.354128475	0.59969143	1.960733681	0.057992586
corr coeff				0.077995968	0.304721863	0.820939605		

	Stage 1, Well 1 (640 acres)			Stage 2, Well 1 (320 acres)					Stage 2, Well 2 (320 acres)				
	1st Year Decline Parameters			20-Year Decline Parameters					20-Year Decline Parameters				
	Qi (MMscf/year)	Di (1/year)	b	Qi (MMscf/year)	Di (1/year)	b	to (year)	Dmin (1/year)	Qi (MMscf/year)	Di (1/year)	b	to (year)	Dmin (1/year)
mean	1417.325454	2745.535707	2.852973224	342.3429646	4.381684839	1.844893989	5.434917597	0.115337908	380.0286546	48.12650189	1.994877593	5.793940534	0.099426452
std dev	1476.410001	6503.888623	0.708232695	234.1481157	1.295915593	0.546051138	1.158981297	0.055173388	247.0786586	880.1403134	0.525878648	1.262092819	0.048913671
corr coeff				0.082952461	0.319002826	0.742729113			0.029826511	0.059907584	0.165993253		

	Stage 1, Well 1 (640 acres)			Stage 2, Well 1 (160 acres)					Stage 2, Well 3 (160 acres)				
	1st Year Decline Parameters			20-Year Decline Parameters					20-Year Decline Parameters				
	Qi (MMscf/year)	Di (1/year)	b	Qi (MMscf/year)	Di (1/year)	b	to (year)	Dmin (1/year)	Qi (MMscf/year)	Di (1/year)	b	to (year)	Dmin (1/year)
mean	1417.325454	2745.535707	2.852973224	339.4088662	5.190551066	1.756079111	5.346518665	0.115432524	376.034896	5.079640652	1.716431261	5.358470257	0.117998285
std dev	1476.410001	6503.888623	0.708232695	211.0952839	3.526969565	0.418217993	1.411561285	0.038905866	243.6482803	2.70100729	0.426903732	1.392107789	0.039688428
corr coeff				0.16367342	0.440108253	0.071211874			0.086641667	-0.10465795	-0.02899776		

	Stage 1, Well 1 (640 acres)			Stage 2, Well 1 (80 acres)					Stage 2, Well 4 (80 acres)				
	1st Year Decline Parameters			20-Year Decline Parameters					20-Year Decline Parameters				
	Qi (MMscf/year)	Di (1/year)	b	Qi (MMscf/year)	Di (1/year)	b	to (year)	Dmin (1/year)	Qi (MMscf/year)	Di (1/year)	b	to (year)	Dmin (1/year)
mean	1417.325454	2745.535707	2.852973224	320.5124769	5.3302376	1.258716002	5.034037555	0.168394617	350.4696269	5.229883699	1.234423123	5.098045331	0.170785748
std dev	1476.410001	6503.888623	0.708232695	198.037214	3.891602954	0.393174269	1.226094305	0.050284693	223.601056	3.8451497	0.408536115	1.150781146	0.051755791
corr coeff				0.18947994	0.552924985	0.028989235			0.112559879	0.017150318	-0.00761268		

Table 19— Statistics of decline curve parameters (mean and standard deviation) and pairwise correlation coefficients between Stage 1 and Stage 2 for downspacing combinations of 320-320, 320-160 and 320-80 (stage length of 1 year).

	Stage 1, Well 2 (320 acres)			Stage 2, Well 2 (320 acres)				
	1st Year Decline Parameters			20-Year Decline Parameters				
	Qi (MMscf/year)	Di (1/year)	b	Qi (MMscf/year)	Di (1/year)	b	to (year)	Dmin (1/year)
mean	1260.617861	1852.531492	2.793315216	330.9932704	4.382637178	1.846951989	5.49488655	0.115771958
std dev	1384.297667	4838.380105	0.635026191	217.9499586	1.449057949	0.567428485	1.347733741	0.057299202
corr coeff				0.187371518	0.420515628	0.887771619		

	Stage 1, Well 2 (320 acres)			Stage 2, Well 2 (160 acres)					Stage 2, Well 3 (160 acres)				
	1st Year Decline Parameters			20-Year Decline Parameters					20-Year Decline Parameters				
	Qi (MMscf/year)	Di (1/year)	b	Qi (MMscf/year)	Di (1/year)	b	to (year)	Dmin (1/year)	Qi (MMscf/year)	Di (1/year)	b	to (year)	Dmin (1/year)
mean	1260.617861	1852.531492	2.793315216	331.6562315	4.61293962	1.713325433	5.149423577	0.122625025	368.6819739	5.008438874	1.721854724	5.316283105	0.118047294
std dev	1384.297667	4838.380105	0.635026191	209.0524148	1.17782453	0.430493697	0.800470542	0.045281897	240.1844923	2.516632446	0.418651282	1.30762142	0.039331516
corr coeff				0.2114321	0.318763385	0.45574339			0.216434609	-0.1707803	0.222598212		

	Stage 1, Well 2 (320 acres)			Stage 2, Well 2 (80 acres)					Stage 2, Well 4 (80 acres)				
	1st Year Decline Parameters			20-Year Decline Parameters					20-Year Decline Parameters				
	Qi (MMscf/year)	Di (1/year)	b	Qi (MMscf/year)	Di (1/year)	b	to (year)	Dmin (1/year)	Qi (MMscf/year)	Di (1/year)	b	to (year)	Dmin (1/year)
mean	1260.617861	1852.531492	2.793315216	311.9238544	5.380223855	1.268979009	4.967582411	0.169185996	343.2427239	5.08021507	1.239711135	5.051593932	0.170889758
std dev	1384.297667	4838.380105	0.635026191	184.4878656	4.096158809	0.393474116	1.045899725	0.053079123	214.2495926	3.26596333	0.404222627	1.038462597	0.051705518
corr coeff				0.320963673	0.696607328	0.297317861			0.364816551	-0.05445479	0.365429005		

Table 20— Statistics of decline curve parameters (mean and standard deviation) and pairwise correlation coefficients between Stage 1 and Stage 2 for downspacing combinations of 160-160 and 160-80 (stage length of 1 year).

	Stage 1, Well 3 (160 acres)			Stage 2, Well 3 (160 acres)				
	1st Year Decline Parameters			20-Year Decline Parameters				
	Qi (MMscf/year)	Di (1/year)	b	Qi (MMscf/year)	Di (1/year)	b	to (year)	Dmin (1/year)
mean	931.637011	467.9336135	2.550808628	320.5928771	4.631699375	1.717984253	5.129644376	0.121957796
std dev	795.7231893	1997.154323	0.317095099	186.2066325	1.162233922	0.420304131	0.747968044	0.043309292
corr coeff				0.416867034	0.185954819	0.814574077		

	Stage 1, Well 3 (160 acres)			Stage 2, Well 3 (80 acres)					Stage 2, Well 4 (80 acres)				
	1st Year Decline Parameters			20-Year Decline Parameters					20-Year Decline Parameters				
	Qi (MMscf/year)	Di (1/year)	b	Qi (MMscf/year)	Di (1/year)	b	to (year)	Dmin (1/year)	Qi (MMscf/year)	Di (1/year)	b	to (year)	Dmin (1/year)
mean	931.637011	467.9336135	2.550808628	298.5873497	4.562552452	1.269784744	4.85691977	0.170816835	339.2811346	5.138004238	1.241648883	5.038260373	0.17070539
std dev	795.7231893	1997.154323	0.317095099	170.0123266	1.444083866	0.388458269	0.320296975	0.052802888	210.9332526	3.35466005	0.401489359	1.041973664	0.051537429
corr coeff				0.446396055	0.428142198	0.684158879			0.426645293	-0.08335355	0.685885313		

Table 21— Statistics of decline curve parameters (mean and standard deviation) and pairwise correlation coefficients between Stage 1 and Stage 2 for downspacing combinations of 80-80 (stage length of 1 year).

	Stage 1, Well 4 (80 acres)			Stage 2, Well 4 (80 acres)				
	1st Year Decline Parameters			20-Year Decline Parameters				
	Qi (MMscf/year)	Di (1/year)	b	Qi (MMscf/year)	Di (1/year)	b	to (year)	Dmin (1/year)
mean	1037.905918	73.91574408	2.183710945	235.3928264	4.729914786	1.335582338	4.738716159	0.16667979
std dev	674.1504223	112.8637855	0.234924767	122.2608855	1.499622347	0.369344376	0.88971759	0.052415262
corr coeff				0.870039588	-0.01467338	0.906601336		

Table 22— Statistics of decline curve parameters (mean and standard deviation) and pairwise correlation coefficients between Stage 1 and Stage 2 for downspacing combinations of 640-640, 640-320, 640-160 and 640-80 (stage length of 3 years).

	Stage 1, Well 1 (640 acres)			Stage 2, Well 1 (640 acres)				
	3-Year Decline Parameters			20-Year Decline Parameters				
	Qi (MMscf/year)	Di (1/year)	b	Qi (MMscf/year)	Di (1/year)	b	to (year)	Dmin (1/year)
mean	581.2792986	145.4158645	2.220772232	228.8042705	10.81902127	2.031741441	5.522539581	0.108100558
std dev	388.666244	1466.206018	0.675621468	169.9352506	154.5379158	0.474227021	2.278895169	0.057475908
corr coeff				0.540825702	0.854786424	0.950010127		

	Stage 1, Well 1 (640 acres)			Stage 2, Well 1 (320 acres)					Stage 2, Well 2 (320 acres)				
	3-Year Decline Parameters			20-Year Decline Parameters					20-Year Decline Parameters				
	Qi (MMscf/year)	Di (1/year)	b	Qi (MMscf/year)	Di (1/year)	b	to (year)	Dmin (1/year)	Qi (MMscf/year)	Di (1/year)	b	to (year)	Dmin (1/year)
mean	581.2792986	145.4158645	2.220772232	227.4747389	4.309346873	1.97866248	5.231155786	0.112167538	301.0245229	38.7262776	2.069884789	5.787289832	0.096955378
std dev	388.666244	1466.206018	0.675621468	168.2603207	13.18252746	0.417240099	1.789202692	0.055064351	278.4089504	543.9133921	0.483138427	1.835540726	0.048527083
corr coeff				0.532545099	0.751657885	0.902840816			0.306940785	-0.00267621	0.134581211		

	Stage 1, Well 1 (640 acres)			Stage 2, Well 1 (160 acres)					Stage 2, Well 3 (160 acres)				
	3-Year Decline Parameters			20-Year Decline Parameters					20-Year Decline Parameters				
	Qi (MMscf/year)	Di (1/year)	b	Qi (MMscf/year)	Di (1/year)	b	to (year)	Dmin (1/year)	Qi (MMscf/year)	Di (1/year)	b	to (year)	Dmin (1/year)
mean	581.2792986	145.4158645	2.220772232	230.5899676	4.637539201	1.902980021	5.111396515	0.112091809	294.2405605	4.471879346	1.82251178	5.101428083	0.117410292
std dev	388.666244	1466.206018	0.675621468	162.8767463	2.587244967	0.343366016	1.682141246	0.040164056	244.0130949	2.213039365	0.39440547	1.447916973	0.042906923
corr coeff				0.548160755	0.358020509	0.114453061			0.345044689	-0.08242712	-0.03046719		

	Stage 1, Well 1 (640 acres)			Stage 2, Well 1 (80 acres)					Stage 2, Well 4 (80 acres)				
	3-Year Decline Parameters			20-Year Decline Parameters					20-Year Decline Parameters				
	Qi (MMscf/year)	Di (1/year)	b	Qi (MMscf/year)	Di (1/year)	b	to (year)	Dmin (1/year)	Qi (MMscf/year)	Di (1/year)	b	to (year)	Dmin (1/year)
mean	581.2792986	145.4158645	2.220772232	220.7119596	5.351706795	1.422207895	4.430289384	0.170360621	282.3521589	4.925212799	1.350614126	4.618035442	0.174377524
std dev	388.666244	1466.206018	0.675621468	150.8391319	4.491025884	0.391054681	1.454778122	0.052868638	225.5642902	3.43985933	0.445104037	1.227653507	0.054202717
corr coeff				0.580192791	0.32253621	0.124424967			0.384970024	-0.04791255	0.022288074		

Table 23— Statistics of decline curve parameters (mean and standard deviation) and pairwise correlation coefficients between Stage 1 and Stage 2 for downspacing combinations of 320-320, 320-160 and 320-80 (stage length of 3 years).

	Stage 1, Well 2 (320 acres)			Stage 2, Well 2 (320 acres)				
	3-Year Decline Parameters			20-Year Decline Parameters				
	Qi (MMscf/year)	Di (1/year)	b	Qi (MMscf/year)	Di (1/year)	b	to (year)	Dmin (1/year)
mean	559.9915417	89.94142642	2.171886807	219.3176703	4.921363496	1.991537118	5.154860229	0.111748951
std dev	375.2221085	963.9178443	0.624443368	159.8290842	30.11693187	0.419970115	1.476801461	0.053836536
corr coeff				0.733493568	0.563743182	0.95705264		

	Stage 1, Well 2 (320 acres)			Stage 2, Well 2 (160 acres)					Stage 2, Well 3 (160 acres)				
	3-Year Decline Parameters			20-Year Decline Parameters					20-Year Decline Parameters				
	Qi (MMscf/year)	Di (1/year)	b	Qi (MMscf/year)	Di (1/year)	b	to (year)	Dmin (1/year)	Qi (MMscf/year)	Di (1/year)	b	to (year)	Dmin (1/year)
mean	559.9915417	89.94142642	2.171886807	220.6653402	4.168806566	1.861611489	4.884177786	0.118432292	285.3295442	4.458998664	1.827720093	5.06241342	0.117029592
std dev	375.2221085	963.9178443	0.624443368	156.8902085	0.932269129	0.324996872	1.322381172	0.042752388	229.3062241	2.151437667	0.387007944	1.276163652	0.041187451
corr coeff				0.726954752	0.010732719	0.460993641			0.369613364	-0.06824618	0.110911349		

	Stage 1, Well 2 (320 acres)			Stage 2, Well 2 (80 acres)					Stage 2, Well 4 (160 acres)				
	3-Year Decline Parameters			20-Year Decline Parameters					20-Year Decline Parameters				
	Qi (MMscf/year)	Di (1/year)	b	Qi (MMscf/year)	Di (1/year)	b	to (year)	Dmin (1/year)	Qi (MMscf/year)	Di (1/year)	b	to (year)	Dmin (1/year)
mean	559.9915417	89.94142642	2.171886807	213.2109216	5.155559829	1.438792798	4.338175038	0.170481617	273.1855965	5.006178529	1.360531213	4.583547219	0.173885691
std dev	375.2221085	963.9178443	0.624443368	144.2495828	3.629037473	0.3741886	1.259245448	0.053914188	218.3728638	3.432401973	0.439144245	1.209521931	0.054035683
corr coeff				0.709006197	0.234899712	0.263623746			0.519235929	-0.03883622	0.162555837		

Table 24— Statistics of decline curve parameters (mean and standard deviation) and pairwise correlation coefficients between Stage 1 and Stage 2 for downspacing combinations of 160-160 and 160-80 (stage length of 3 years).

	Stage 1, Well 3 (160 acres)			Stage 2, Well 3 (160 acres)				
	3-Year Decline Parameters			20-Year Decline Parameters				
	Qi (MMscf/year)	Di (1/year)	b	Qi (MMscf/year)	Di (1/year)	b	to (year)	Dmin (1/year)
mean	553.5476481	10.40736776	2.017442335	197.823603	4.189314839	1.877603769	4.817489584	0.117850566
std dev	349.6321087	15.28311484	0.417705785	109.882807	0.881781382	0.286753213	1.162730758	0.041601648
corr coeff				0.7905628	0.229672389	0.933771538		

	Stage 1, Well 3 (160 acres)			Stage 2, Well 3 (80 acres)					Stage 2, Well 4 (80 acres)				
	3-Year Decline Parameters			20-Year Decline Parameters					20-Year Decline Parameters				
	Qi (MMscf/year)	Di (1/year)	b	Qi (MMscf/year)	Di (1/year)	b	to (year)	Dmin (1/year)	Qi (MMscf/year)	Di (1/year)	b	to (year)	Dmin (1/year)
mean	553.5476481	10.40736776	2.017442335	188.3997357	4.36729383	1.450213388	4.137979384	0.173247018	258.4636938	5.055136843	1.370582292	4.579289266	0.173366312
std dev	349.6321087	15.28311484	0.417705785	102.676301	1.229285182	0.336229309	0.564011319	0.055227196	203.1847485	3.83402701	0.421897471	1.525452308	0.053647398
corr coeff				0.793027281	0.277599158	0.727803544			0.52384636	-0.14742369	0.386324732		

Table 25— Statistics of decline curve parameters (mean and standard deviation) and pairwise correlation coefficients between Stage 1 and Stage 2 for downspacing combinations of 80-80 (stage length of 3 years).

	Stage 1, Well 4 (80 acres)			Stage 2, Well 4 (80 acres)				
	3-Year Decline Parameters			20-Year Decline Parameters				
	Qi (MMscf/year)	Di (1/year)	b	Qi (MMscf/year)	Di (1/year)	b	to (year)	Dmin (1/year)
mean	522.5572019	10.32835129	1.593210461	116.9092495	4.80379468	1.61915838	4.038033409	0.161353508
std dev	322.9292143	6.861598773	0.483950197	60.2836749	1.248891941	0.24830814	1.247064849	0.053829103
corr coeff				0.663889726	0.52470373	0.933279135		

Table 26— Statistics of decline curve parameters (mean and standard deviation) and pairwise correlation coefficients between Stage 1 and Stage 2 for downspacing combinations of 640-640, 640-320, 640-160 and 640-80 (stage length of 5 years).

	Stage 1, Well 1 (640 acres)			Stage 2, Well 1 (640 acres)				
	5-Year Decline Parameters			20-Year Decline Parameters				
	Qi (MMscf/year)	Di (1/year)	b	Qi (MMscf/year)	Di (1/year)	b	to (year)	Dmin (1/year)
mean	485.8140538	29.71721177	1.914712496	175.3291377	6.926296197	2.119121265	5.633505441	0.101059478
std dev	313.1800035	515.7909688	0.684292847	139.885264	91.03236405	0.427833457	2.477021128	0.053593724
corr coeff				0.571008684	0.991858869	0.962650383		

	Stage 1, Well 1 (640 acres)			Stage 2, Well 1 (320 acres)					Stage 2, Well 2 (320 acres)				
	5-Year Decline Parameters			20-Year Decline Parameters					20-Year Decline Parameters				
	Qi (MMscf/year)	Di (1/year)	b	Qi (MMscf/year)	Di (1/year)	b	to (year)	Dmin (1/year)	Qi (MMscf/year)	Di (1/year)	b	to (year)	Dmin (1/year)
mean	485.8140538	29.71721177	1.914712496	174.896954	5.923618678	2.064659417	5.335553419	0.104965859	259.0760912	26.4871274	2.144917899	5.787371169	0.09285755
std dev	313.1800035	515.7909688	0.684292847	139.9080261	59.40489093	0.366260373	2.012829382	0.051372421	244.2412383	344.2703107	0.480491641	1.552647066	0.047567712
corr coeff				0.567182521	0.062590124	0.934161106			0.265751468	-0.00268877	0.134946232		

	Stage 1, Well 1 (640 acres)			Stage 2, Well 1 (160 acres)					Stage 2, Well 3 (160 acres)				
	5-Year Decline Parameters			20-Year Decline Parameters					20-Year Decline Parameters				
	Qi (MMscf/year)	Di (1/year)	b	Qi (MMscf/year)	Di (1/year)	b	to (year)	Dmin (1/year)	Qi (MMscf/year)	Di (1/year)	b	to (year)	Dmin (1/year)
mean	485.8140538	29.71721177	1.914712496	176.9792909	4.770236285	1.987621407	5.182147657	0.105230611	247.7718523	4.5434288	1.886092488	5.200177699	0.112115366
std dev	313.1800035	515.7909688	0.684292847	132.6307907	3.027140078	0.323677206	1.622269907	0.03760409	227.0431232	3.348501025	0.393836166	1.549469164	0.042460053
corr coeff				0.525278847	0.210731273	0.055955881			0.365604858	-0.02653814	-0.01185563		

	Stage 1, Well 1 (640 acres)			Stage 2, Well 1 (80 acres)					Stage 2, Well 4 (80 acres)				
	5-Year Decline Parameters			20-Year Decline Parameters					20-Year Decline Parameters				
	Qi (MMscf/year)	Di (1/year)	b	Qi (MMscf/year)	Di (1/year)	b	to (year)	Dmin (1/year)	Qi (MMscf/year)	Di (1/year)	b	to (year)	Dmin (1/year)
mean	485.8140538	29.71721177	1.914712496	171.0471923	5.245958231	1.508736662	4.35156934	0.163394297	243.1239173	5.028070724	1.407440901	4.591847451	0.168880334
std dev	313.1800035	515.7909688	0.684292847	128.0886527	3.773129772	0.384298168	1.299525172	0.054593831	225.6225626	3.704931512	0.439550538	1.315822539	0.056165562
corr coeff				0.532135947	0.184600245	0.062968802			0.403547946	-0.0304221	-0.02054983		

Table 27— Statistics of decline curve parameters (mean and standard deviation) and pairwise correlation coefficients between Stage 1 and Stage 2 for downspacing combinations of 320-320, 320-160 and 320-80 (stage length of 5 years).

	Stage 1, Well 2 (320 acres)			Stage 2, Well 2 (320 acres)				
	5-Year Decline Parameters			20-Year Decline Parameters				
	Qi (MMscf/year)	Di (1/year)	b	Qi (MMscf/year)	Di (1/year)	b	to (year)	Dmin (1/year)
mean	479.3151368	8.500446252	1.859945013	163.1803929	4.090240011	2.078071211	5.400943194	0.103871558
std dev	320.841138	62.76197864	0.628207014	118.9712655	1.550732291	0.357795263	2.229821079	0.052480874
corr coeff				0.558766382	0.445432594	0.971386068		

	Stage 1, Well 2 (320 acres)			Stage 2, Well 2 (160 acres)					Stage 2, Well 3 (160 acres)				
	5-Year Decline Parameters			20-Year Decline Parameters					20-Year Decline Parameters				
	Qi (MMscf/year)	Di (1/year)	b	Qi (MMscf/year)	Di (1/year)	b	to (year)	Dmin (1/year)	Qi (MMscf/year)	Di (1/year)	b	to (year)	Dmin (1/year)
mean	479.3151368	8.500446252	1.859945013	164.6139255	4.283546019	1.953463311	4.941789511	0.111392283	242.4828292	4.572464847	1.891497035	5.185836648	0.111661219
std dev	320.841138	62.76197864	0.628207014	118.8282325	0.967019756	0.292555324	1.213660181	0.043054179	225.8211266	2.285859054	0.389837921	1.403102098	0.042389849
corr coeff				0.547739607	0.01570099	0.392848259			0.332550232	-0.05241105	0.053149647		

	Stage 1, Well 2 (320 acres)			Stage 2, Well 2 (80 acres)					Stage 2, Well 4 (80 acres)				
	5-Year Decline Parameters			20-Year Decline Parameters					20-Year Decline Parameters				
	Qi (MMscf/year)	Di (1/year)	b	Qi (MMscf/year)	Di (1/year)	b	to (year)	Dmin (1/year)	Qi (MMscf/year)	Di (1/year)	b	to (year)	Dmin (1/year)
mean	479.3151368	8.500446252	1.859945013	159.2867735	5.336341334	1.523176203	4.230308011	0.163328033	236.4673815	5.049740833	1.417061344	4.500864329	0.168823455
std dev	320.841138	62.76197864	0.628207014	109.5767332	3.899764133	0.358572577	0.81545058	0.054072716	218.1246319	3.858261302	0.431007122	0.991305726	0.05405207
corr coeff				0.508686789	0.143233227	0.158508906			0.512434412	-0.02947199	0.132985969		

Table 28— Statistics of decline curve parameters (mean and standard deviation) and pairwise correlation coefficients between Stage 1 and Stage 2 for downspacing combinations of 160-160 and 160-80 (stage length of 5 years).

	Stage 1, Well 3 (160 acres)			Stage 2, Well 3 (160 acres)				
	5-Year Decline Parameters			20-Year Decline Parameters				
	Qi (MMscf/year)	Di (1/year)	b	Qi (MMscf/year)	Di (1/year)	b	to (year)	Dmin (1/year)
mean	478.5713852	5.549329094	1.71271402	138.7045337	4.332962622	1.983136409	4.939411211	0.109244443
std dev	308.570522	5.69527044	0.49232269	79.35779206	0.945920571	0.257564713	1.225447191	0.040314353
corr coeff				0.556777192	0.326848876	0.969623649		

	Stage 1, Well 3 (160 acres)			Stage 2, Well 3 (80 acres)					Stage 2, Well 4 (80 acres)				
	5-Year Decline Parameters			20-Year Decline Parameters					20-Year Decline Parameters				
	Qi (MMscf/year)	Di (1/year)	b	Qi (MMscf/year)	Di (1/year)	b	to (year)	Dmin (1/year)	Qi (MMscf/year)	Di (1/year)	b	to (year)	Dmin (1/year)
mean	478.5713852	5.549329094	1.71271402	132.5096783	4.517508136	1.546207951	4.133422964	0.163253656	217.9034305	5.037750021	1.438539236	4.462805719	0.167548176
std dev	308.570522	5.69527044	0.49232269	74.00262308	1.335080694	0.313786457	0.815618414	0.052962768	208.3574471	3.350374099	0.41591677	1.112022204	0.054758275
corr coeff				0.55033082	0.397354949	0.78100275			0.391869267	-0.20560503	0.374233963		

Table 29— Statistics of decline curve parameters (mean and standard deviation) and pairwise correlation coefficients between Stage 1 and Stage 2 for downspacing combinations of 80-80 (stage length of 5 years).

	Stage 1, Well 4 (80 acres)			Stage 1, Well 4 (80 acres)				
	5-Year Decline Parameters			20-Year Decline Parameters				
	Qi (MMscf/year)	Di (1/year)	b	Qi (MMscf/year)	Di (1/year)	b	to (year)	Dmin (1/year)
mean	447.3407145	4.3990145	1.249097065	72.93520615	5.04828331	1.740665617	4.079123001	0.148007864
std dev	312.3629193	2.059627729	0.448752208	42.60404376	1.343717336	0.215874448	1.009873844	0.049779749
corr				0.280279248	0.695493083	0.970189451		

CHAPTER VI
DECISION MODEL

The research team led by Dr. Eric Bickel (Industrial & Systems Engineering Department in University of Texas at Austin, UT) developed a practical and flexible decision model to evaluate a variety of two-stage development scenarios and assess the full spectrum of potential economic outcomes.

The model follows a practical approach for capturing the dependence between these stages and determines an optimal strategy that exploits the information provided by primary stage production results from the reservoir simulation. Production results are integrated to the decision model using the decline curve analysis approach described in the previous chapter **(Fig. 30).**

To fully model dependence between primary and secondary development plans, joint probability distributions of the decline parameters are constructed from a set of pairwise probability and correlation assessments. These distributions are then used to calculate the expected net present value which will form the basis of our decision.

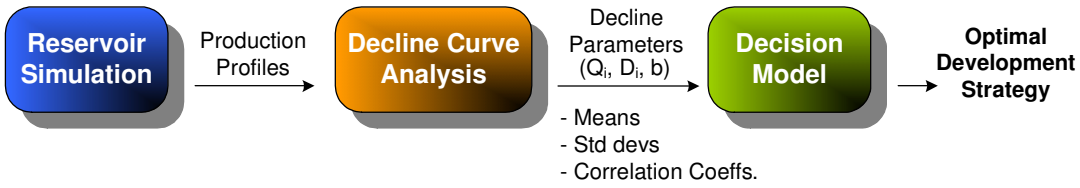

Fig. 30— Schematic outlining the approach used in the decision model. Production profiles from the reservoir simulation are input into the decline curve analysis to generate the decline parameters. Means, standard deviations and correlation coefficients of the decline parameters are then calculated and input into the decision model. The decision model processes these inputs and yields the optimal development strategy.

This chapter briefly describes the decision model employed in this work and provides the results obtained from the model. The preliminary decision model that will be outlined in the following section only uses the initial production rate, q_i in the analysis and evaluates only the 1-year and 3-year results.

6.1 Methodology

When making sequential development decisions, one needs to capture the dependence between stages and use the primary production results to make more informed decisions for the next stages. **Fig. 31** shows the influence diagram for the decision on the development plan of the Berland River area. The net present value (NPV) is the objective variable, i.e., the quantitative criterion that will be maximized. In other words, the decision model selects the optimal development strategy with the objective of maximizing profitability. The optimal strategy consists of optimal primary and secondary well spacings which are decision variables in the influence diagram. Decline parameters provided in terms of probability distributions are the uncertain variables used in calculation of the expected NPV. **Fig. 32** shows a partial decision tree which demonstrates the structure of the sequential development program.

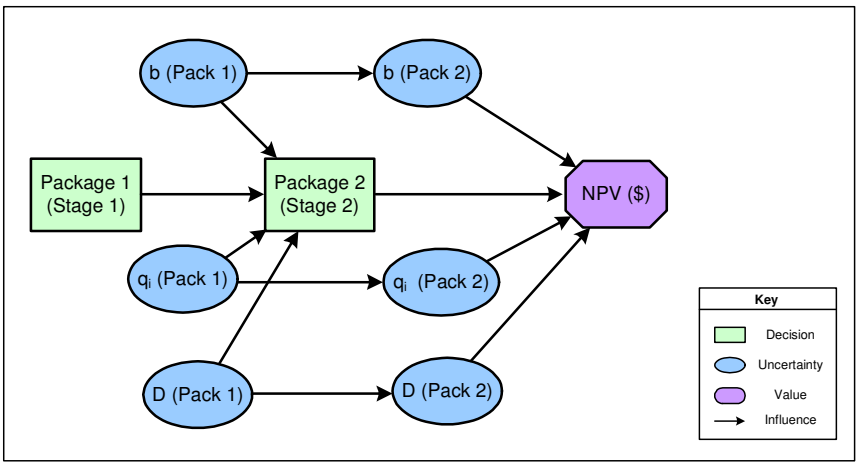

Fig. 31— Influence diagram for the Berland River area development plan decision.

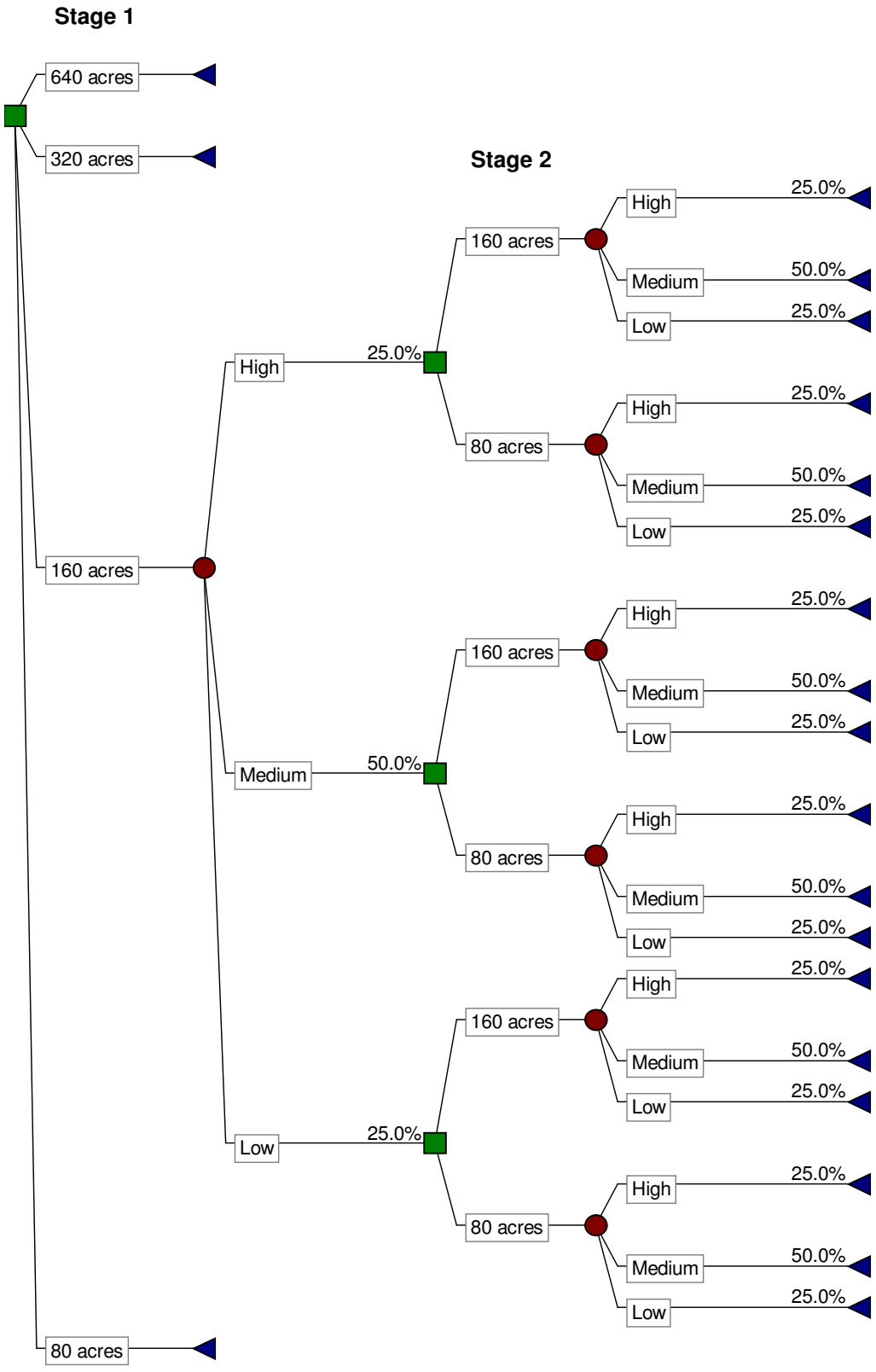

Fig. 32— Partial decision tree for the Berland River area development plan.

The decline curve analysis results indicate that the initial production rates are log-normally distributed (Fig. 29). Therefore, first stage q_i values are transformed to fit a log-normal distribution by using the following equations,

$$mean = e^{\left(\mu + \frac{\sigma^2}{2}\right)}$$

$$std.dev = \left(e^{\sigma^2} - 1\right)\left(e^{2\mu+\sigma^2}\right)$$

The 90th, 50th and 10th percentiles (P90, P50 and P10) are also computed, which represent high, medium and low production rates at Stage 1 and are assigned with probabilities of 25%, 50% and 25%, respectively. These percentiles along with the pairwise correlation coefficients will be used in computing the conditional means and standard deviations of Stage 2 given Stage 1 to construct the joint probability distributions. The following equations are used in this calculation,

$$\mu_{x|y} = \mu_x + \rho\frac{\sigma_x}{\sigma_y}\left(y - \mu_y\right)$$

$$\sigma^2{}_{x|y} = \left(1 - \rho^2\right)\sigma_x{}^2$$

After specifying the joint probability distribution of q_i over all possible combinations of outcomes, the corresponding cumulative productions are calculated at a discount rate of 10%. Based on the discounted cumulative production and price environment, the expected net present value (NPV) of future cash flows is determined for each scenario.

6.2 Results of the Decision Model

The decision model has been employed in two different price environments (low and high) and results for each scenario are analyzed and compared. **Table 30** shows the low price environment where gas price, marginal costs, fixed costs, drilling cost and discount rate are the major parameters. Based on these values, the decision model calculates the expected NPV for each scenario and selects the one with the highest.

Table 30— Low price environment.

Parameter	Units	Value
Gas Price	$/MCF	**5.50**
Marginal Costs	$/MCF	**1.00**
Fixed Costs	MM $/yr/well	**0.05**
Drilling Cost	MM $/well	**1.00**
Discout Rate		**0.10**

Table 31 shows the decision model results in the low price environment, for stage length of 1 year. Results indicate that if the initial production q_i is high, the downspacing alternative that maximizes NPV is the 160 acre-spacing. This means that, the optimal strategy is to start development on 640 acres and downspace to 160 acres if high production is observed. However, if production is low, continuing development on 640 acres would be the best choice. It is worthwhile to mention that, the dynamic 640-acre strategy is better than the static 160-acre strategy by $660K (i.e., $2.09MM - $1.43MM = $0.66MM).

Similarly, **Table 32** outlines the decision model results in the low price environment, for stage length of 3 years. It is seen that for the primary stage, development on 640 acres and for the secondary stage downspacing to 160 acres should be selected.

Table 31— Decision model results showing the optimal development plan in low price environment. Stage length is 1 year.

			Stage 2					
Stage 1	Prob	Qi	640	320	160	80	Opt D	Value
640	0.25	H	$4.2	$3.4	$4.9	$0.1	160	$4.9
$2.09	0.5	M	$1.5	$0.7	$1.4	($3.6)	640	$1.5
	0.25	L	$0.4	($0.5)	($0.3)	($5.6)	640	$0.4

			Stage 2					
Stage 1	Prob	Qi	640	320	160	80	Opt D	Value
320	0.25	H		$3.0	$4.5	($0.4)	160	$4.5
$1.72	0.5	M		$0.6	$1.4	($3.7)	160	$1.4
	0.25	L		($0.5)	($0.3)	($5.6)	160	($0.3)

			Stage 2					
Stage 1	Prob	Qi	640	320	160	80	Opt D	Value
160	0.25	H			$3.7	($1.1)	160	$3.7
$1.43	0.5	M			$1.2	($3.9)	160	$1.2
	0.25	L			($0.4)	($5.6)	160	($0.4)

			Stage 2					
Stage 1	Prob	Qi	640	320	160	80	Opt D	Value
80	0.25	H				($0.3)	80	($0.3)
($3.27)	0.5	M				($3.6)	80	($3.6)
	0.25	L				($5.5)	80	($5.5)

Comparing the results for stage lengths of 1 year and 3 years, it is seen that the expected NPVs for a 3-year stage is lower than a 1-year stage. Regardless, the dynamic (640-acre) strategy is still better than the static (160-acre) strategy (i.e., $0.72MM - $0.63MM = $0.09MM).

Next, the decision model is employed in the high price environment **(Table 33),** for stage length of 1 year. The decision model results indicate that, selecting 640-acre spacing for the primary stage and downspacing to 160-acre is the best option, unless low initial production is observed **(Table 34).**

However, in the high price environment and for a stage length of 3 years, the optimal development strategy is to start development on 160 acre-spacing and not to downspace **(Table 35).**

Table 32— Decision model results showing the optimal development plan in low price environment. Stage length is 3 years.

			Stage 2					
Stage 1	Prob	Qi	640	320	160	80	Opt D	Value
640	0.25	H	$1.4	$1.4	$3.4	($1.0)	160	$3.4
$0.72	0.5	M	$0.0	($0.4)	($0.0)	($4.8)	640	$0.0
	0.25	L	($0.6)	($1.4)	($2.1)	($7.2)	640	($0.6)

			Stage 2					
Stage 1	Prob	Qi	640	320	160	80	Opt D	Value
320	0.25	H		$1.4	$3.4	($0.9)	160	$3.4
$0.48	0.5	M		($0.4)	($0.0)	($4.8)	160	($0.0)
	0.25	L		($1.4)	($2.1)	($7.2)	320	($1.4)

			Stage 2					
Stage 1	Prob	Qi	640	320	160	80	Opt D	Value
160	0.25	H			$4.0	($0.3)	160	$4.0
$0.63	0.5	M			$0.2	($4.6)	160	$0.2
	0.25	L			($2.0)	($7.0)	160	($2.0)

			Stage 2					
Stage 1	Prob	Qi	640	320	160	80	Opt D	Value
80	0.25	H				($0.6)	80	($0.6)
($4.26)	0.5	M				($4.7)	80	($4.7)
	0.25	L				($7.1)	80	($7.1)

Table 33— High price environment.

Parameter	Units	Value
Gas Price	$/MCF	**9.00**
Marginal Costs	$/MCF	**1.00**
Fixed Costs	MM $/yr/well	**0.05**
Drilling Cost	MM $/well	**2.00**
Discout Rate		**0.10**

Table 34— Decision model results showing the optimal development plan in high price environment. Stage length is 1 year.

			Stage 2					
Stage 1	Prob	Qi	640	320	160	80	Opt D	Value
640	0.25	H	$7.6	$6.4	$9.4	$1.3	160	$9.4
$4.14	0.5	M	$2.8	$1.5	$3.2	($5.2)	160	$3.2
	0.25	L	$0.8	($0.6)	$0.0	($8.7)	640	$0.8

			Stage 2					
Stage 1	Prob	Qi	640	320	160	80	Opt D	Value
320	0.25	H		$5.6	$8.6	$0.5	160	$8.6
$3.66	0.5	M		$1.4	$3.0	($5.4)	160	$3.0
	0.25	L		($0.6)	$0.0	($8.7)	160	$0.0

			Stage 2					
Stage 1	Prob	Qi	640	320	160	80	Opt D	Value
160	0.25	H			$7.3	($0.8)	160	$7.3
$3.14	0.5	M			$2.7	($5.7)	160	$2.7
	0.25	L			($0.1)	($8.7)	160	($0.1)

			Stage 2					
Stage 1	Prob	Qi	640	320	160	80	Opt D	Value
80	0.25	H				$0.6	80	$0.6
($4.60)	0.5	M				($5.2)	80	($5.2)
	0.25	L				($8.6)	80	($8.6)

Table 35— Decision model results showing the optimal development plan in high price environment. Stage length is 3 years.

			Stage 2					
Stage 1	Prob	Qi	640	320	160	80	Opt D	Value
640	0.25	H	$2.6	$2.7	$6.6	($0.5)	160	$6.6
$1.67	0.5	M	$0.2	($0.5)	$0.5	($7.4)	160	$0.5
	0.25	L	($1.0)	($2.2)	($3.1)	($11.5)	640	($1.0)

			Stage 2					
Stage 1	Prob	Qi	640	320	160	80	Opt D	Value
320	0.25	H		$2.8	$6.7	($0.4)	160	$6.7
$1.38	0.5	M		($0.5)	$0.5	($7.4)	160	$0.5
	0.25	L		($2.2)	($3.1)	($11.5)	320	($2.2)

			Stage 2					
Stage 1	Prob	Qi	640	320	160	80	Opt D	Value
160	0.25	H			$7.8	$0.7	160	$7.8
$1.72	0.5	M			$1.0	($6.9)	160	$1.0
	0.25	L			($2.9)	($11.3)	160	($2.9)

			Stage 2					
Stage 1	Prob	Qi	640	320	160	80	Opt D	Value
80	0.25	H				$0.2	80	$0.2
($6.35)	0.5	M				($7.1)	80	($7.1)
	0.25	L				($11.4)	80	($11.4)

In this chapter, a practical and flexible framework was presented which fully models the dependence between development stages and decides on the next stage based on the previous stage information. The decision model presented herein provides quick recommendations to operators on development strategies and will prove to be useful in determining an optimal development strategy.

CHAPTER VII
CONCLUSIONS AND RECOMMENDATIONS

7.1 Conclusions

In this work, we developed a probabilistic reservoir model which allows prediction of production profiles under different development scenarios. These production profiles are integrated to a Bayesian decision model and allow calculation of the expected net present value for each scenario. To facilitate the integration of the reservoir and decision models, the simulated production profiles are fit with decline curves and the corresponding decline parameters are determined to serve as inputs to the decision model. The model distinguishes itself from existing technologies, by its speed, cost-effectiveness, ability to model production uncertainty and spatial dependence between wells. The integration of Monte Carlo techniques with reservoir simulations yields random combinations of the uncertain parameters, hence to permit the modeling of reservoir heterogeneity.

A VBA code was developed which allowed thousands of simulations to be performed automatically; thereby providing a full spectrum of production profiles. Incorporation of these production profiles to the decision model rendered a tool that can offer recommendations to operators on selecting the optimal development strategy with the objective of maximizing profitability.

The reservoir and decision modeling tools developed in this project were applied to UGR's tight gas assets in Berland River, Alberta to determine the optimal well spacing in the area. The decision context modeled consisted of 2 development decisions: the primary and secondary well spacings. In particular, the plan is to start development on a specific well spacing (Stage 1) and then decide on whether to downspace or not (Stage 2) based on the primary production results. Also, to understand the trade-off between Stage 1 duration and spacing, results were evaluated for 2 different stage lengths (1- and 3- year).

The decision model was employed in two different price environments: In a low price environment, for both 1 and 3 year-stage lengths, the optimal strategy is 640 acres to start and then downspace to 160 acres if high production is observed. When a higher price environment is considered, for stage length of 1 yr, the optimal strategy is to select 640 acres for primary stage and then downspace to 160 acres unless low production is observed. On the other hand, again in the high price environment but for stage length of 3 yrs, the optimal strategy is to start development on 160-acre spacing and not to downspace. In terms of profitability, in the low price environment, the expected NPVs for a 3-year stage are lower than a 1-year stage; however, the opposite holds for the high price environment.

7.2 Limitations

As with any modeling approach, the method presented in this study is also based on certain approximations. These approximations are the major cause for divergence of the model from the real case. Some limitations of the probabilistic reservoir model developed in this study are as follows: (1) The current single-well approach can model the reservoir heterogeneity to a certain extent but it cannot provide a full representation. (2) Pressure interference between wells cannot be modeled perfectly. (3) While the reservoir model is built based on the assumption that at most 8 wells will be drilled in a section due to lengthy simulation times, only 4 representative wells are modeled. However, modeling all the wells would yield more precise results.

7.3 Recommended Future Work

The reservoir model can be improved to model completion efficiency (stimulation failure) in more detail and the developed tool can be extended to yield the optimal well completion strategy in addition to the primary and secondary optimal well spacings.

The reservoir model can be applied to other fields to confirm and extends functionality. Once the model's applicability on other fields is verified and after further

refinements, the tools and methods developed in this project may be transformed into a fully functional and flexible software module used for determining optimal development strategies for unconventional tight gas reservoirs.

In future research, a multi-well model approach can be investigated to better model the reservoir heterogeneity and the pressure interference between Stage 1 and Stage 2 wells.

NOMENCLATURE

a = the range beyond which variogram remains essentially constant, m

a_0 = regression coefficient used in the moving window technology

a_1 = regression coefficient used in the moving window technology

a_2 = regression coefficient used in the moving window technology

a_3 = regression coefficient used in the moving window technology

a_C = main diagonal of coefficient Matrix A, scf . cp/psi^2 . D

a_N, a_W = north and west flow coefficient, scf . cp/psi^2 . D

a_E, a_S = east and south flow coefficient, scf . cp/psi^2 . D

A = well spacing, acre

b = hyperbolic exponent

B = formation volume factor, reservoir ft^3/scf

BY = best 12 consecutive months of production divided by 12, MSCM/M

c_t = total system compressibility, psi^{-1}

C_0 = nugget

C_1 = difference between sill and nugget

C_1 = intermediate result in the reservoir model of moving window technology

C_2 = intermediate result in the reservoir model of moving window technology

C_3 = intermediate result in the reservoir model of moving window technology

$C(h)$ = covariance function

d = right-side column vector of the 2D flow equation

D = decline rate, 1/year

Di = initial decline rate, 1/year

F_{cD} = dimensionless fracture conductivity

Gp = cumulative production, standard cubic feet

h = lag distance between pairs, ft

h = net pay thickness, ft

J' = well index

k = permeability, md

k_{gas} = gas permeability, md

k_f = fracture permeability, md

L_f = fracture length, ft

Np = cumulative production, MMscf

p = the vector of well block pressure, psi

pi = initial reservoir pressure, psia

p_p = real-gas pseudopressure, m/Lt^3 , psi^2/cp

pwf = flowing bottomhole pressure, psi

$p^n_{pi,j}$ = real-gas pseudopressure in (i,j) grid at n time step, m/Lt^3 , psi^2/cp

$p^{n+1}_{pi,j-1}$ = real-gas pseudopressure in (i,j-1) grid at n+1 time step, m/Lt^3 , psi^2/cp

$p^{n+1}_{pi-1,j}$ = real-gas pseudopressure in (i-1,j) grid at n+1 time step, m/Lt^3 , psi^2/cp

$p^{n+1}_{pi,j}$ = real-gas pseudopressure in (i,j) grid at n+1 time step, m/Lt^3 , psi^2/cp

$p^{n+1}_{pi+1,j}$ = real-gas pseudopressure in (i+1,j) grid at n+1 time step, m/Lt^3 , psi^2/cp

$p^{n+1}_{pi,j+1}$ = real-gas pseudopressure in (i,j+1) grid at n+1 time step, m/Lt^3 , psi^2/cp

q = production rate, Mscf/D

q_i = initial production rate, Mscf/D

r_o = equivalent radius of well gridblock, L, ft

r_w = wellbore radius, L, ft

s = skin factor, dimensionless

t_o = transition time, years

T = temperature, T, ºR

T_{sc} = temperature at standard condition, ºR

Δt = timestep, t, days

V_p = pore volume of gridblock, L^3, ft^3

VBY = virgin best year, MSCM/M

α = coefficient in the a_C equation

$\rho(h)$ = correlation function

$\gamma(h)$ = semi-variogram

μ = viscosity, cp

ϕ = porosity, fraction

w = fracture width, ft

z = z factors

REFERENCES

Cheng, Y., Lee, W.J., and McVay, D.A. 2008a. Improving Reserves Estimates from Decline-Curve Analysis of Tight and Multilayer Gas Wells. *SPE Reservoir Evaluation & Engineering* **11** (5): 912-920. SPE-108176-PA. doi: 10.2118/108176-PA.

Cheng, Y., McVay, D.A., and Lee, J.W. 2006b. Optimal Infill Drilling Design for Marginal Gas Reservoirs Using a Simulation-Based Inversion Approach. Paper SPE 104574 presented at the SPE Eastern Regional Meeting, Canton, Ohio, USA, 11-13 October.

Cheng, Y., McVay, D.A., Wang, J. et al. 2006a. Simulation-Based Technology for Rapid Assessment of Redevelopment Potential in Stripper-Gas-Well Fields: Technology Advances and Validation in the Garden Plains Field, Western Canada Sedimentary Basin. Paper SPE 100583 presented at the SPE Gas Technology Symposium, Calgary, Alberta, Canada, 15-17 May.

Cheng, Y., McVay, D.A., Wang, J. et al. 2008b. Simulation-Based Technology for Rapid Assessment of Redevelopment Potential in Marginal Gas Fields--Technology Advances and Validation in Garden Plains Field, Western Canada Sedimentary Basin. *SPE Reservoir Evaluation & Engineering* **11** (3): 521-534. SPE-100583-PA. doi: 10.2118/100583-PA.

Cipolla, C.L. and Wood, M.C. 1996. A Statistical Approach to Infill-Drilling Studies: Case History of the Ozona Canyon Sands. *SPE Reservoir Engineering* **11** (3): 196-202. SPE-35628-PA. doi: 10.2118/35628-PA.

Fattah, K.A., 2006. Predicting Production Performance Using a Simplified Model. *World Oil*. April: 147-150.

Gao, H. and McVay, D.A. 2004. Gas Infill Well Selection Using Rapid Inversion Methods. Paper SPE 90545 presented at the Annual Technical Conference and Exhibition, Houston, Texas, 26-29 September.

Guan, L. and Du, Y. 2004. Fast Method Finds Infill Drilling Potentials in Mature-Tight Reservoirs. Paper SPE 91755 presented at the SPE International Petroleum Conference in Mexico, Puebla, Mexico, 8-9 November.

Guan, L., McVay, D.A., Jensen, J.L. et al. 2002. Evaluation of a Statistical Infill Candidate Selection Technique. Paper 75718 presented at the SPE Gas Technology Symposium, Calgary, Alberta, Canada, 30 April-2 May.

Guan, L., McVay, D.A., and Jensen, J.L. 2004. Parameter Sensitivity Study of a Statistical Technique for Fast Infill Evaluation of Mature Tight-Gas Reservoirs. Paper PETSOC 2004-164 presented at the Canadian International Petroleum Conference, Calgary, Alberta, 8-10 June.

Gunter, G.W., Finneran, J.M., Hartmann, D.J. et al. 1997a. Early Determination of Reservoir Flow Units Using an Integrated Petrophysical Method. Paper SPE 38679 presented at the SPE Annual Technical Conference and Exhibition, San Antonio, Texas, 5-8 October.

Gunter, G.W., Pinch, J.J., Finneran, J.M. et al. 1997b. Overview of an Integrated Process Model to Develop Petrophysical Based Reservoir Descriptions. Paper SPE 38748 presented at the SPE Annual Technical Conference and Exhibition, San Antonio, Texas, 5-8 October.

Hudson, J.W., Jochen, J.E., and Jochen, V.A. 2000. Practical Technique to Identify Infill Potential in Low-Permeability Gas Reservoirs Applied to the Milk River Formation in Canada. Paper SPE 59779 presented at the SPE/CERI Gas Technology Symposium, Calgary, Alberta, Canada, 3-5 April.

Hudson, J.W., Jochen, J.E., and Spivey, J.P. 2001. Practical Methods to High-Grade Infill Opportunities Applied to the Mesaverde, Morrow, and Cotton Valley Formations. Paper SPE 68598 presented at the SPE Hydrocarbon Economics and Evaluation Symposium, Dallas, Texas, 2-3 April.

Isaaks E.H., and Srivastava, R.M. 1989. *Applied Geostatistics*. New York: Oxford University Press.

Kyte, D.G. and Meehan, D.N. 1996. Horizontal Spacing, Depletion, and Infill Potential in the Austin Chalk. Paper SPE 36721 presented at the SPE Annual Technical Conference and Exhibition, Denver, Colorado, 6-9 October.

Masters, J.A. 1979. Deep Basin Gas Trap, Western Canada: **AAPG Bulletin**, 63: 152-181.

McCain, W.D., Voneiff, G.W., Hunt, E.R. et al. 1993. A Tight Gas Field Study: Carthage (Cotton Valley) Field. Paper SPE 26141 presented at the SPE Gas Technology Symposium, Calgary, Alberta, Canada, 28-30 June.

McKinney, P.D., Rushing, J.A., and Sanders, L.A. 2002. Applied Reservoir Characterization for Maximizing Reserve Growth and Profitability in Tight Gas Sands: A Paradigm Shift in Development Strategies for Low-Permeability Gas Reservoirs. Paper SPE 75708 presented at the SPE Gas Technology Symposium, Calgary, Alberta, Canada, 30 April-2 May.

Newsham, K.E. and Rushing, J.A. 2001. An Integrated Work-Flow Model to Characterize Unconventional Gas Resources: Part I - Geological Assessment and Petrophysical Evaluation. Paper SPE 71351 presented at the SPE Annual Technical Conference and Exhibition, New Orleans, Louisiana, 30 September-3 October.

Rushing, J.A. and Newsham, K.E. 2001. An Integrated Work-Flow Model to Characterize Unconventional Gas Resources: Part II - Formation Evaluation and Reservoir Modeling. Paper SPE 71352 presented at the SPE Annual Technical Conference and Exhibition, New Orleans, Louisiana, 30 September-3 October.

Smith, D.G, Zorn, C.E., and Sneider, R.M. 1984. The Paleogeography of the Lower Cretaceous of Western Alberta and Northeastern British Columbia in and Adjacent to the Deep Basin of the Elmworth Area.

Stark, P., Chew, K., and Fryklund, B. 2007. The Role of Unconventional Hydrocarbon Resources in Shaping the Energy Future. Paper IPTC 11806 presented at the International Petroleum Technology Conference, Dubai, UAE, 4-6 December.

Voneiff, G.W. and Cipolla, C. 1996. A New Approach to Large-Scale Infill Evaluations Applied to the Ozona (Canyon) Gas Sands. Paper SPE 35203 presented at the Permian Basin Oil and Gas Recovery Conference, Midland, Texas, 27-29 March.

Xiong, H. and Holditch, S.A. 2006. Will the Blossom of Unconventional Natural Gas Development in North America Be Repeated in China. Paper SPE 103775 presented at the International Oil & Gas Conference and Exhibition in China, Beijing, China, 5-7 December.

Zahid, S., Bhatti, A.A., Khan, H.A. et al. 2007. Development of Unconventional Gas Resources: Stimulation Perspective. Paper SPE 107053 presented at the Production and Operations Symposium, Oklahoma City, Oklahoma, USA, 31 March-3 April.

APPENDIX A
ADDITIONAL PROBABILITY DISTRIBUTION PLOTS OF DISCOUNTED CUMULATIVE GAS PRODUCTION FOR THE FIRST RESERVOIR MODEL

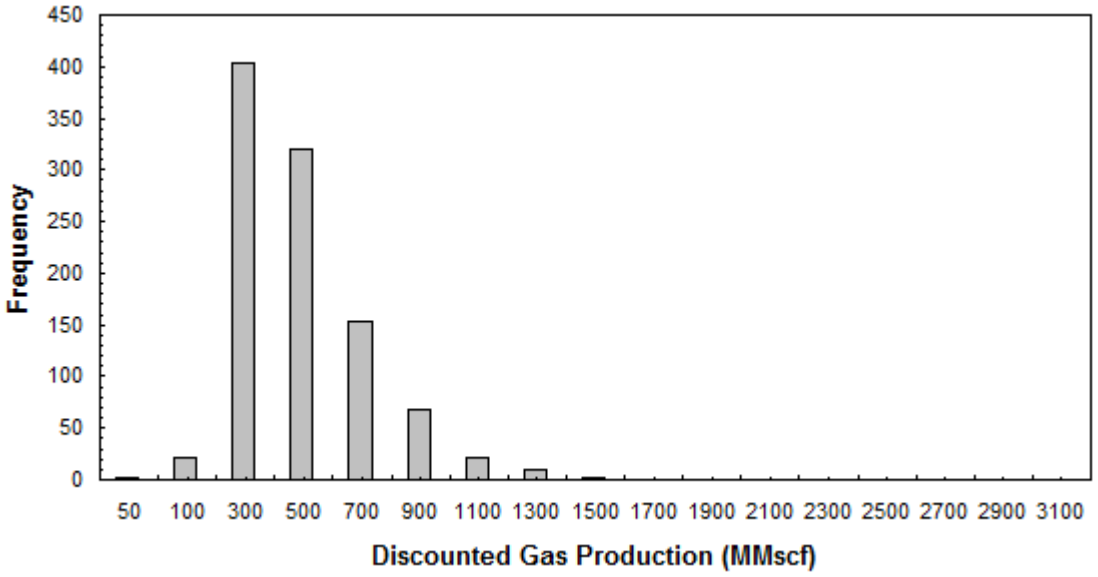

Fig. A1— Probability distribution plot of 20-year discounted cumulative gas production for Well 1 on 210 acre-spacing (Stage 2 – Option 1).

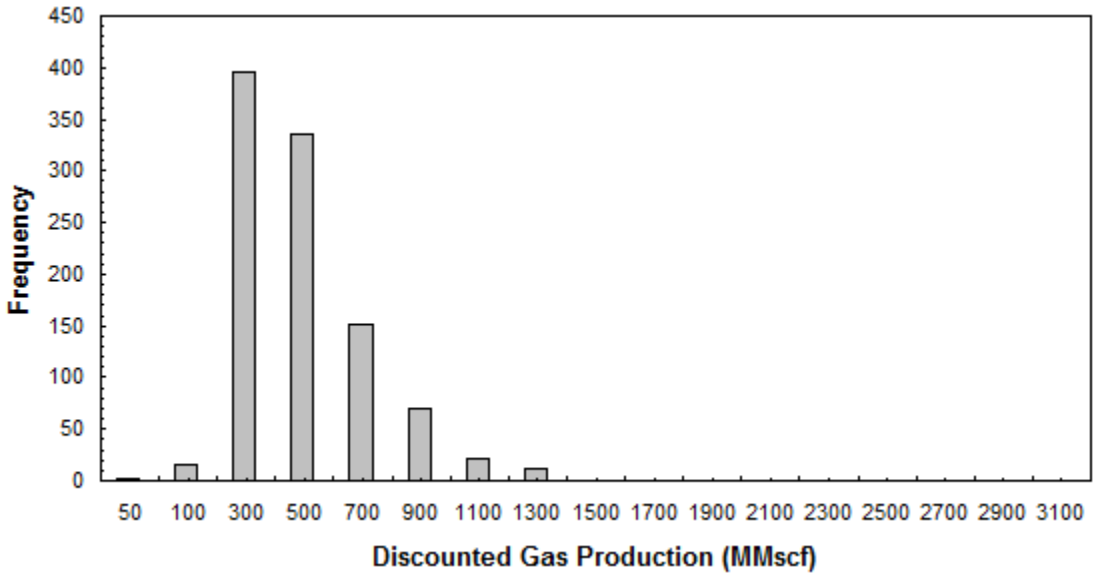

Fig. A2— Probability distribution plot of 20-year discounted cumulative gas production for Well 1 on 160 acre-spacing (Stage 2 – Option 2).

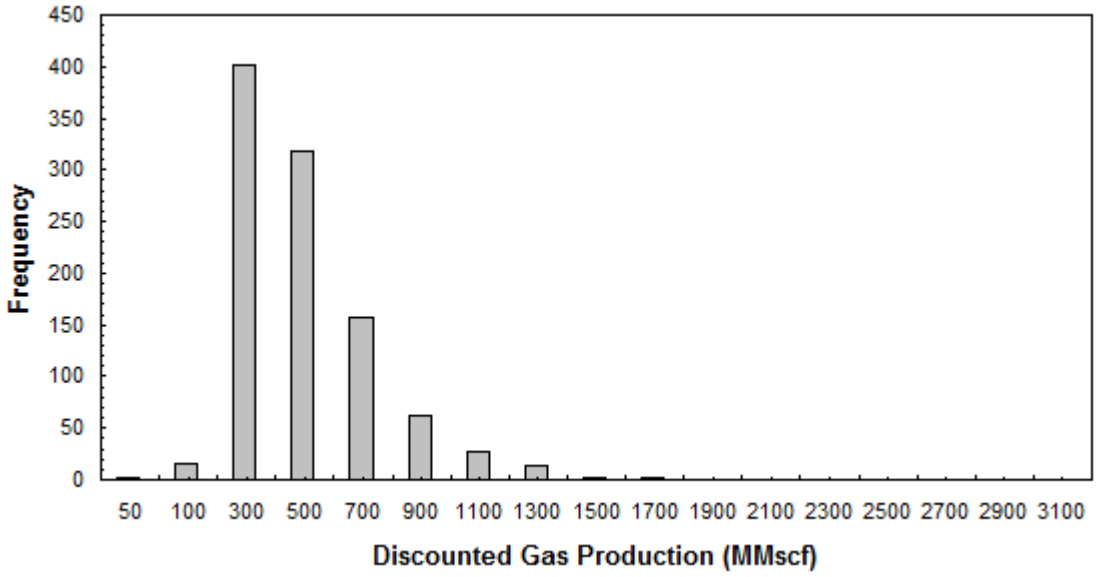

Fig. A3— Probability distribution plot of 20-year discounted cumulative gas production for Well 2 on 160 acre-spacing (Stage 2 – Option 2).

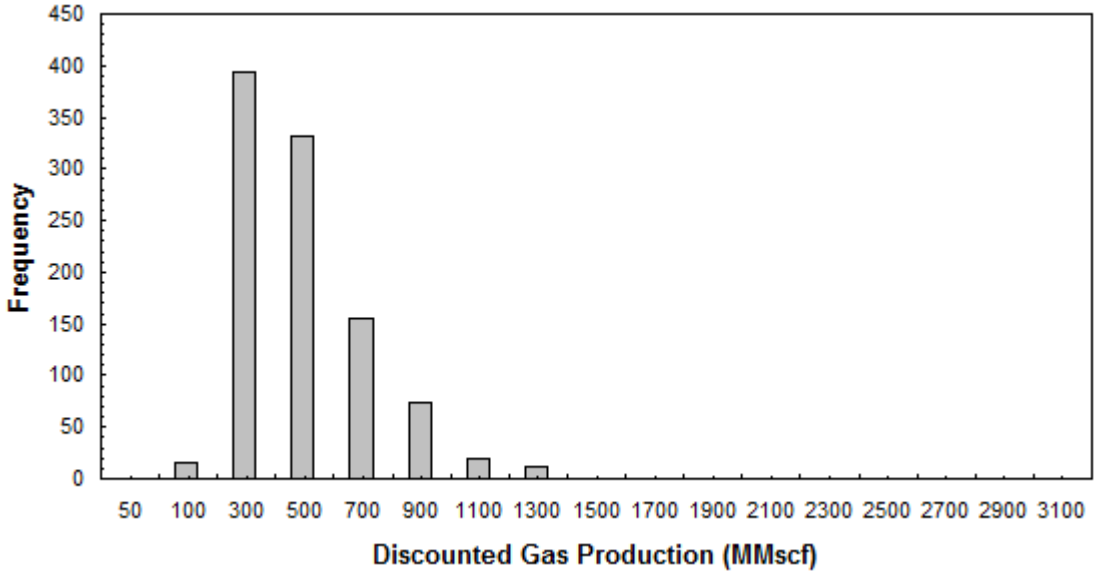

Fig. A4— Probability distribution plot of 20-year discounted cumulative gas production for Well 1 on 160 acre-spacing (Stage 2 – Option 3).

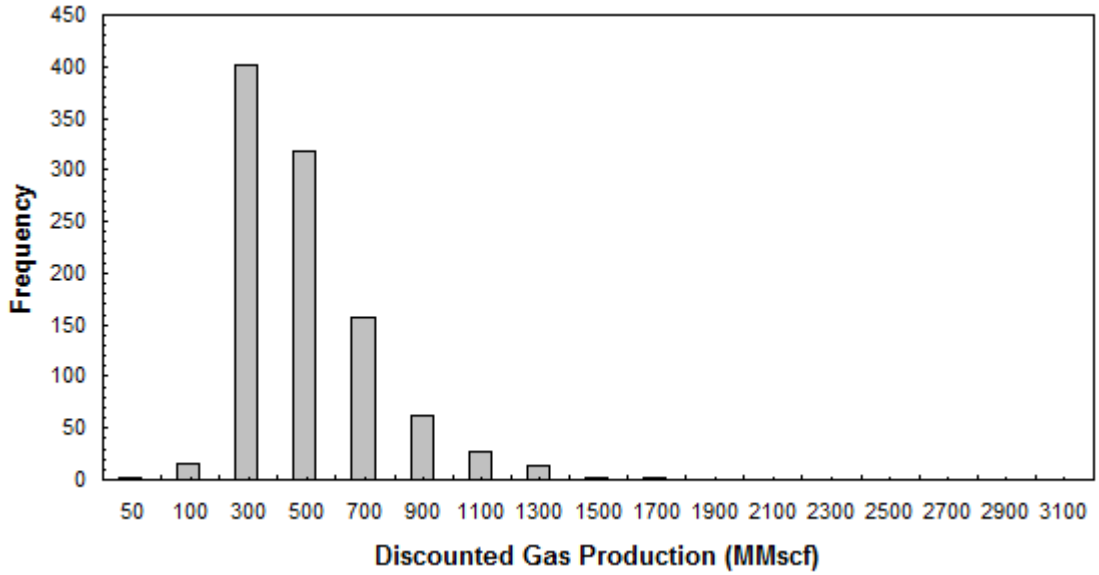

Fig. A5— Probability distribution plot of 20-year discounted cumulative gas production for Well 2 on 160 acre-spacing (Stage 2 – Option 3).

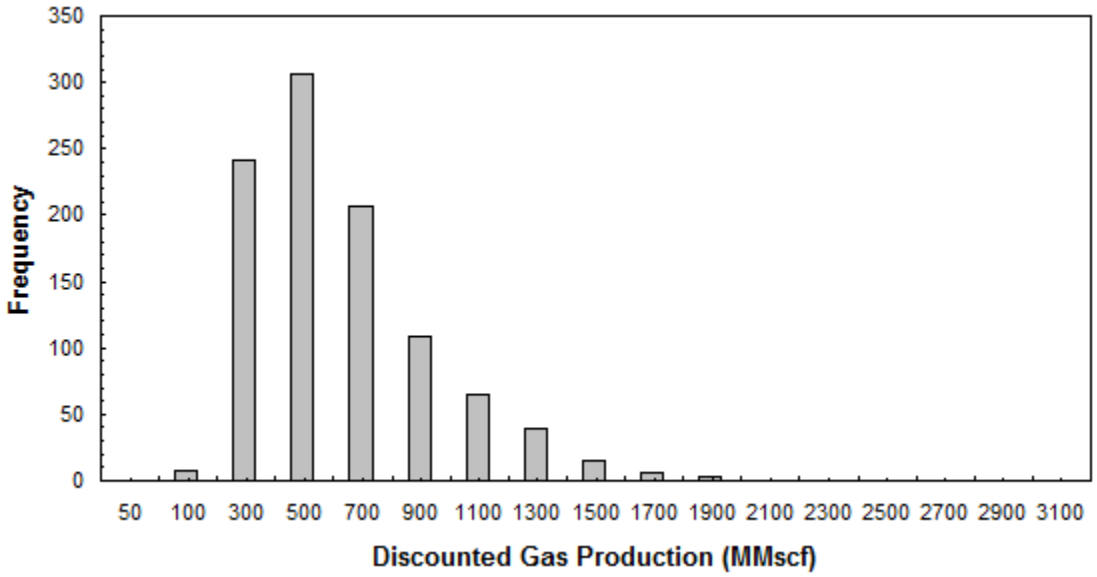

Fig. A6— Probability distribution plot of 20-year discounted cumulative gas production for Well 3 on 210 acre-spacing (Stage 2 – Option 3).

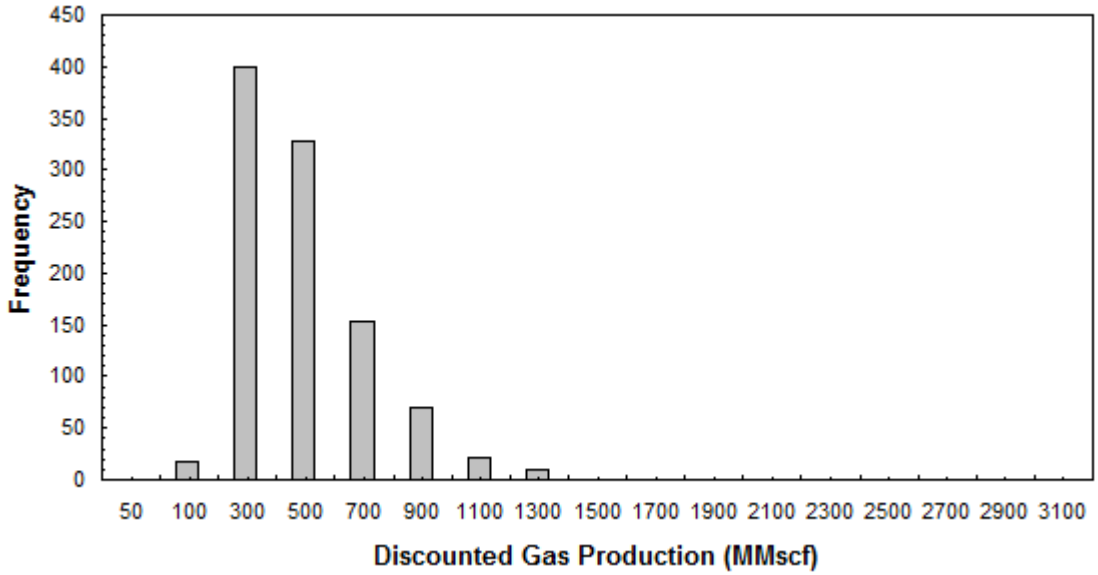

Fig. A7— Probability distribution plot of 20-year discounted cumulative gas production for Well 1 on 160 acre-spacing (Stage 2 – Option 4).

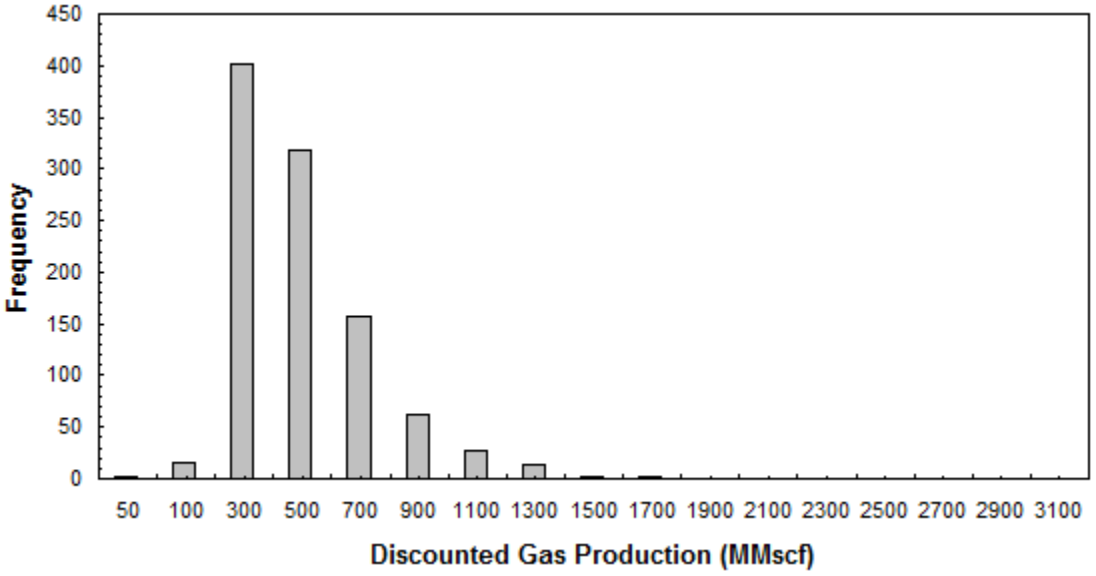

Fig. A8— Probability distribution plot of 20-year discounted cumulative gas production for Well 2 on 160 acre-spacing (Stage 2 – Option 4).

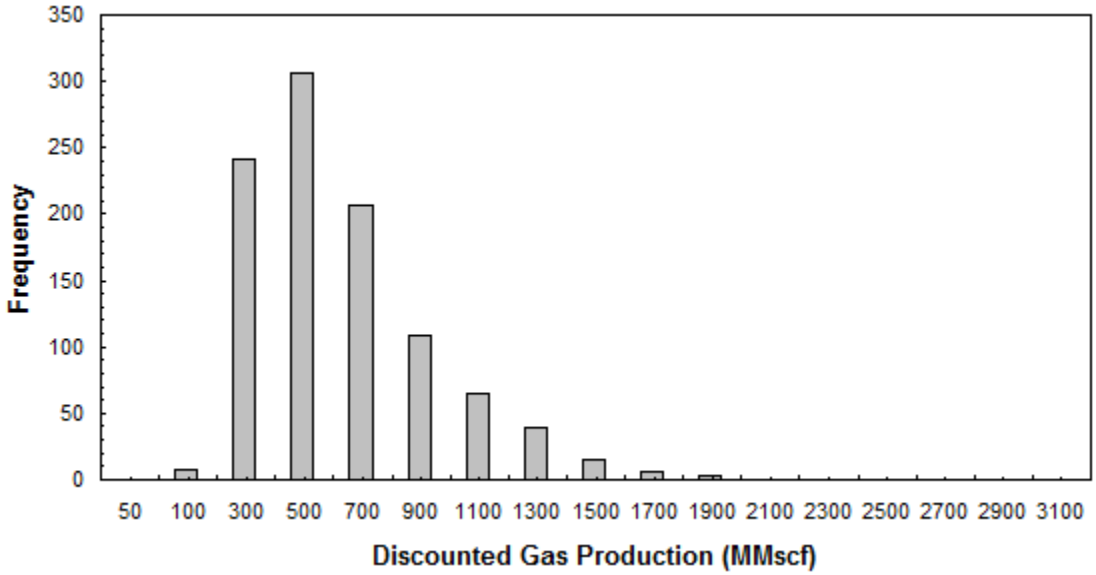

Fig. A9— Probability distribution plot of 20-year discounted cumulative gas production for Well 3 on 210 acre-spacing (Stage 2 – Option 4).

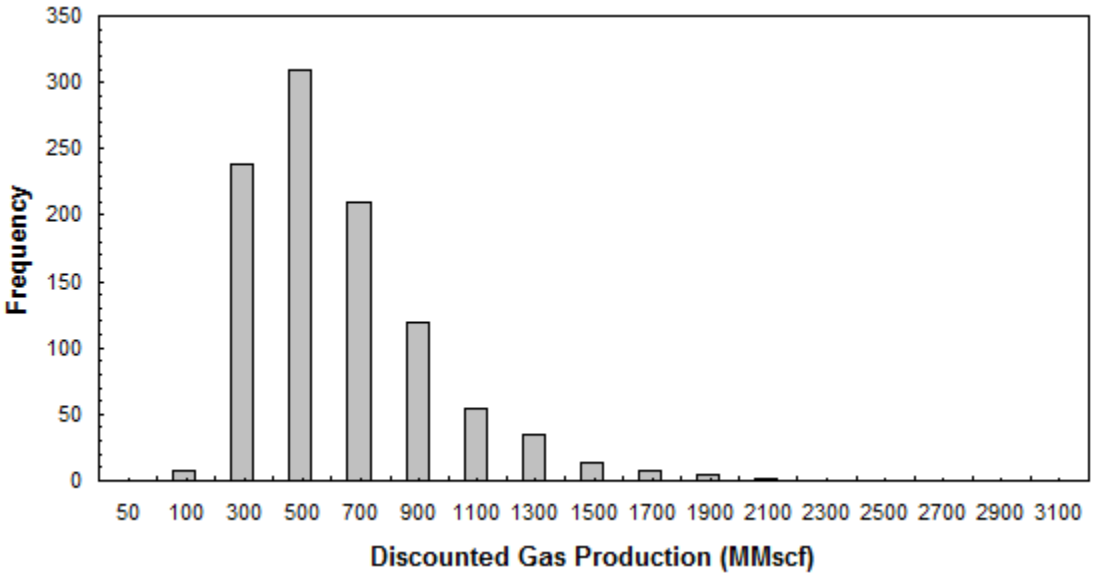

Fig. A10— Probability distribution plot of 20-year discounted cumulative gas production for Well 4 on 210 acre-spacing (Stage 2 – Option 4).

APPENDIX B

CROSSPLOTS OF STAGE 1 VS STAGE 2 DISCOUNTED CUMULATIVE GAS PRODUCTIONS FOR THE FIRST RESERVOIR MODEL

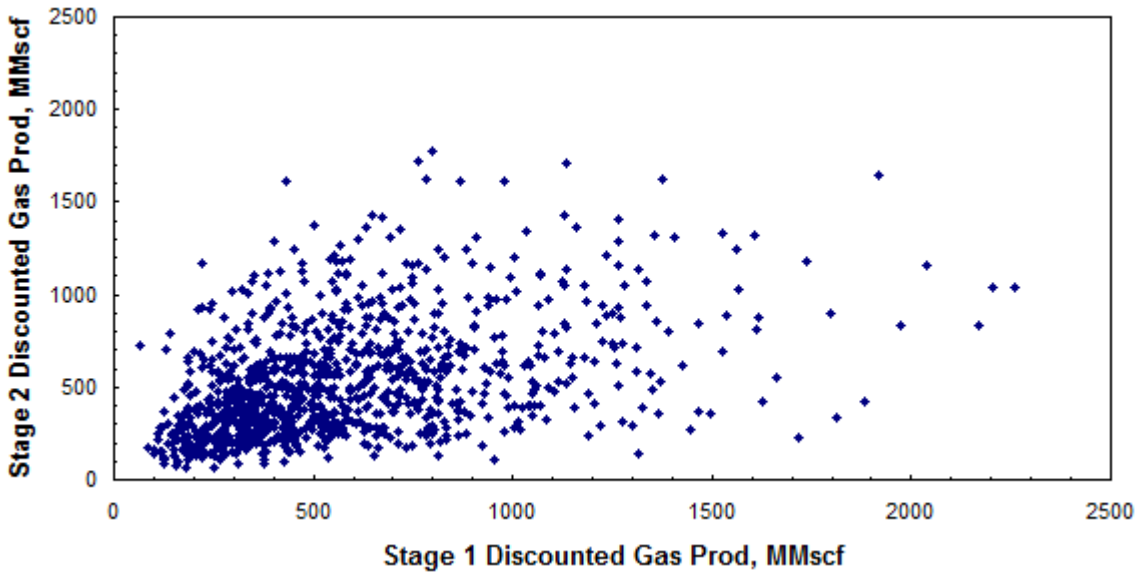

Fig. B1— Crossplot of Well 1 (Stage 1) vs. Well 3 (Stage 2) 20-year discounted cumulative gas productions (Option 3).

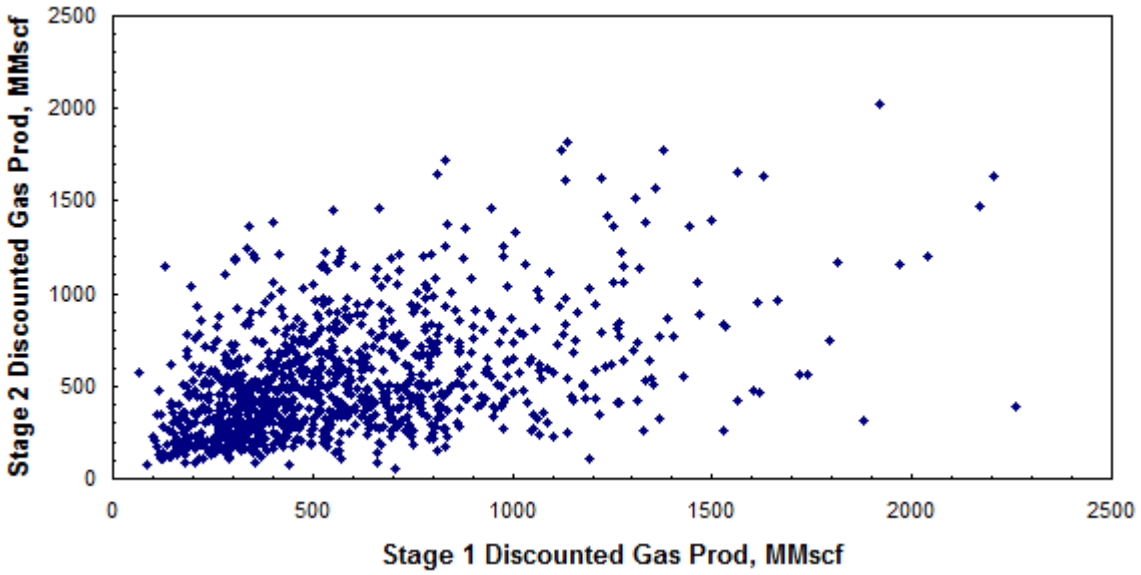

Fig. B2— Crossplot of Well 1 (Stage 1) vs. Well 4 (Stage 2) 20-year discounted cumulative gas productions (Option 4).

APPENDIX C

ADDITIONAL PROBABILITY DISTRIBUTION PLOTS OF STAGE GAS PRODUCTION FOR THE PRELIMINARY VERSION OF THE SECOND RESERVOIR MODEL

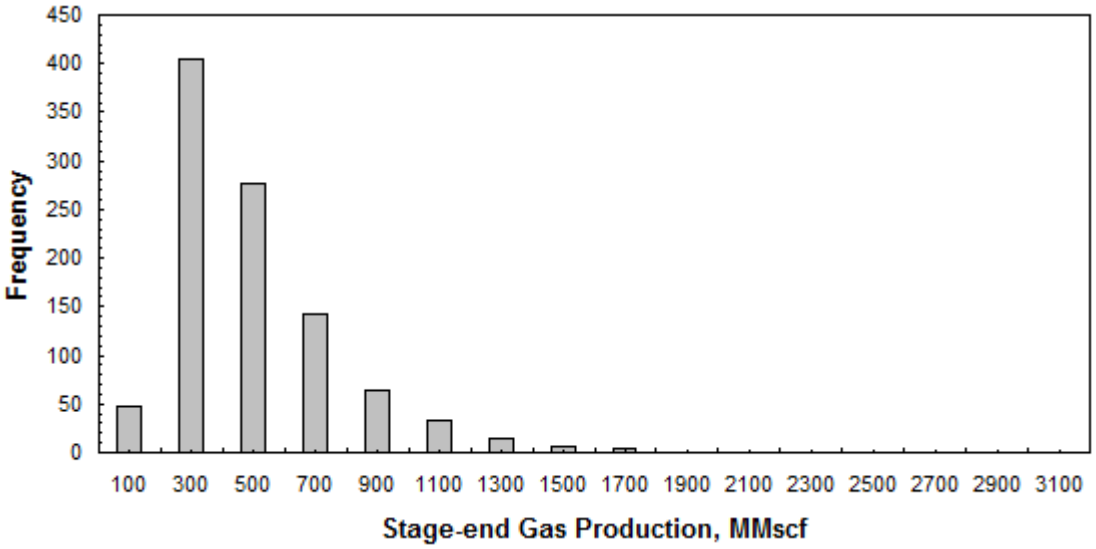

Fig. C1— Probability distribution plot of stage-end average gas production for Well 1 on 640 acre-spacing (Stage 2, 640-640).

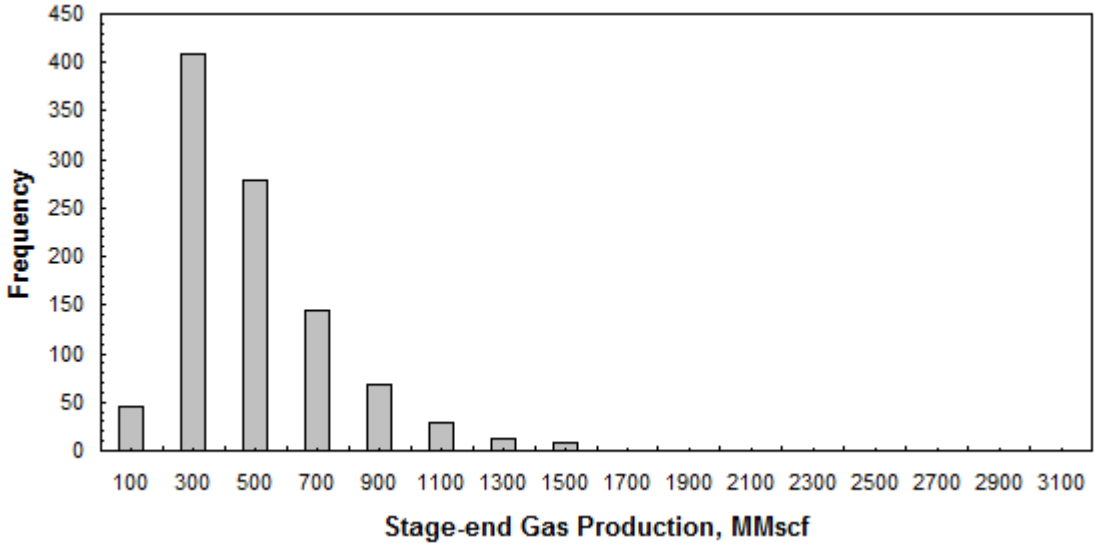

Fig. C2— Probability distribution plot of stage-end average gas production for Well 1 on 320 acre-spacing (Stage 2, 640-320).

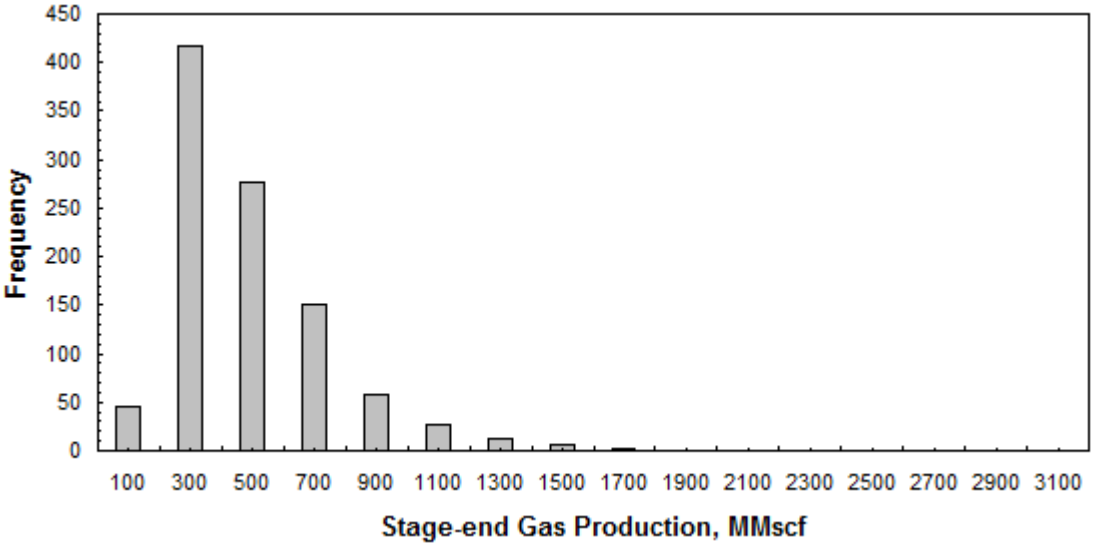

Fig. C3— Probability distribution plot of stage-end average gas production for Well 2 on 320 acre-spacing (Stage 2, 640-320).

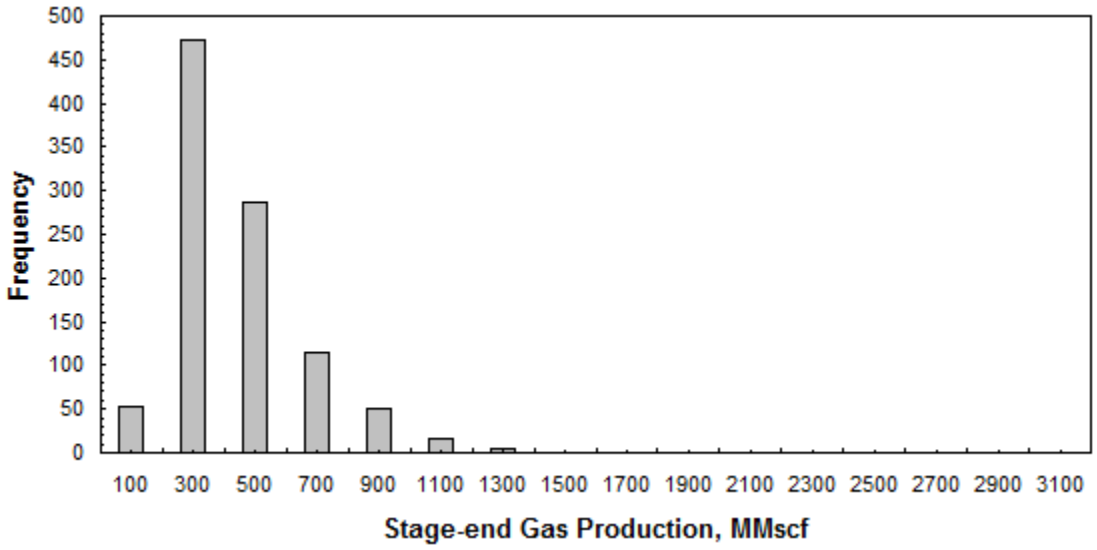

Fig. C4— Probability distribution plot of stage-end average gas production for Well 1 on 160 acre-spacing (Stage 2, 640-160).

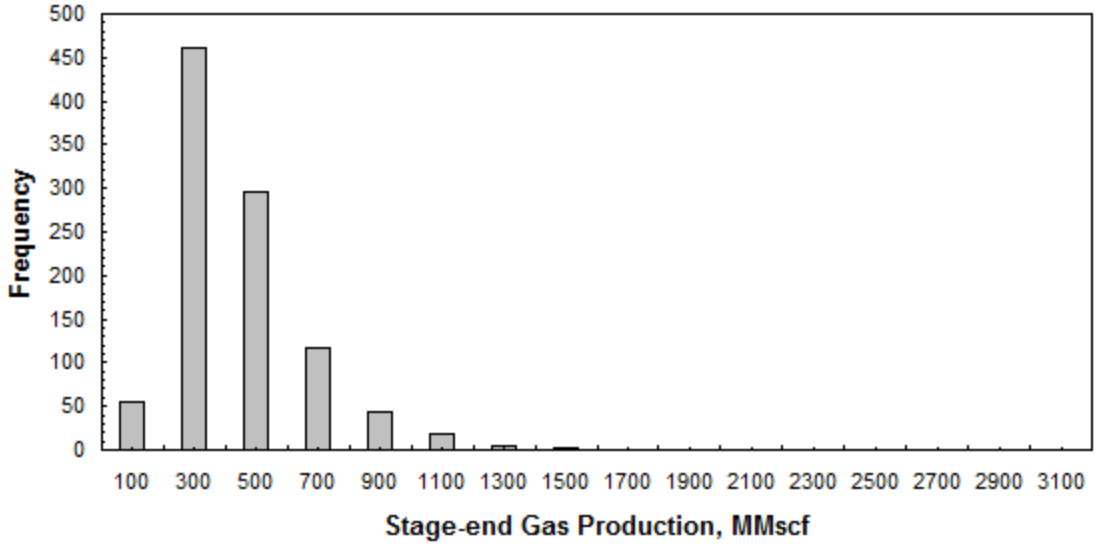

Fig. C5— Probability distribution plot of stage-end average gas production for Well 2 on 160 acre-spacing (Stage 2, 640-160).

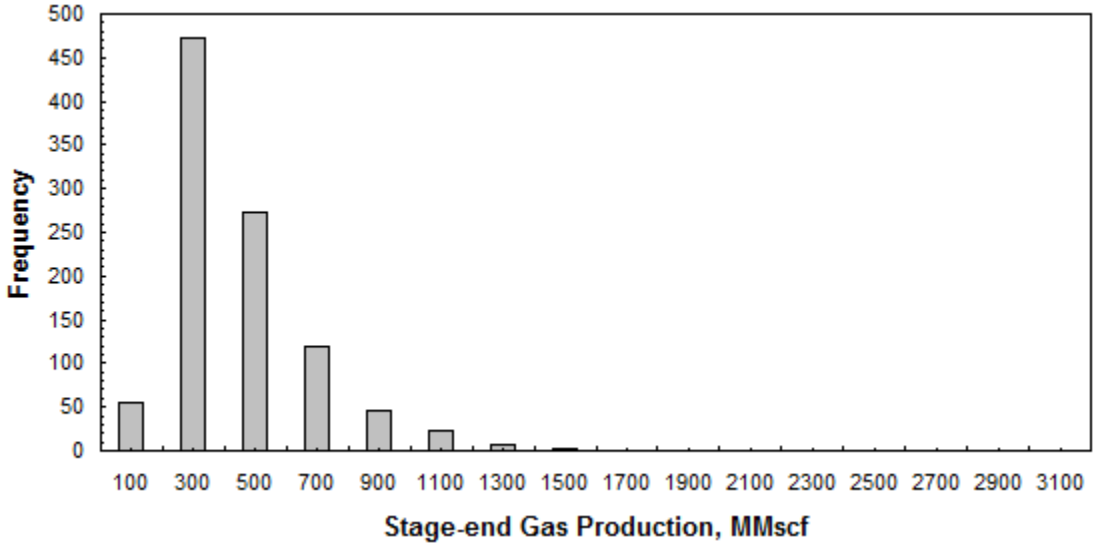

Fig. C6— Probability distribution plot of stage-end average gas production for Well 3 on 160 acre-spacing (Stage 2, 640-160).

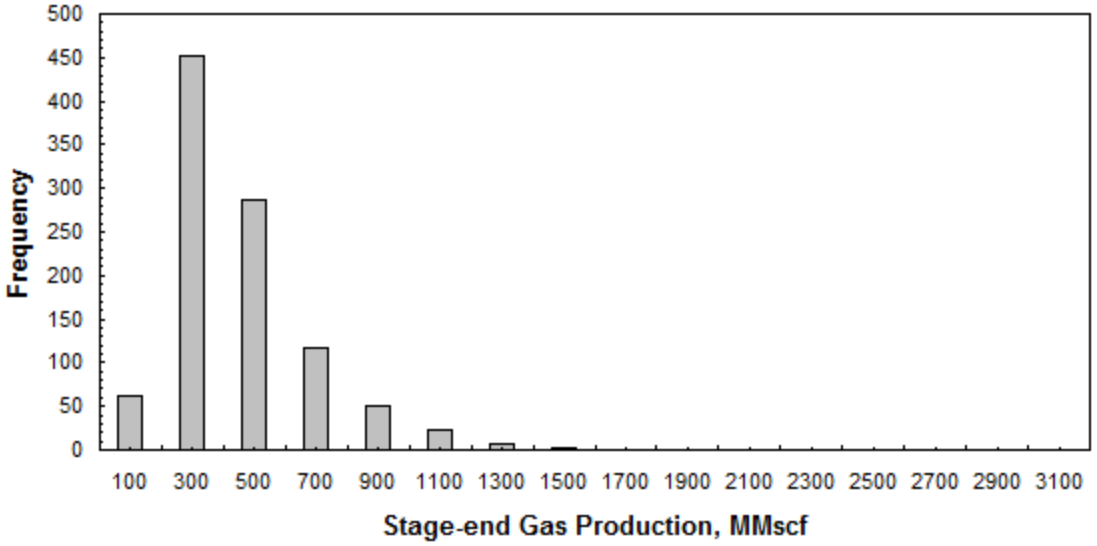

Fig. C7— Probability distribution plot of stage-end average gas production for Well 4 on 160 acre-spacing (Stage 2, 640-160).

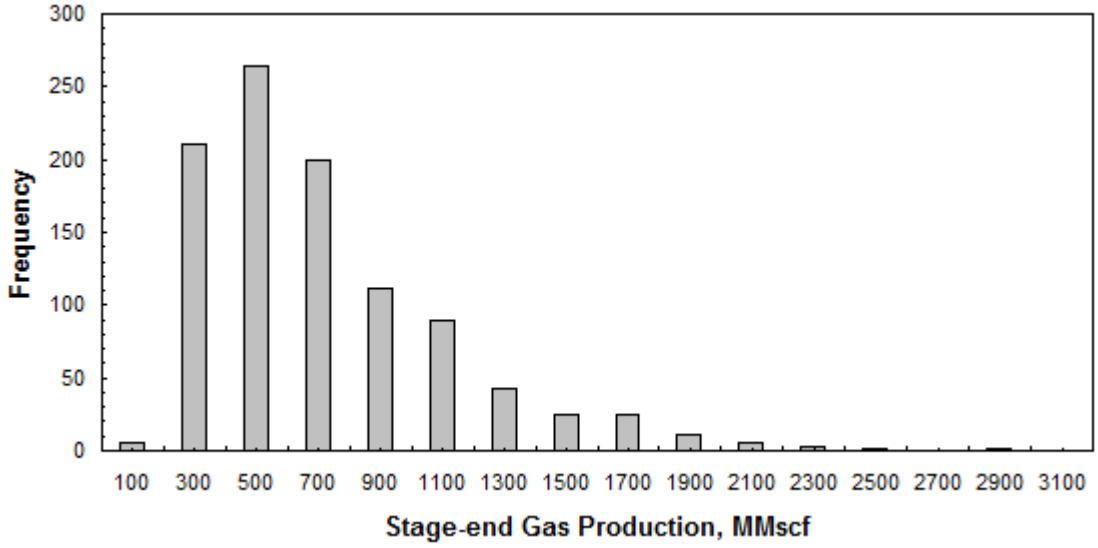

Fig. C8— Probability distribution plot of stage-end average gas production for Well 1 on 320 acre-spacing (Stage 1).

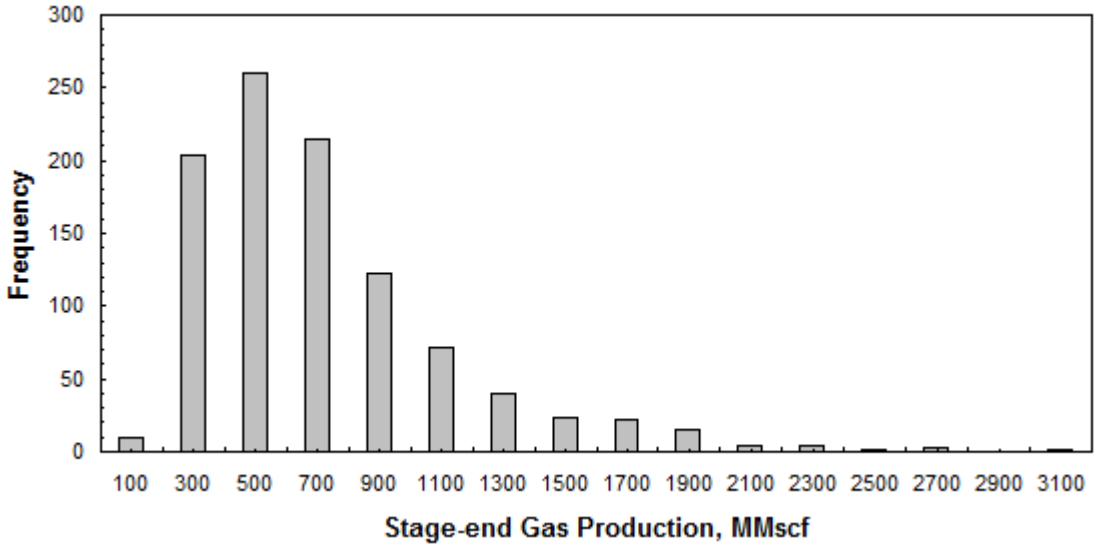

Fig. C9— Probability distribution plot of stage-end average gas production for Well 2 on 320 acre-spacing (Stage 1).

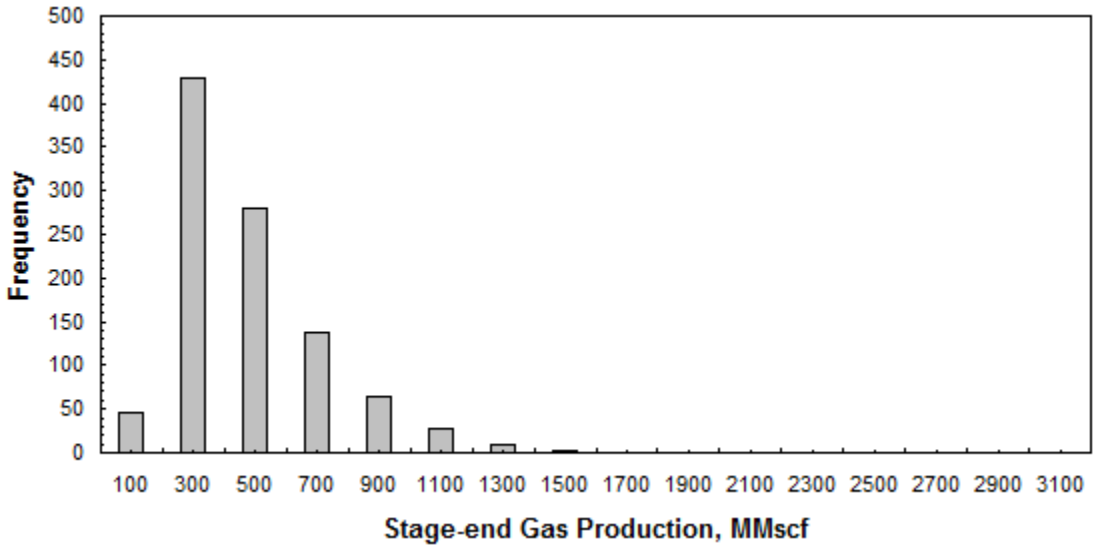

Fig. C10— Probability distribution plot of stage-end average gas production for Well 1 on 320 acre-spacing (Stage 2, 320-320).

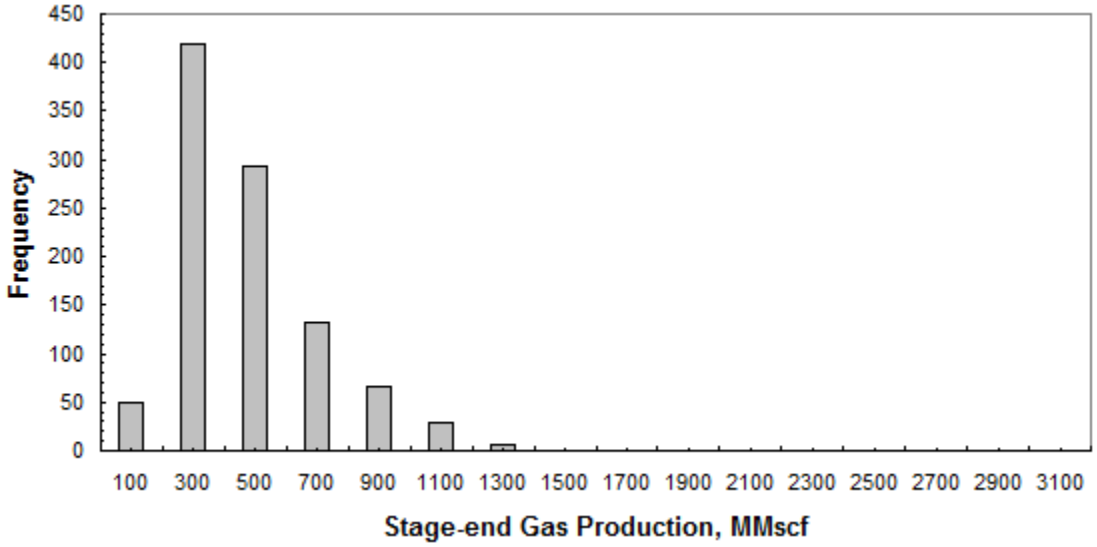

Fig. C11— Probability distribution plot of stage-end average gas production for Well 2 on 320 acre-spacing (Stage 2, 320-320).

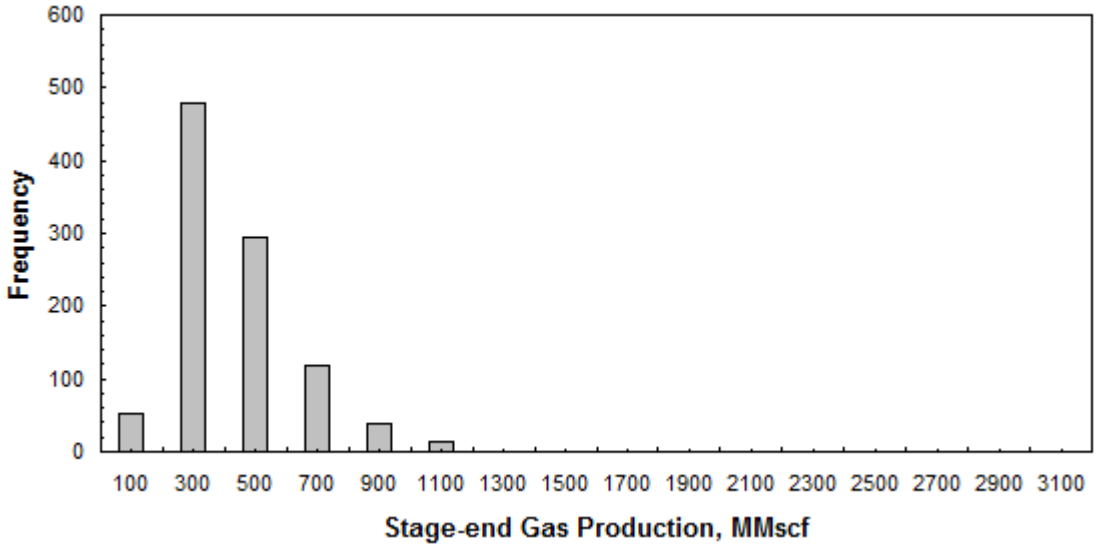

Fig. C12— Probability distribution plot of stage-end average gas production for Well 1 on 160 acre-spacing (Stage 2, 320-160).

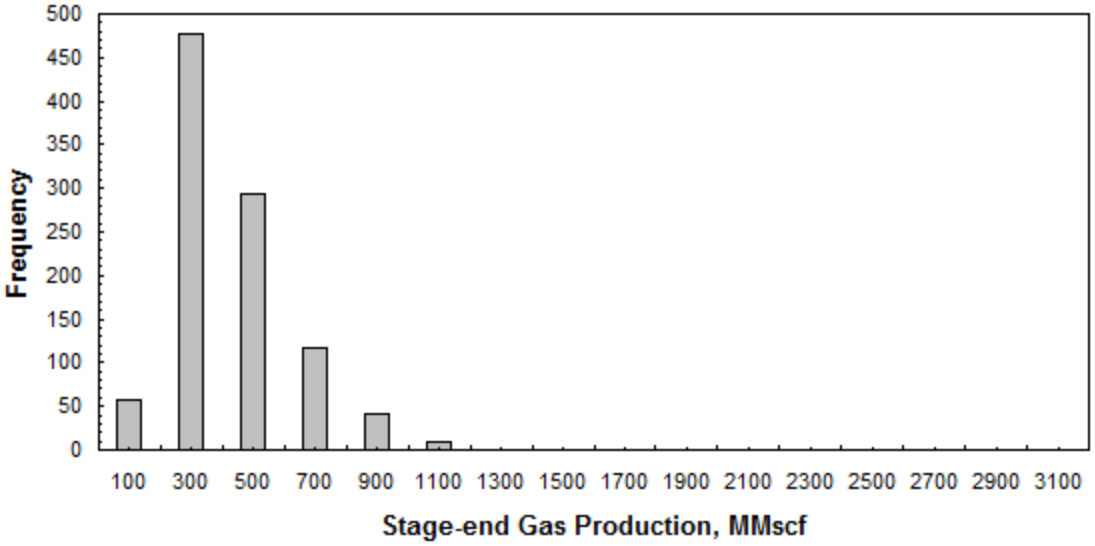

Fig. C13— Probability distribution plot of stage-end average gas production for Well 2 on 160 acre-spacing (Stage 2, 320-160).

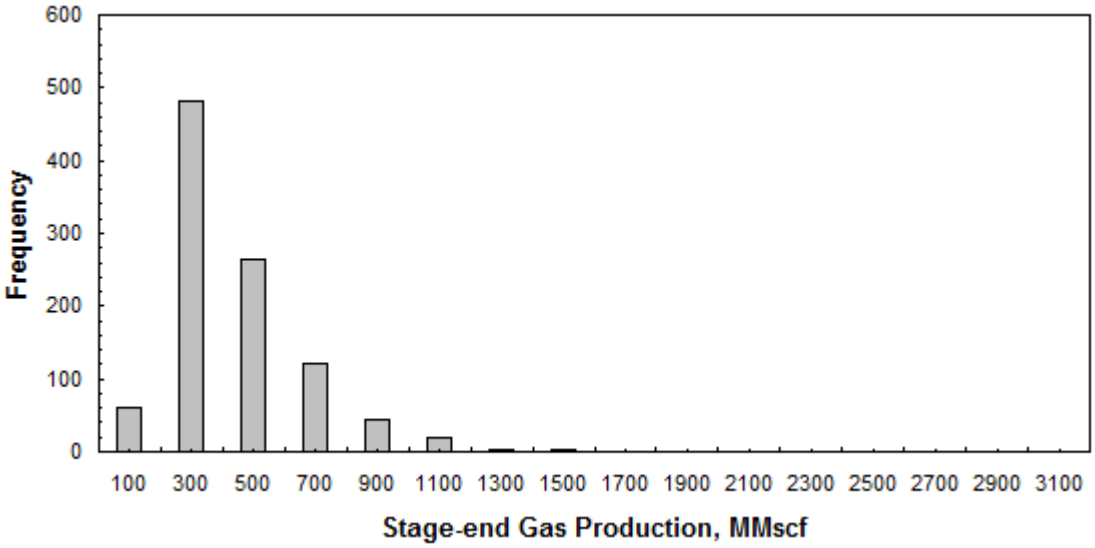

Fig. C14— Probability distribution plot of stage-end average gas production for Well 3 on 160 acre-spacing (Stage 2, 320-160).

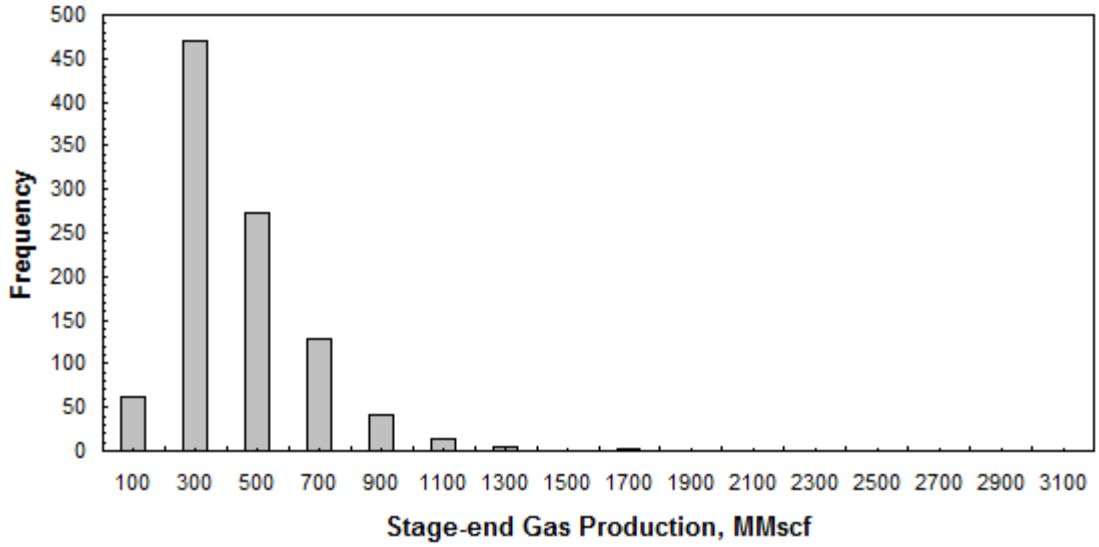

Fig. C15— Probability distribution plot of stage-end average gas production for Well 4 on 160 acre-spacing (Stage 2, 320-160).

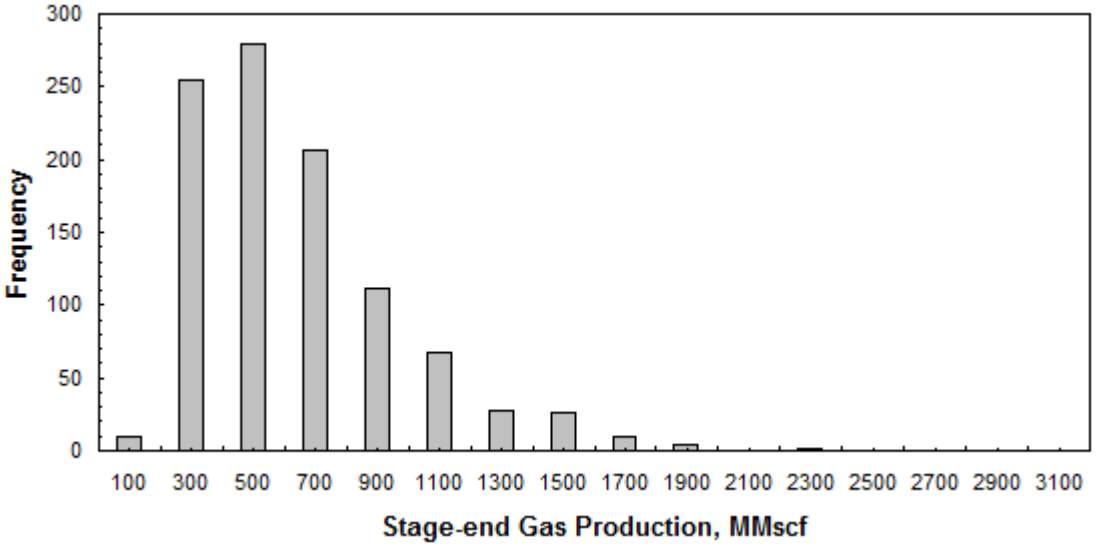

Fig. C16— Probability distribution plot of stage-end average gas production for Well 1 on 160 acre-spacing (Stage 1).

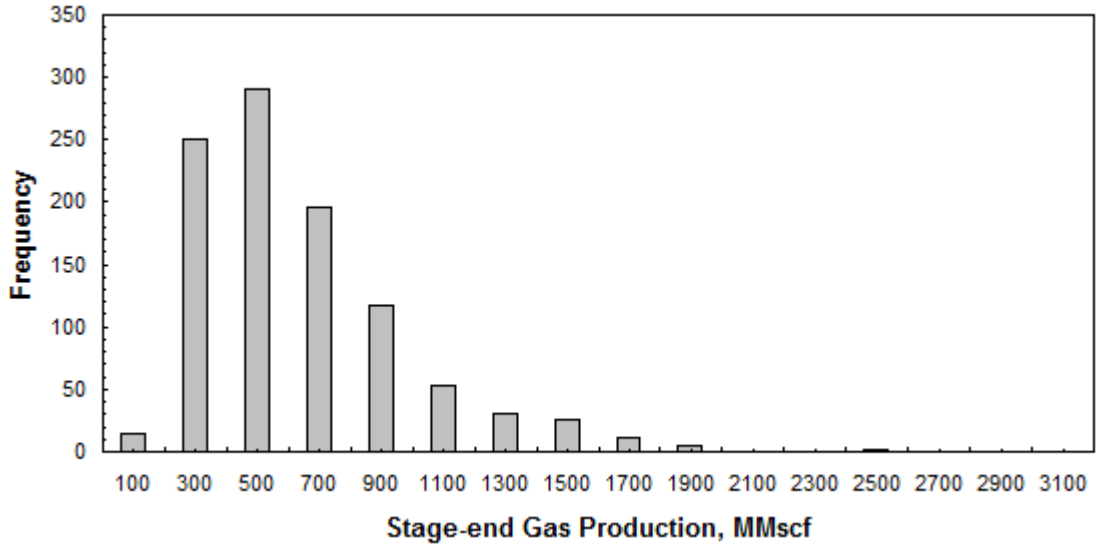

Fig. C17— Probability distribution plot of stage-end average gas production for Well 2 on 160 acre-spacing (Stage 1).

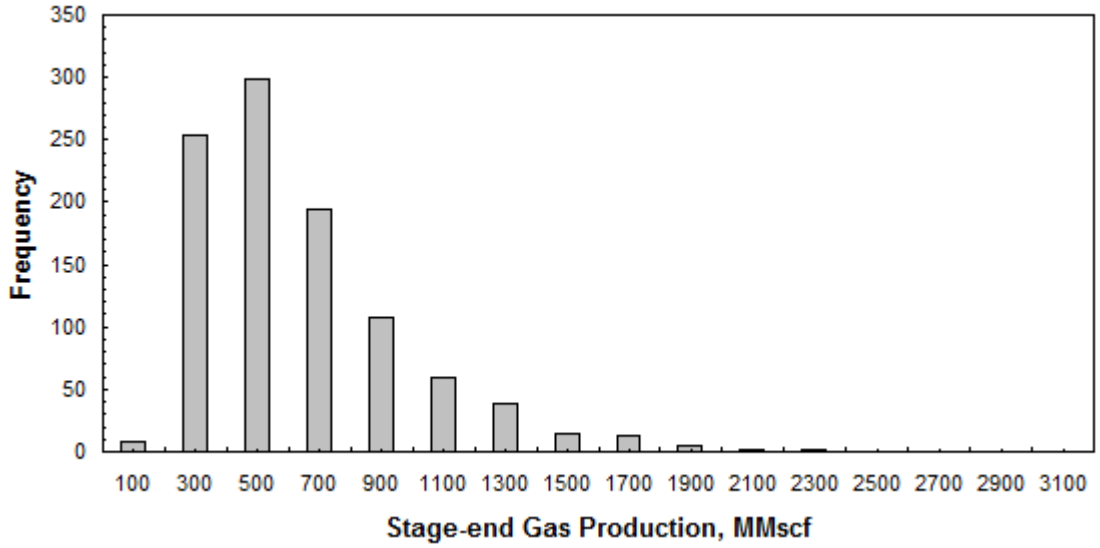

Fig. C18— Probability distribution plot of stage-end average gas production for Well 3 on 160 acre-spacing (Stage 1).

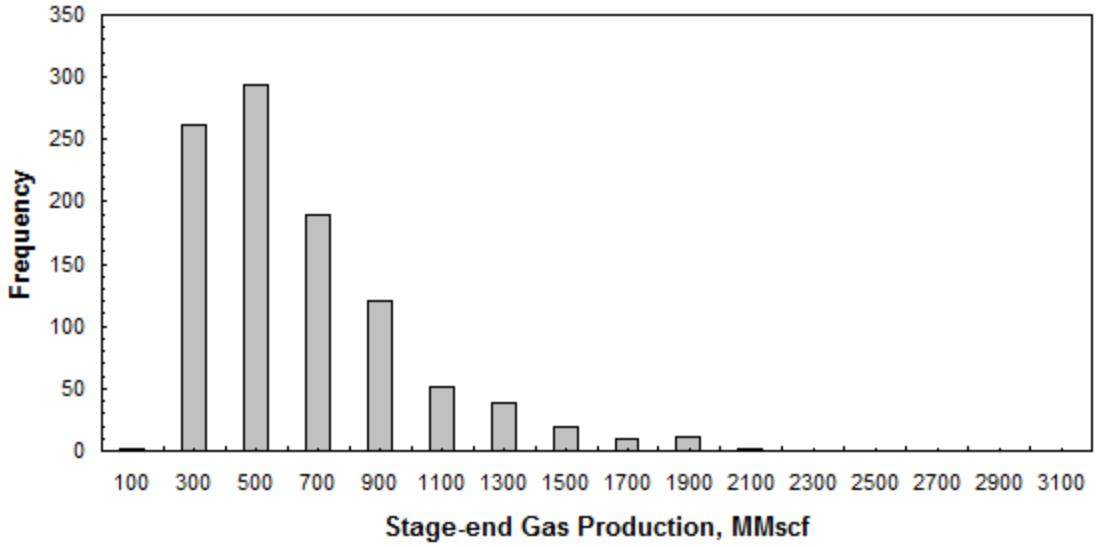

Fig. C19— Probability distribution plot of stage-end average gas production for Well 4 on 160 acre-spacing (Stage 1).

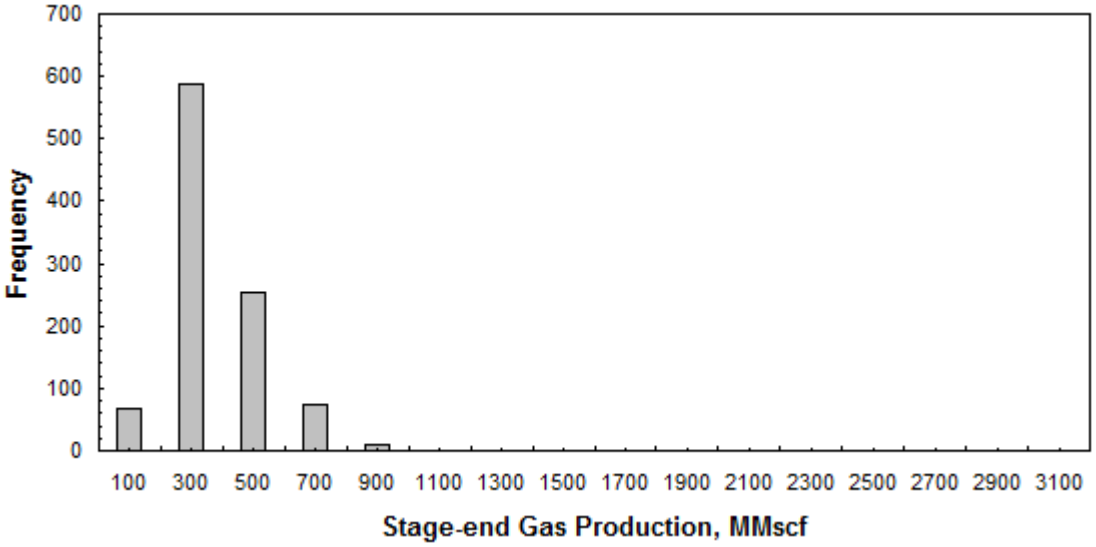

Fig. C20— Probability distribution plot of stage-end average gas production for Well 1 on 160 acre-spacing (Stage 2, 160-160).

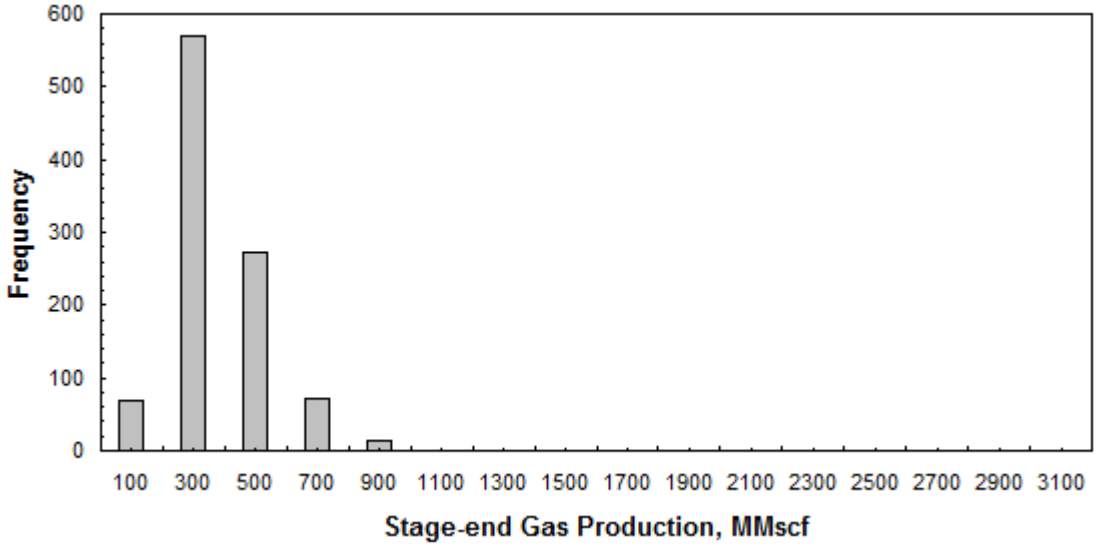

Fig. C21— Probability distribution plot of stage-end average gas production for Well 2 on 160 acre-spacing (Stage 2, 160-160).

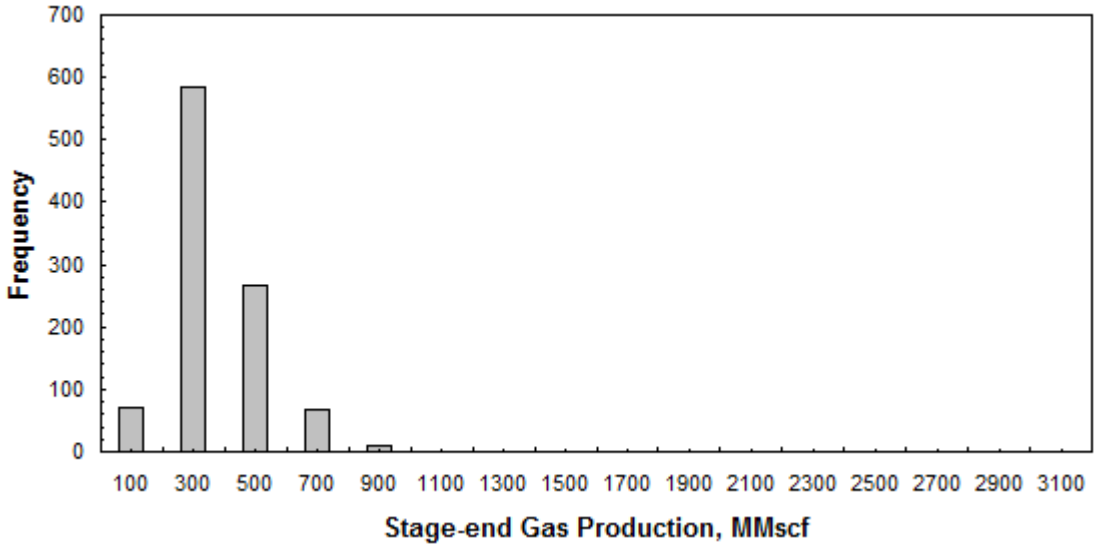

Fig. C22— Probability distribution plot of stage-end average gas production for Well 3 on 160 acre-spacing (Stage 2, 160-160).

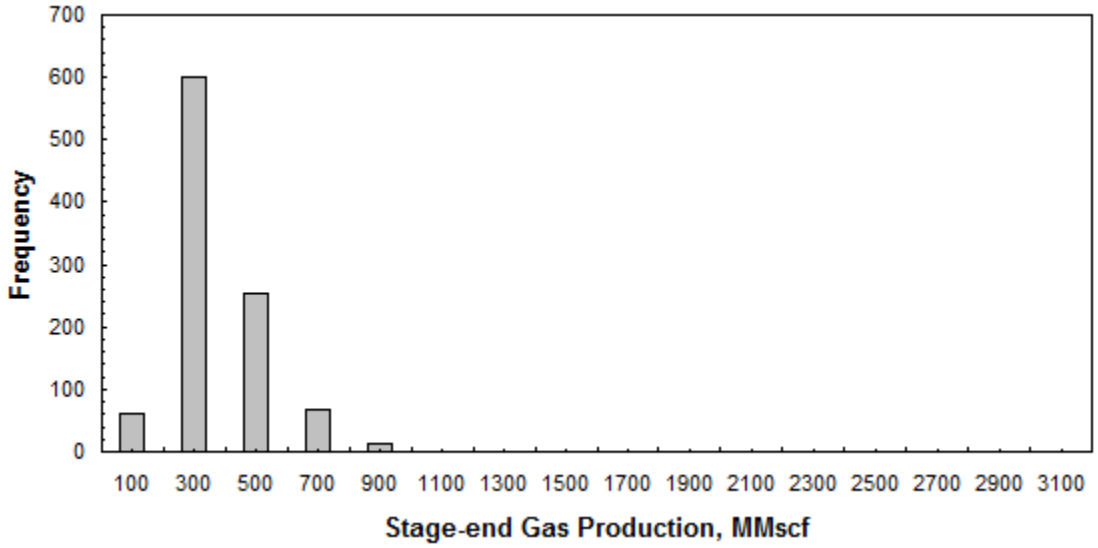

Fig. C23— Probability distribution plot of stage-end average gas production for Well 4 on 160 acre-spacing (Stage 2, 160-160).

APPENDIX D

CROSSPLOTS OF STAGE 1 VS STAGE 2 GAS PRODUCTIONS FOR THE PRELIMINARY VERSION OF THE SECOND RESERVOIR MODEL

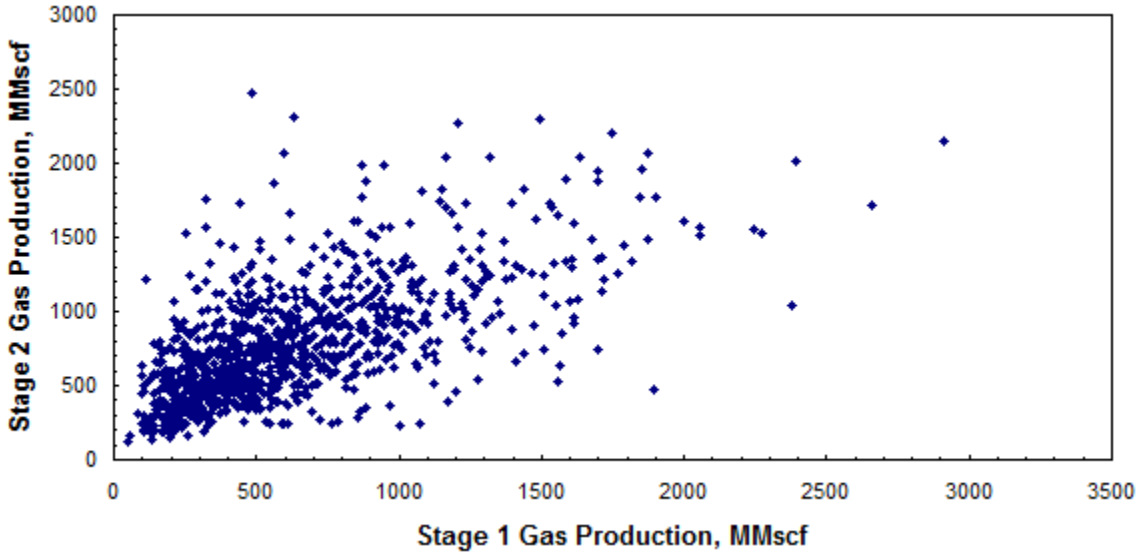

Fig. D1— Crossplot of Stage 1 (640 acres) vs. Stage 2 (320 acres) gas productions.

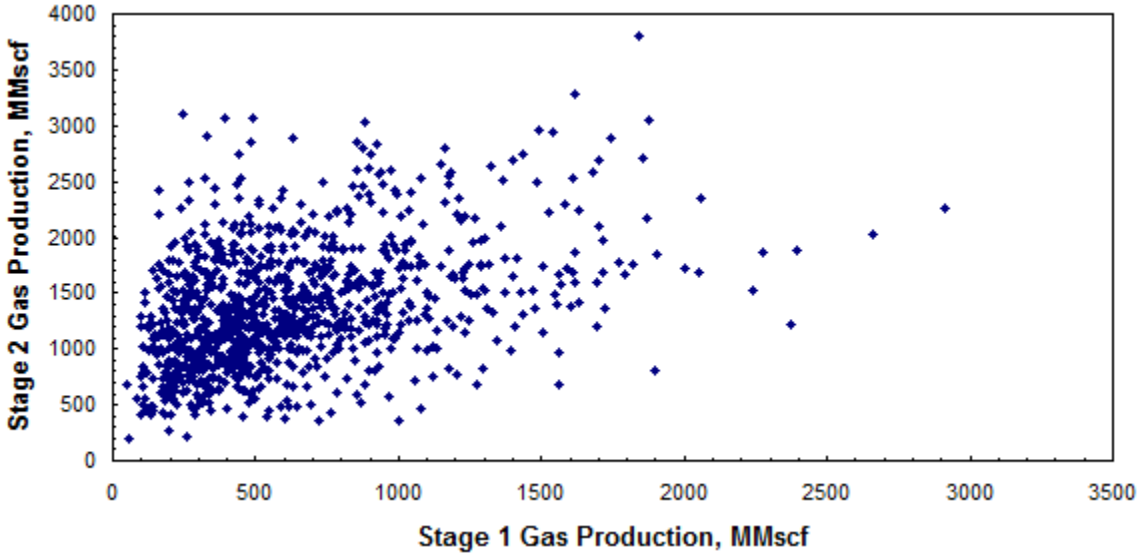

Fig. D2— Crossplot of Stage 1 (640 acres) vs. Stage 2 (160 acres) gas productions.

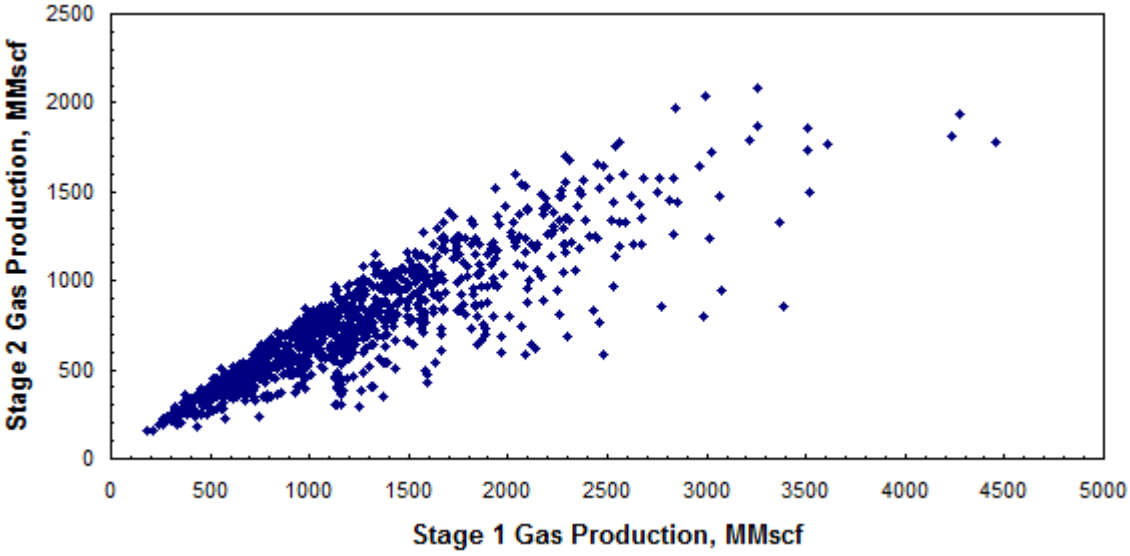

Fig. D3— Crossplot of Stage 1 (320 acres) vs. Stage 2 (320 acres) gas productions.

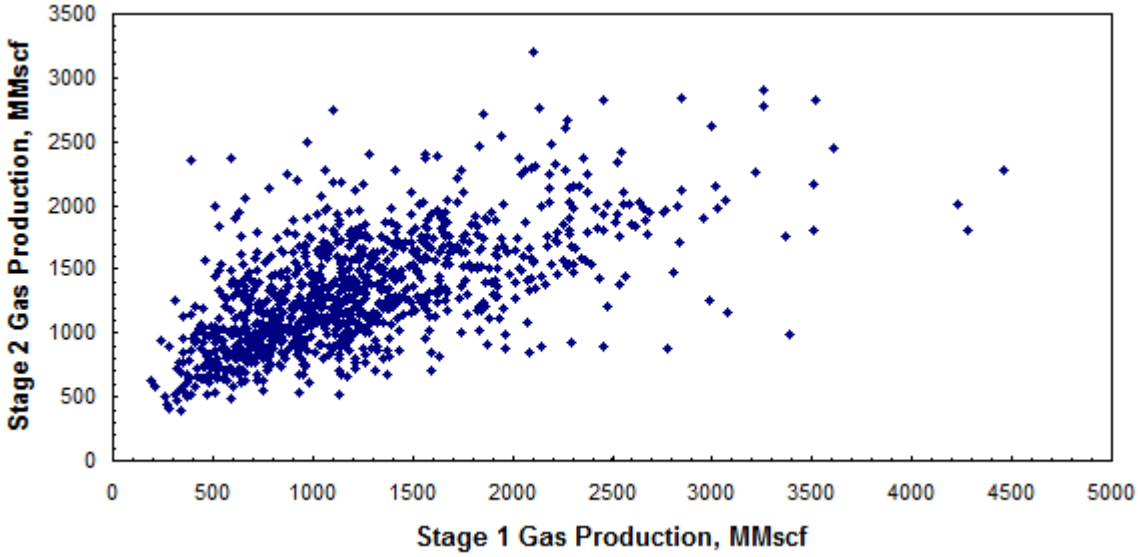

Fig. D4— Crossplot of Stage 1 (320 acres) vs. Stage 2 (160 acres) gas productions.

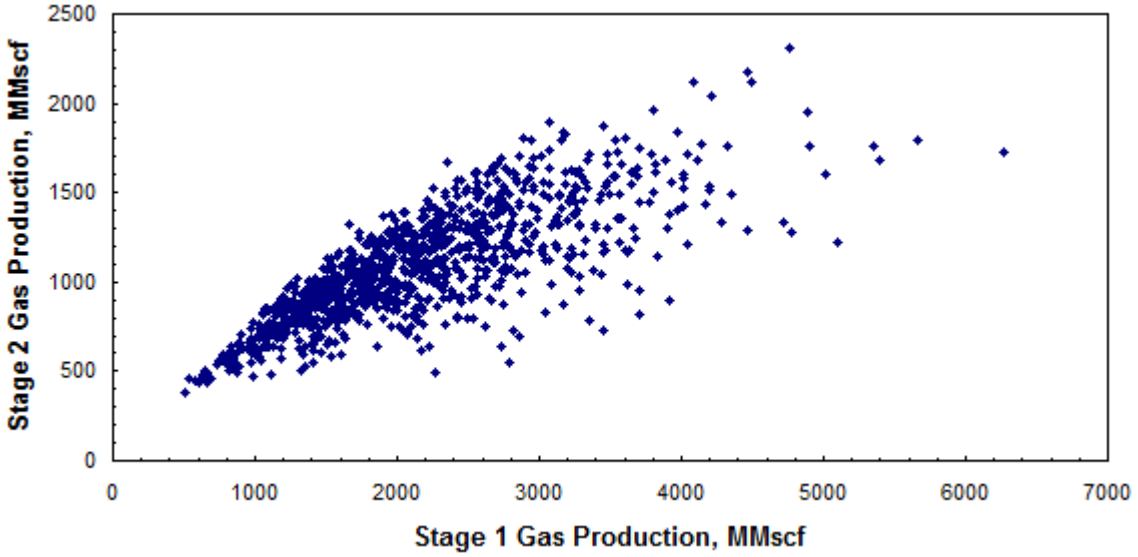

Fig. D5— Crossplot of Stage 1 (160 acres) vs. Stage 2 (160 acres) gas productions.

APPENDIX E

CUMULATIVE DISTRIBUTION PLOTS OF INITIAL PRODUCTION RATE, qi

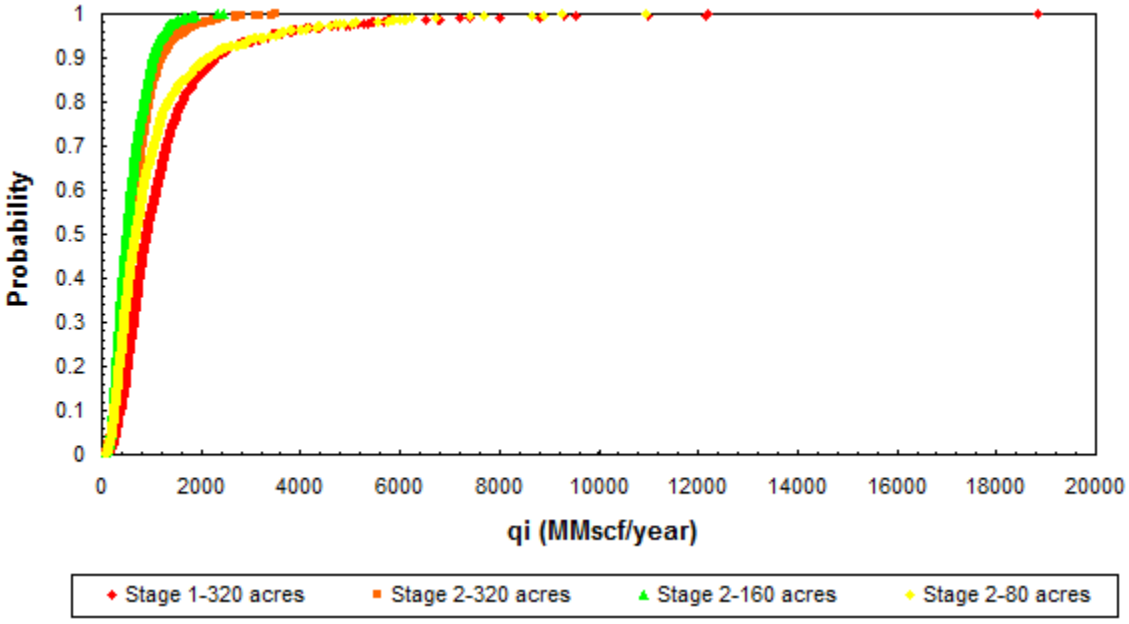

(a)

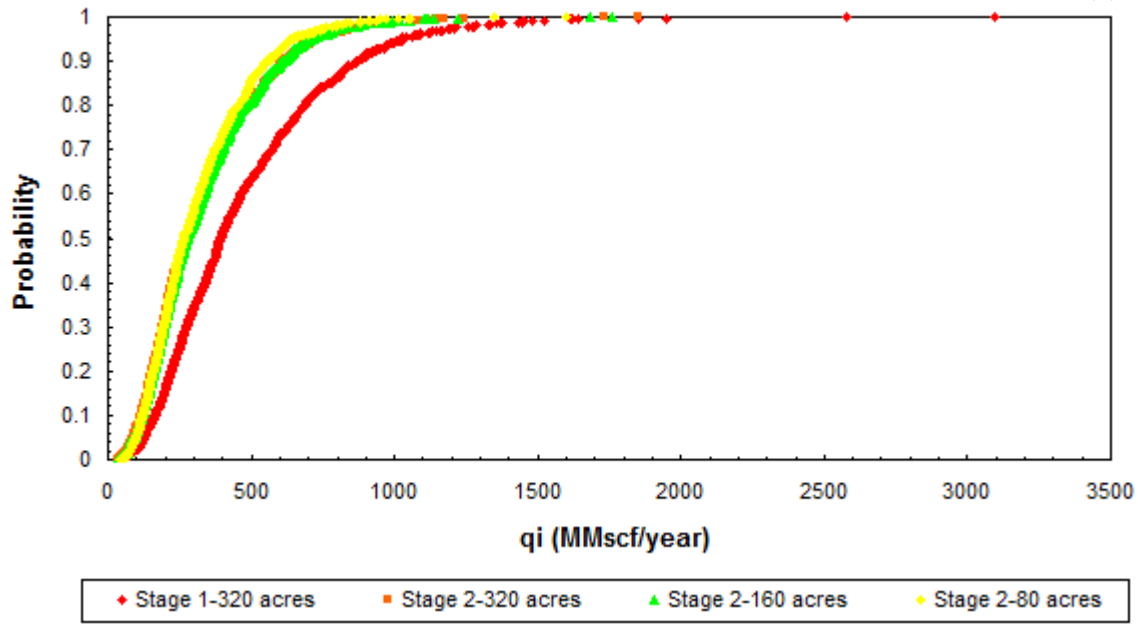

(b)

Fig. E1— Cumulative distribution plot of qi for Well 2, stage-length of 1 year: (a) 1 year-qi (Stage 1), (b) 20 year-qi (Stage 1 + Stage 2).

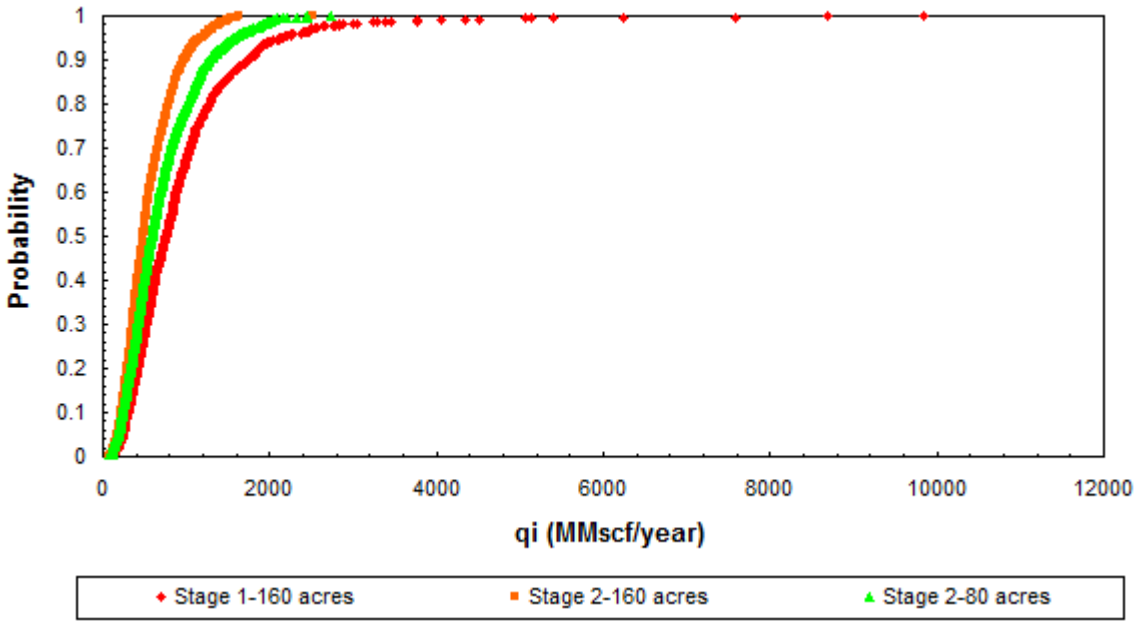

(a)

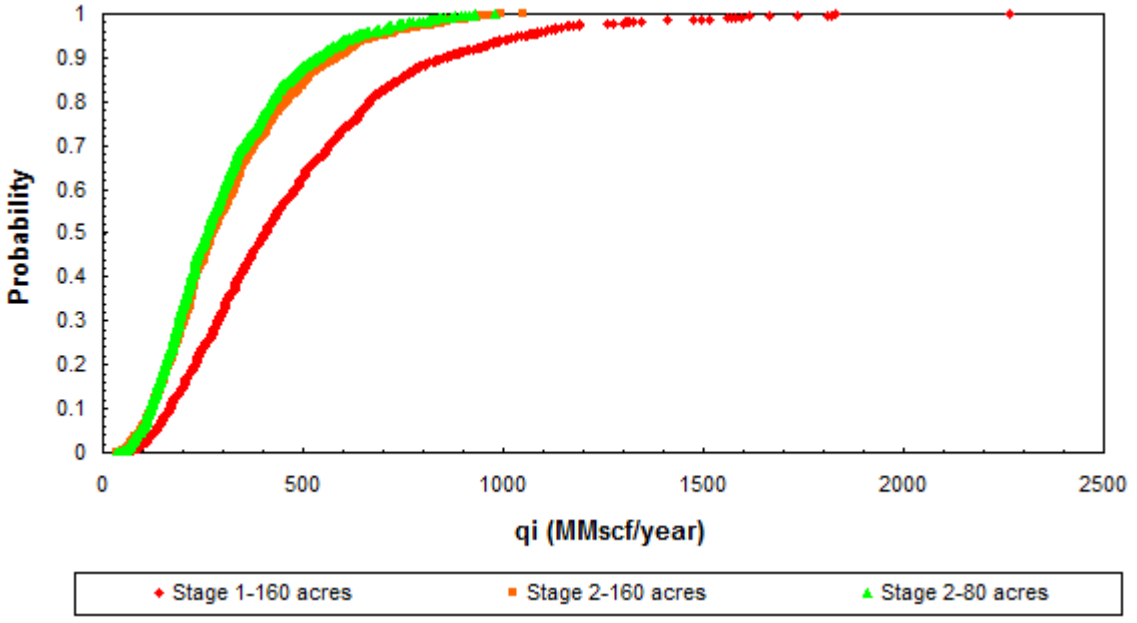

(b)

Fig. E2— Cumulative distribution plot of *qi* for Well 3, stage-length of 1 year: (a) 1 year-*qi* (Stage 1), (b) 20 year-*qi* (Stage 1 + Stage 2).

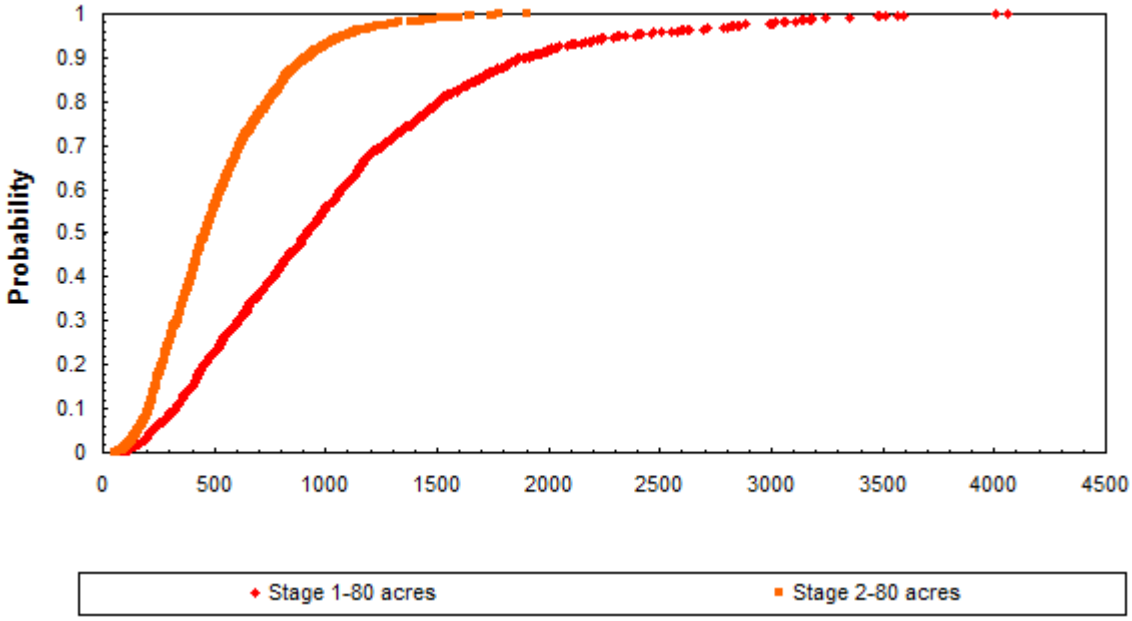

(a)

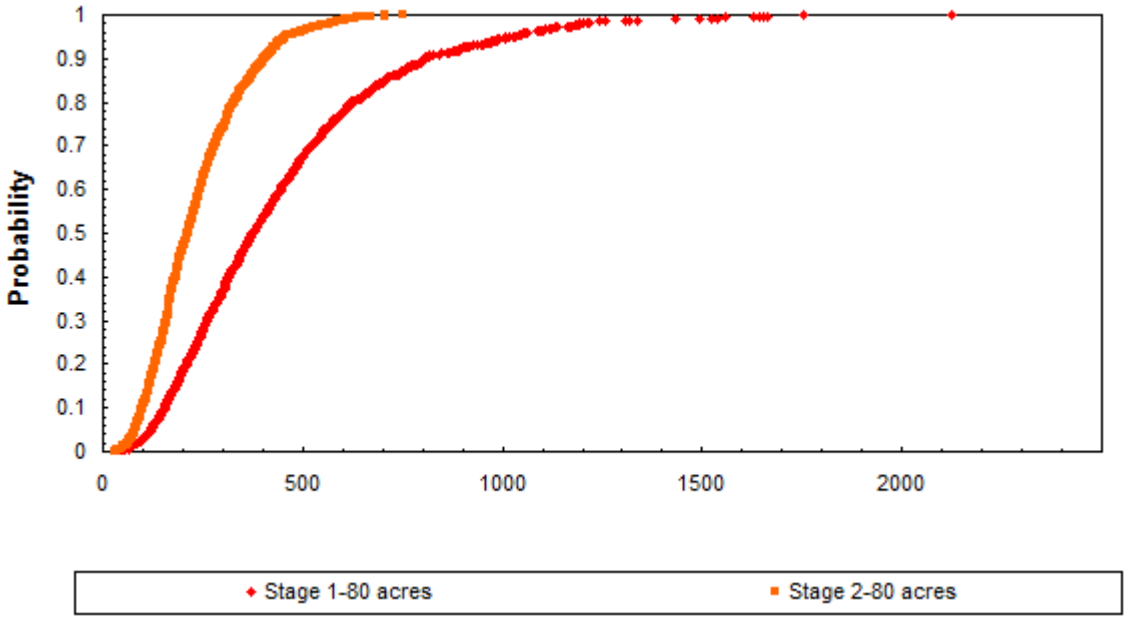

(b)

Fig. E3— Cumulative distribution plot of *qi* for Well 4, stage-length of 1 year: (a) 1 year-*qi* (Stage 1), (b) 20 year-*qi* (Stage 1 + Stage 2).

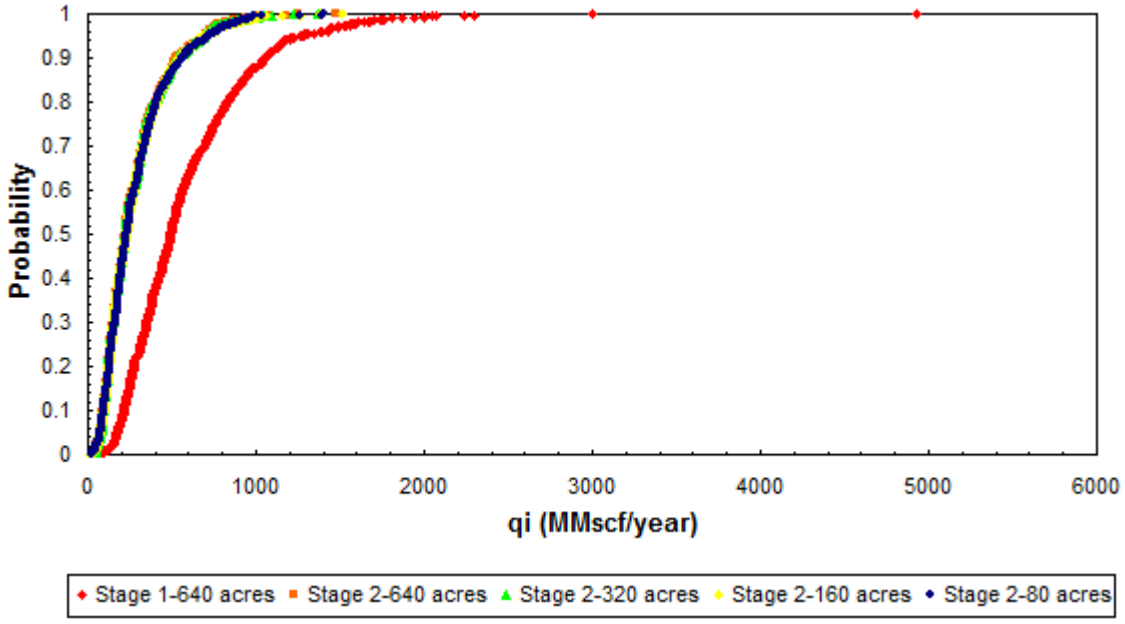

(a)

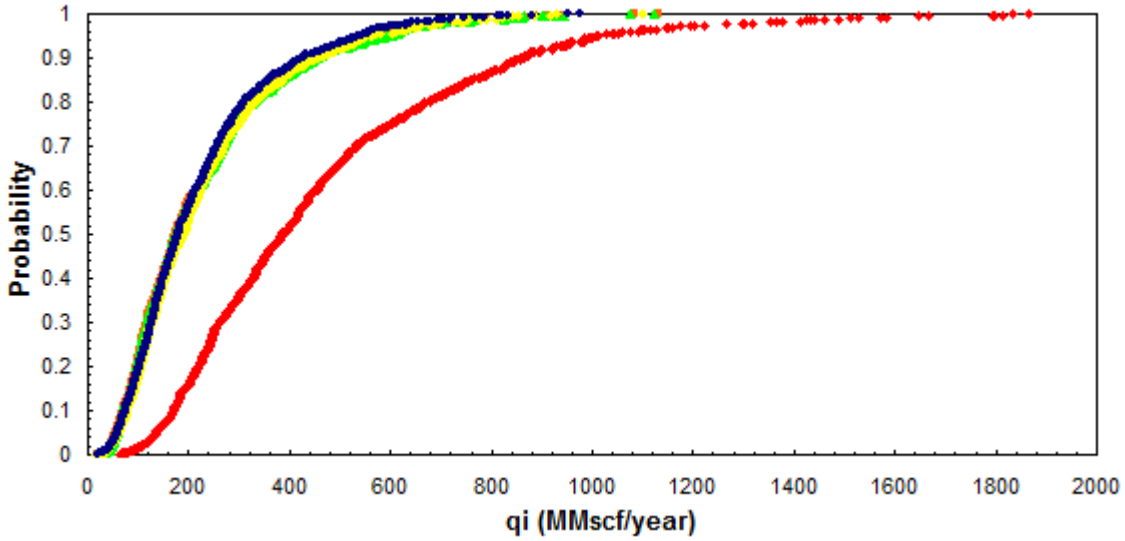

(b)

Fig. E4— Cumulative distribution plot of *qi* for Well 1, stage-length of 3 years: (a) 3 year-*qi* (Stage 1), (b) 20 year-*qi* (Stage 1 + Stage 2).

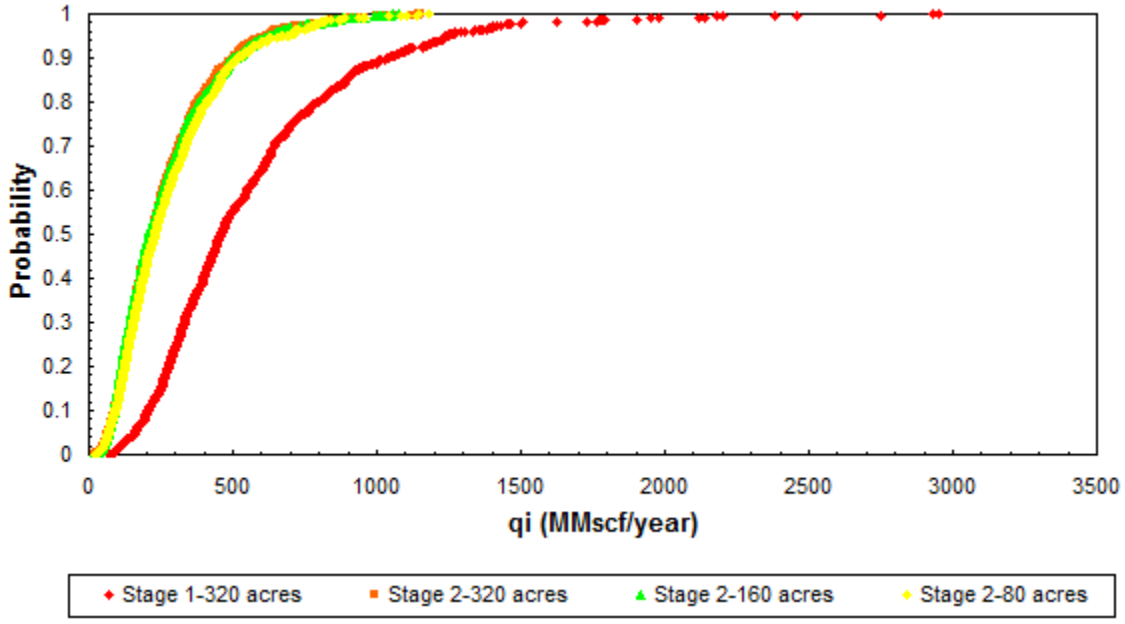

(a)

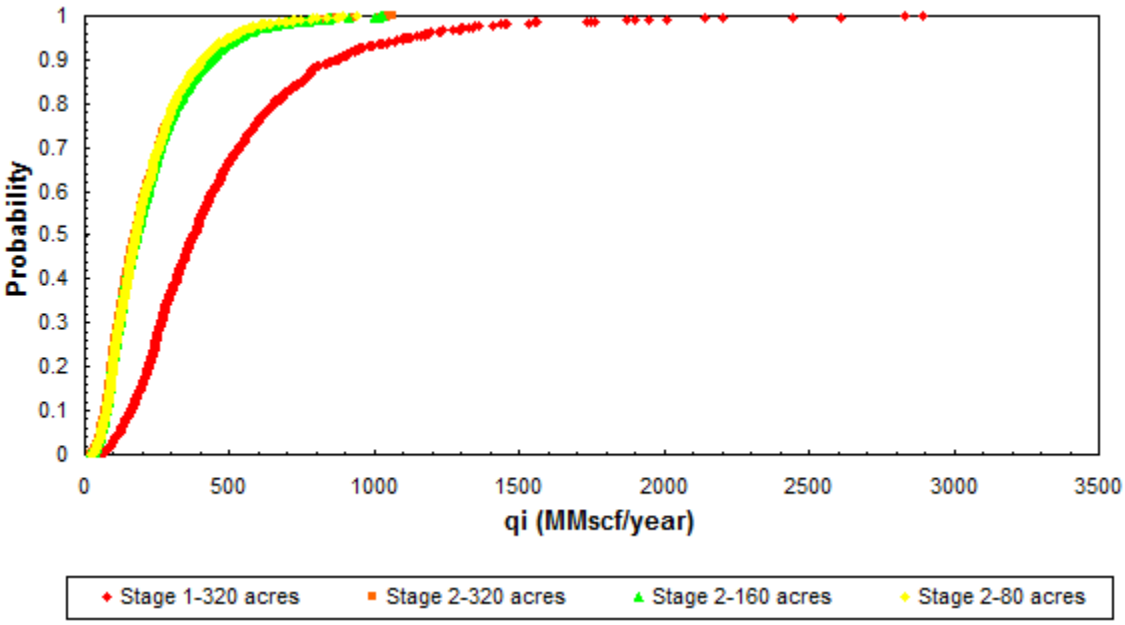

(b)

Fig. E5— Cumulative distribution plot of *qi* for Well 2, stage-length of 3 years: (a) 3 year-*qi* (Stage 1), (b) 20 year-*qi* (Stage 1 + Stage 2).

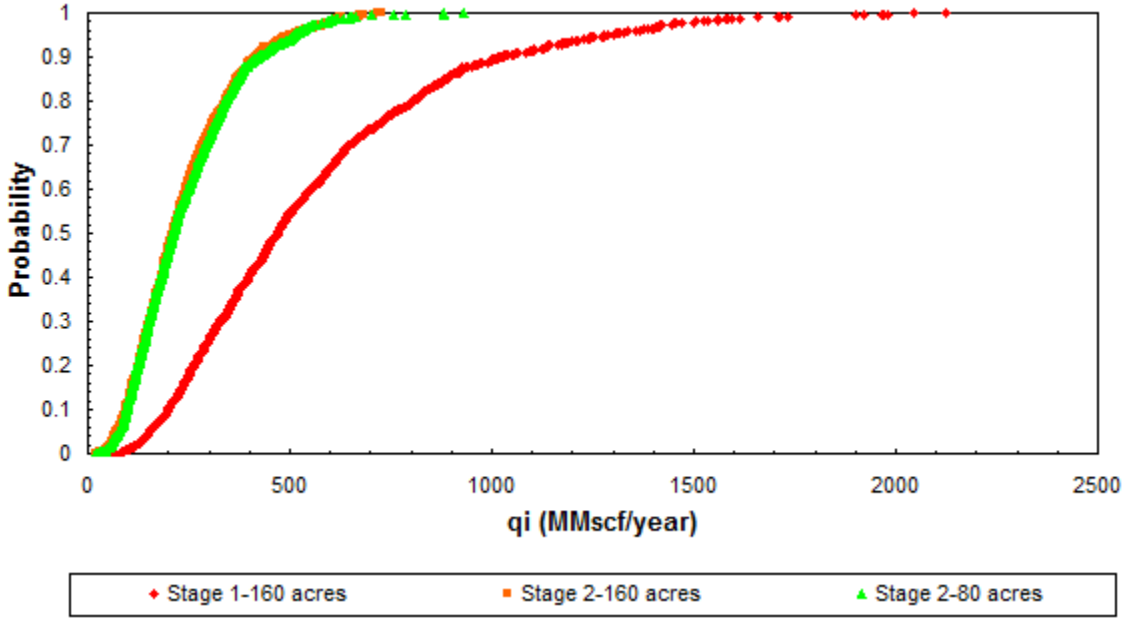

(a)

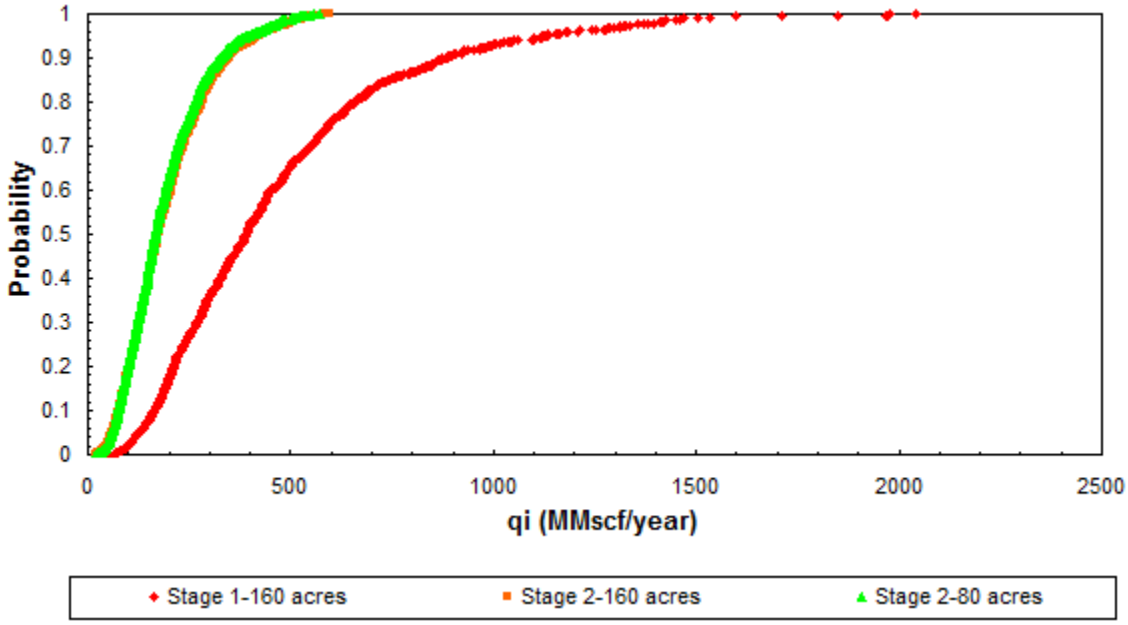

(b)

Fig. E6— Cumulative distribution plot of *qi* for Well 3, stage-length of 3 years: (a) 3 year-*qi* (Stage 1), (b) 20 year-*qi* (Stage 1 + Stage 2).

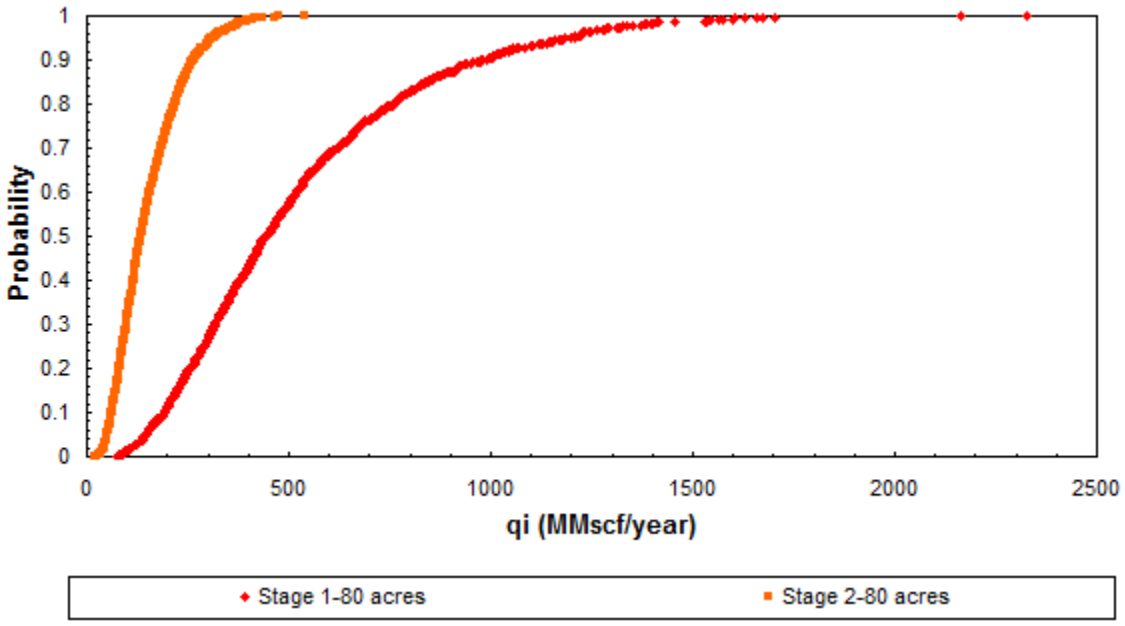

(a)

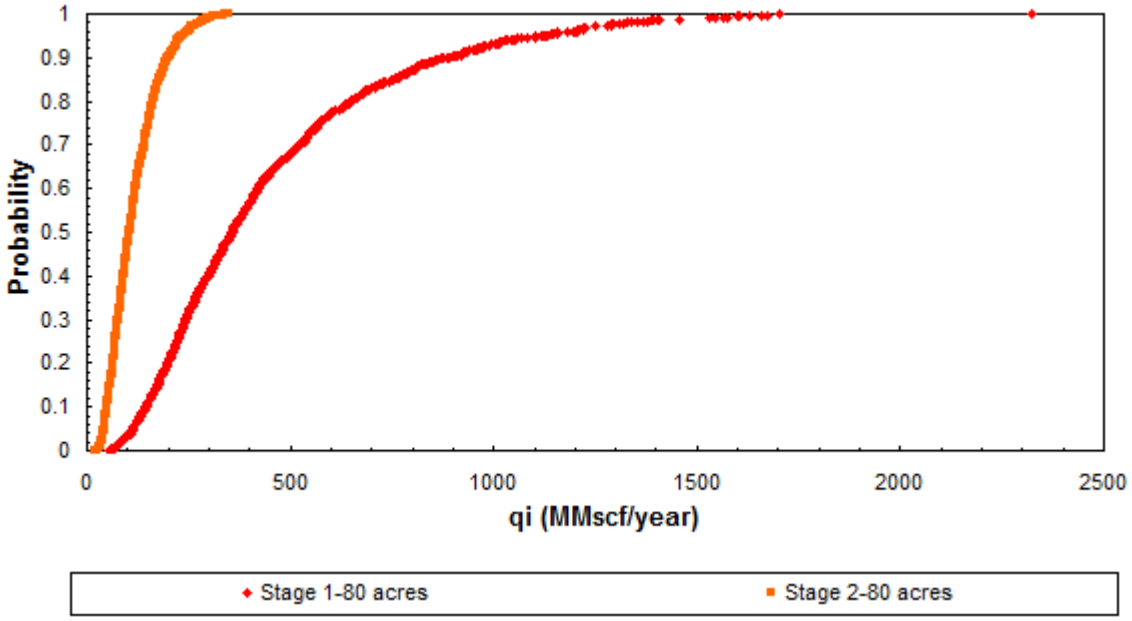

(b)

Fig. E7— Cumulative distribution plot of *qi* for Well 4, stage-length of 3 years: (a) 3 year-*qi* (Stage 1), (b) 20 year-*qi* (Stage 1 + Stage 2).

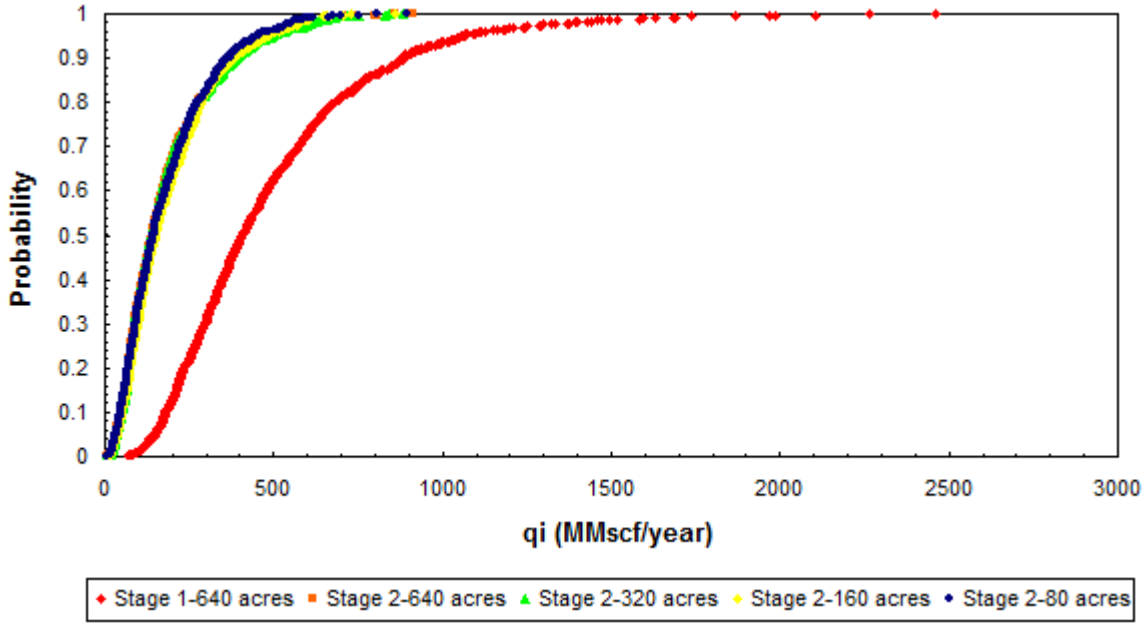

(a)

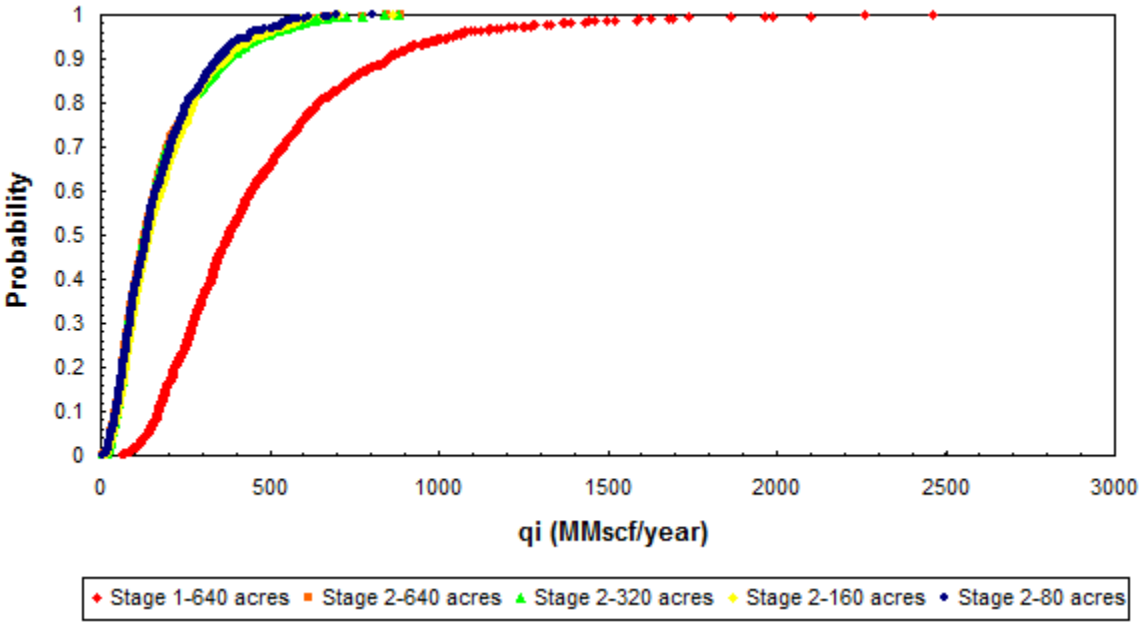

(b)

Fig. E8— Cumulative distribution plot of *qi* for Well 1, stage-length of 5 years: (a) 5 year-*qi* (Stage 1), (b) 20 year-*qi* (Stage 1 + Stage 2).

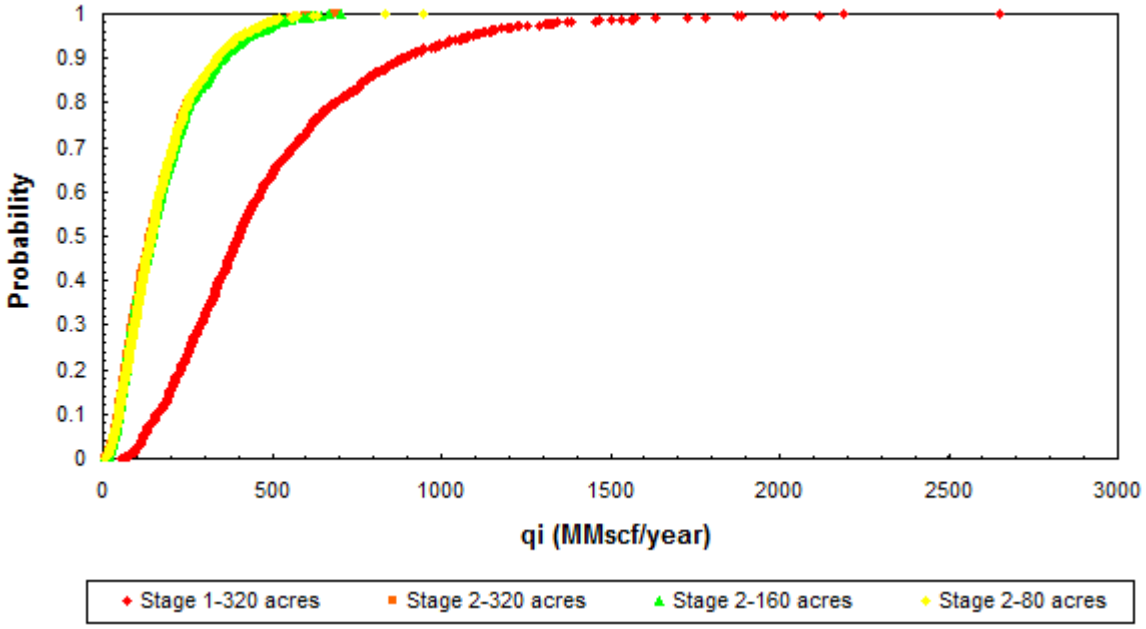

(a)

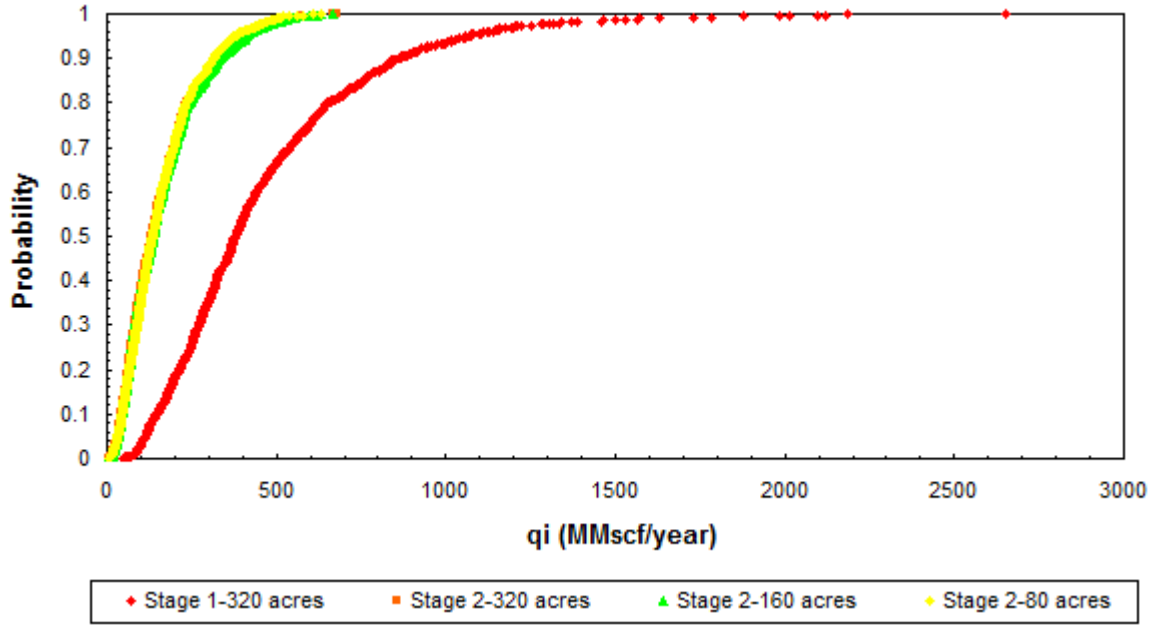

(b)

Fig. E9— Cumulative distribution plot of *qi* for Well 2, stage-length of 5 years: (a) 5 year-*qi* (Stage 1), (b) 20 year-*qi* (Stage 1 + Stage 2).

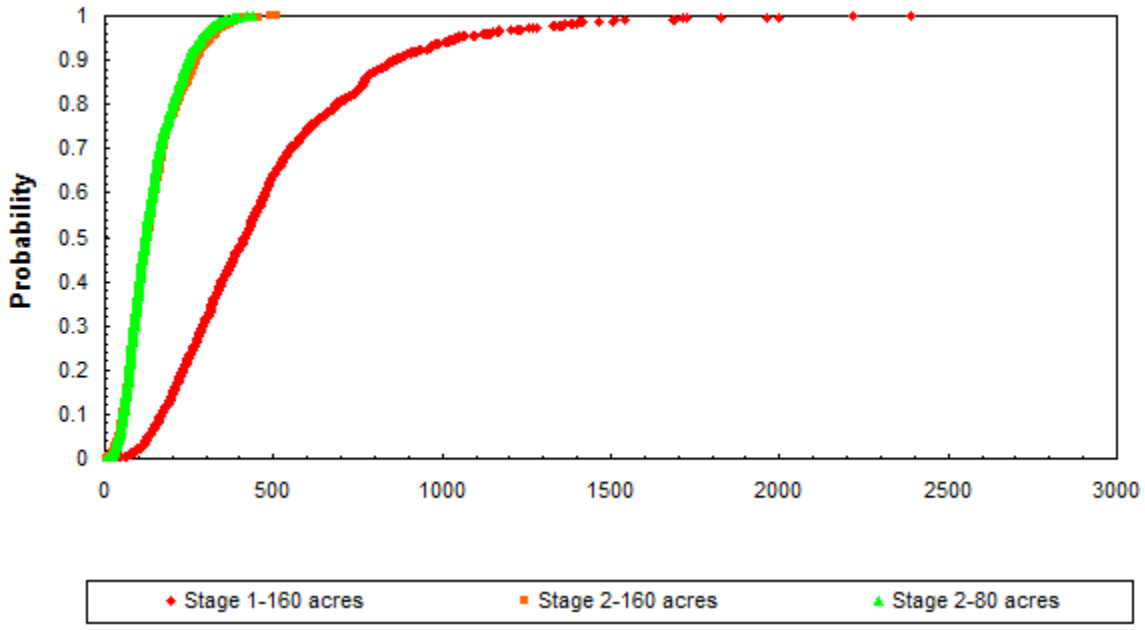

(a)

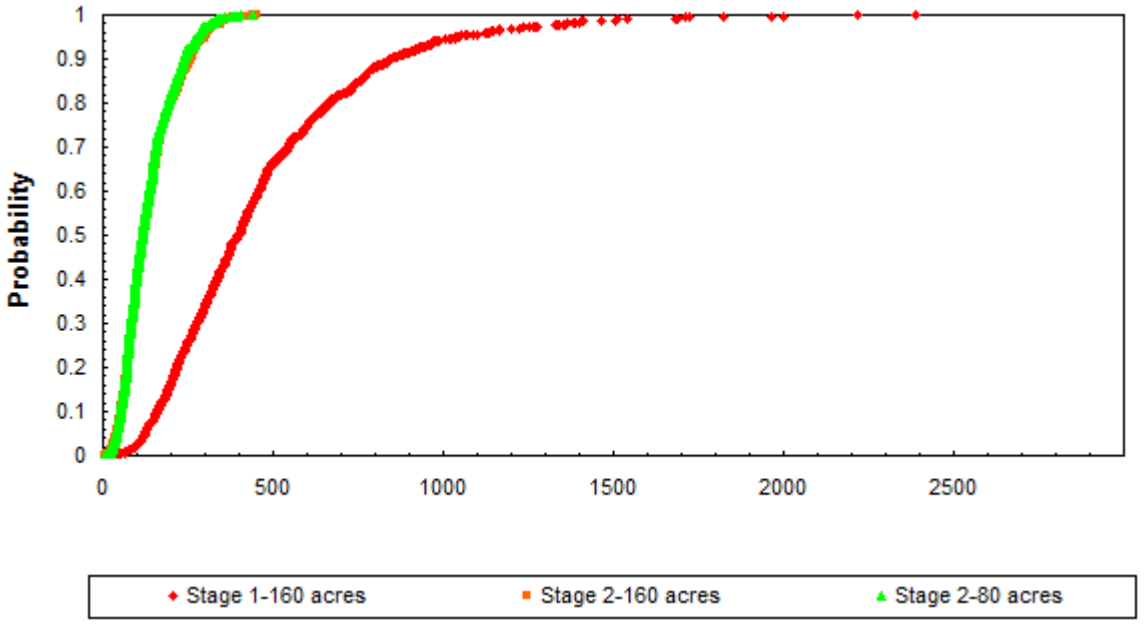

(b)

Fig. E10— Cumulative distribution plot of *qi* for Well 3, stage-length of 5 years: (a) 5 year-*qi* (Stage 1), (b) 20 year-*qi* (Stage 1 + Stage 2).

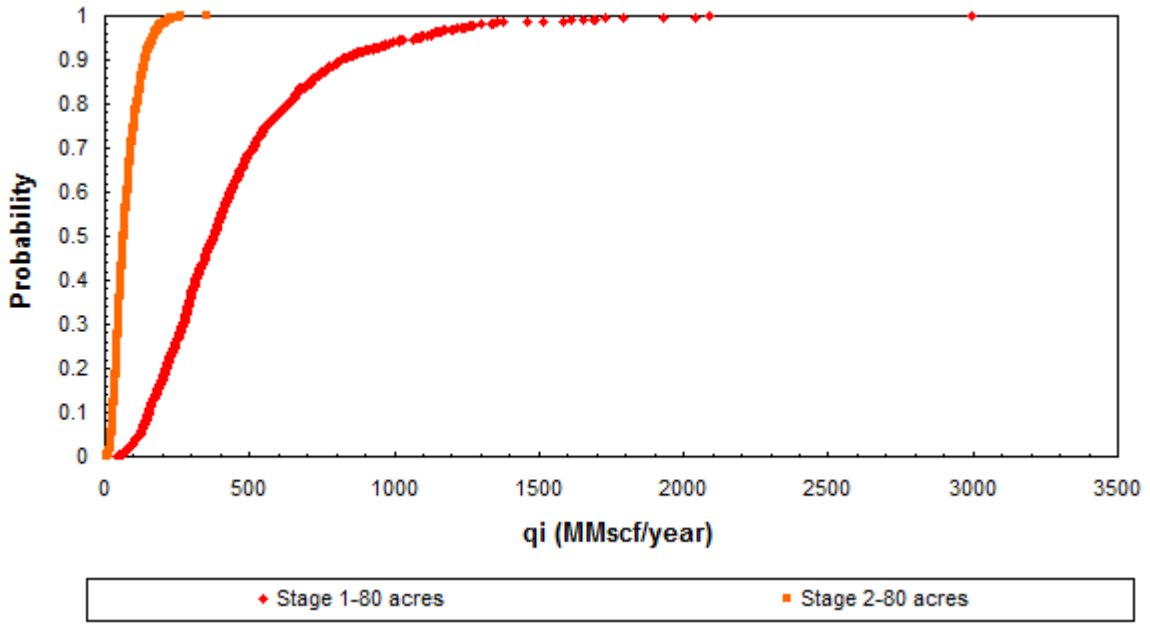

(a)

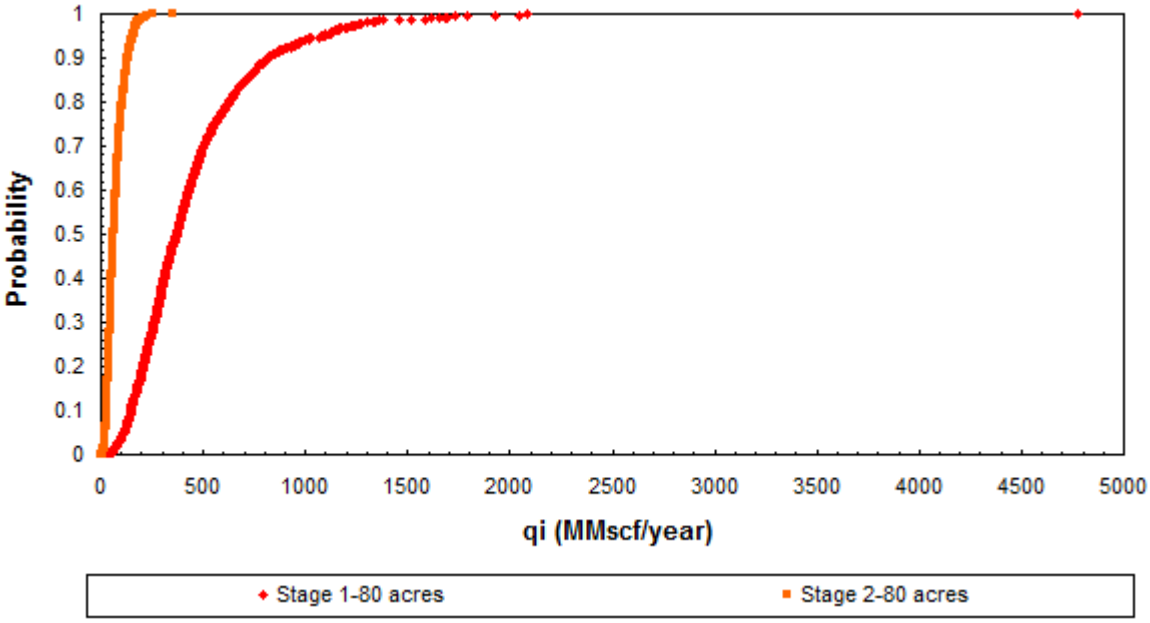

(b)

Fig. E11— Cumulative distribution plot of *qi* for Well 3, stage-length of 5 years: (a) 5 year-*qi* (Stage 1), (b) 20 year-*qi* (Stage 1 + Stage 2).

VITA

Gulcan Turkarslan was born in Ankara, Turkey in 1985. She received her high school baccalauréat diploma at Le Lycée Tevfik Fikret d'Ankara and graduated as the valedictorian of class of 2003. She continued her studies at the Middle East Technical University (METU), Ankara, and graduated 1st in her class with a Bachelor of Science degree in Petroleum & Natural Gas Engineering. In 2008, she joined the Department of Petroleum Engineering at Texas A&M University, College Station to pursue her Master of Science degree. Her research interests focus on reservoir engineering, reservoir simulation and unconventional resources. In the future, she plans to further develop and apply her skills as a reservoir engineer. She can be reached at her permanent address:

Umit Mahallesi, 2436 Sok. 18/1
Umitkoy, Ankara
Turkey